UNIVERSITY OF TRENTO - Italy

International PhD Program in Biomolecular Sciences

Centre for Integrative Biology

29th Cycle

"PERSISTENCE AND ADAPTATION OF PSEUDOMONAS AERUGINOSA IN CYSTIC FIBROSIS AIRWAY"

Tutor

Olivier JOUSSON

Centre for Integrative Biology (CIBIO)

Advisor

Irene BIANCONI

Centre for Integrative Biology (CIBIO)

Ph.D. Thesis of

Silvia D'ARCANGELO

Centre for Integrative Biology (CIBIO)

Academic Year 2015/2016

DECLARATION

I (Silvia D'Arcangelo) confirm that this is my own work and the use of all material from other sources has been properly and fully acknowledged.

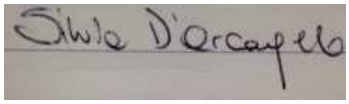

CONTRIBUTIONS

My PhD project was focused on the understanding of dynamics that *Pseudomonas aeruginosa* undergoes during the adaptation in cystic fibrosis patients airway. Professor Olivier Jousson, Dr Irene Bianconi and I designed the experimental workflow, with the valuable contributions of Dr Kate Bailey at CIBIO – Centre for Integrative Biology, University of Trento, Trento, Italy.

Experiments involving Artificial Sputum Medium were performed in collaboration with Prof. Craig Winstanley and Dr Jo Fothergill at the Institute of Infection and Global Health, University of Liverpool, Liverpool, UK.

Mutagenesis experimental procedures were carried out in collaboration with Prof. Alain Filloux and Dr Thomas Wood at the Centre for Molecular Bacteriology and Infection, Imperial College London, London, UK.

Experiments on *Galleria mellonella* were performed with the help of Prof. Giovanni Di Bonaventura and Dr Arianna Pompilio at the Laboratory of Clinical Microbiology, Department of Medical, Oral and Biotechnological Sciences, School of Medicine and Health Sciences, University of Chieti-Pescara "Gabriele D'Annunzio", Chieti, Italy.

Phenotypic assays were performed with the precious help of Elena Piffer, Postgraduate student, CIBIO, University of Trento, Trento, Italy.

Internalization assay was carried out with the contribution of Wojtek Berkowicz, Master student from University of Warsaw, Warsaw, Poland.

Antibiograms were performed in collaboration with Dr Paola Gualdi, Dr Marco Vizzini and Loredana Barberi, at Laboratorio di Patologia Clinica, Ospedale "Santa Maria del Carmine", Rovereto, Italy.

Bioinformatic analyses were performed with the contributions of Dr Alfonso Esposito and Dr Mattia Benedet, CIBIO, University of Trento, Trento, Italy.

Publications

- "Draft Genome Sequences of 40 *Pseudomonas aeruginosa* Clinical Strains Isolated from the Sputum of a Single Cystic Fibrosis Patient Over an 8-Year Period."
  Irene Bianconi, Silvia D'Arcangelo, Mattia Benedet, Kate E. Bailey, Alfonso Esposito, Elena Piffer, Alex Mariotto, Ermanno Baldo, Grazia Dinnella, Paola Gualdi, Michele Schinella, Claudio Donati and Olivier Jousson. *Genome Announcements*, 2016 Nov-Dec; 4(6): e01205-16.
- "Persistence and microevolution of *Pseudomonas aeruginosa* in the Cystic Fibrosis lung: a single-patient longitudinal genomic study."
  Irene Bianconi, Silvia D'Arcangelo, Alfonso Esposito, Mattia Benedet, Elena Piffer, Grazia Dinnella, Paola Gualdi, Michele Schinella, Ermanno Baldo, Claudio Donati and Olivier Jousson, submitted to BMC Microbiology.

Conference abstracts

- "The role of Type VI Secretion System on the competitiveness of *P. aeruginosa* clinical isolates."
  Silvia D'Arcangelo et al., 16th International Conference on Pseudomonas, 5-9th September 2017, Liverpool, UK
- "A population genomics longitudinal study of *P. aeruginosa* reveals adaptive changes related to the acquisition of multidrug-resistant phenotypes during persistence in cystic fibrosis airways."
  Irene Bianconi, Silvia D'Arcangelo et al., 30th Annual North American Cystic Fibrosis Conference, 27-29th October 2016, Orlando, FL, USA
- "A longitudinal study focusing on population genomics and phenotypic factors leading to adaptation of *Pseudomonas aeruginosa* in a Cystic Fibrosis patient."
  Silvia D'Arcangelo et al., Cortona Procarioti 2016, 12-14th May 2016, Cortona, Italy
- "A longitudinal study focusing on population genomics and phenotypic factors leading to adaptation of *Pseudomonas aeruginosa* in a cystic fibrosis patient."
  Silvia D'Arcangelo et al., 31st Meeting of SIMGBM – Società Italiana di Microbiologia Generale e Biotecnologie Microbiche, 23-26th September 2015, Ravenna, Italy
- "A longitudinal investigation of genomic and phenotypic factors leading to adaptation of *Pseudomonas aeruginosa* in a cystic fibrosis patient."
  Silvia D'Arcangelo et al., 38th European Cystic Fibrosis Conference, 10-13th June 2015, Brussels, Belgium.

CONTENTS

1. ABSTRACT

Background. Infections caused by *Pseudomonas aeruginosa* are the main cause of morbidity and mortality in Cystic Fibrosis (CF) patients and occur via primary colonisation of the airway followed by the accumulation of pathoadaptive mutations in the bacterial genome which increase fitness in the lung environment and result in chronicization. A better understanding of i) the evolutionary dynamics occurring during chronic airway infections in CF patients and ii) the genetic adaptation of strains to the CF lung environment, might give further clues for preventive measures or novel therapies to control CF infections in the future. In this work, we obtained genomic sequences of 40 *P. aeruginosa* isolates from a single CF patient collected over an eight-year period (2007-2014) and analysed the population in terms of clonality of the isolates, phylogenetic relationships, and presence of polymorphisms and variants between the strains.

Population structure and microevolution. *In silico* Multilocus Sequence Typing (MLST) analysis revealed a characteristic single clonal population dominated by a previously characterized sequence type (ST390) and a small number of new, closely related ST variants (ST1863, ST1864, ST1923). EBURST analysis of the sequence types revealed that all members of this population belong to the same clonal lineage and likely evolved from a single ancestral colonizing strain. Furthermore, the phylogenetic analysis based on SNPs also divided the population into two subpopulations derived from the evolution of the first infecting strain.

The annotation of SNPs allowed us to identify mutations with moderate or high impact. Genes with high impact variants encoded respiratory nitrate reductase subunit gamma *nail*, polyprotein signal peptidase *lspA*, the ABC transporter-binding protein *aaltP*, the copper resistance protein A precursor *pcoA*in, and four hypothetical proteins.

The evolution of strains in the CF airway is characterized by the loss of many virulence traits, including motility and protease secretion, along with the acquisition of multidrug resistance. Functional phenotypic assays of the collection, including motility and secretion of proteases, showed a decrease over time in the persistent isolates. We also determined the antibiotic susceptibility profile of the collection; while early isolates were found to be susceptible to almost all these antibiotics, resistant phenotypes dramatically increased over time in the population.

Functional studies on specific strains. To identify additional functional variations related to pathoadaptive mutations occurring in the course of chronic infection in CF, we then selected three isolates for further characterization: one early CF isolate (TNCF_23 isolated in 2007); one clonal late CF isolate (TNCF_175 isolated in 2014); one clinical isolate (VrPa97) from a non-CF patient belonging to the same sequence type (ST390) as the former isolates. With this approach, we aimed to identify additional phenotypic and functional variations between isolates with a very homogeneous genomic background, in an attempt to find out new pathoadaptive mutations occurring in the course of chronic infection in CF.

Specifically, the following traits were investigated: killing of *C. elegans* and *G. mellonella* (in vivo virulence); immunomodulatory properties (IL-8 ELISA assay); competitive growth in Artificial Sputum Medium (ASM); functionality of Type Six Secretion System (T6SS). Despite their close genetic relatedness, considerable variations were observed between the three isolates, among which the late isolate TNCF_175 showed several alterations

putatively resulting from the adaptation process to the CF lung. TNCF_175 presented a mutation in *tssK3,* part of H3-T6SS; this mutation (C958T) was therefore introduced in the reference strains PAO1 and PA14, and mutated strains were subsequently complemented; killing rate on *C. elegans* and growth rate in ASM in mutant and complemented strains were evaluated.

Conclusions. A rare feature of this strain collection is the consistent number of clonal isolates obtained from a single patient over a rather long period of 8 eight years, thus providing a model to look at microevolutionary trends within a highly homogenous bacterial population, and avoiding potential biases due to the host genetic background and clinical history. In spite of the close genomic relatedness of all isolates, a surprisingly high diversity was observed for the majority of tested phenotypes. Investigating the competitive ability of early versus late strains we propose a role for T6SS in the adaptation process to the CF lung environment. Our data suggest that once persistence has been established, a strain no longer requires its T6SS, allowing loss of function mutations to occur. Conversely, acute and early CF strains still carry a number of virulence factors, including T6SS that potentially provide an advantage in outcompeting other microorganisms in the initial stage of CF infection.

2. INTRODUCTION

2.1. Pathogenesis of Cystic fibrosis

Cystic fibrosis is the most common autosomal lethal genetic disease among the caucasian population, and it affects approximately one child out of 3000 [1]. The disease is characterized by high levels of epithelial chloride, pancreatic insufficiency, recurring lung infections and bronchiectasis, leading to death from respiratory failure [2].

It is caused by a defect in the Cystic Fibrosis Transmembrane Conductance Regulator (CFTR) gene, which is located on the long arm of chromosome 7 and encodes a 1480-amino acid membrane protein. In healthy individuals with non-impaired CFTR, the ion conductance across the membrane is well-regulated [3].

CFTR belongs to the adenosine triphosphate (ATP)-binding cassette (ABC) transporter protein family. ABC transporters regulate the transmembrane transport of small molecules. CFTR consists of two homologous cytoplasmic nucleotide-binding domains (NBDs) and two membrane-spanning domains (MSDs) [4]. In normal conditions, CFTR allows chloride passage and regulates electrolytes exchange through the cellular membrane. Malfunctioning of CFTR protein causes a diminished Cl^- secretion and increased Na^+ absorption.

Up until now, over 2000 mutations have been identified in the CFTR gene, but only 242 were confirmed to cause CF [5]. The most common mutations in CF patients are divided into six classes, based on the mechanisms that cause aberrant synthesis or function of the protein (Fig.1) [5][6]:

- Class I mutations: presence of a premature stop codon in mRNA or presence of major insertions and deletions that disrupt translation. The protein is not produced;
- Class II mutations: abnormal protein processing or trafficking. The protein is not delivered to the membrane. ΔF508, the most common mutation present in 85-90% of white CF patients, belongs to this class [5]. The mutation consists of a three-base-pair deletion leading to the loss of a phenylalanine residue. This deletion leads to the production of a misfolded CFTR that is not delivered to the cellular membrane and is degraded by the proteasome;
- Class III mutations: abnormal protein regulation. The protein is not activated;
- Class IV mutations: lead to changes in conductivity of the protein, causing abnormal chloride permeability;
- Class V mutations: mutations present in promoter or splice regions. The protein is produced but at lower level;
- Class VI mutations: CFTR is present at the cell surface but with a reduced stability, leading to an increased turnover of the protein.

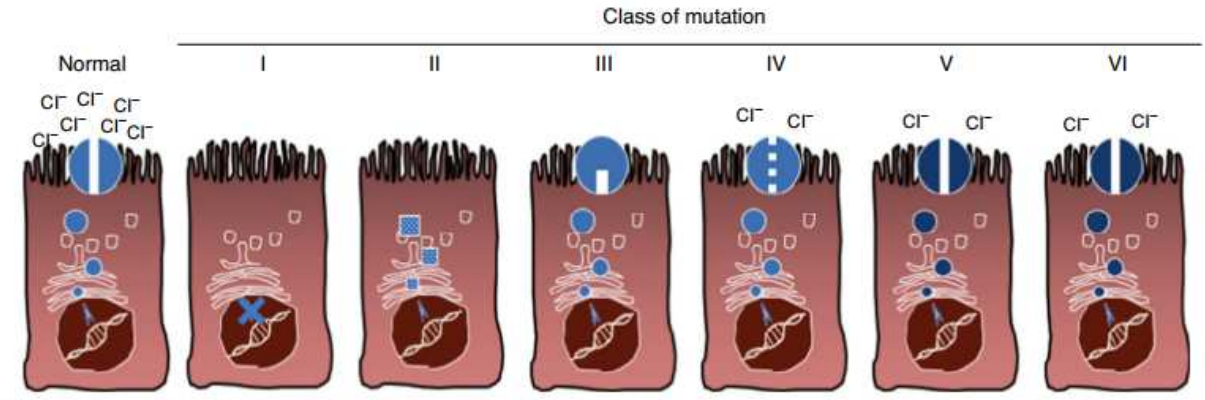

Molecular defect	No synthesis	Block in processing	Block in regulation	Reduced conductance	Reduced synthesis	Reduced half-life
Functional abnormality	Protein is not synthesized	Folding defect	Channel opening defect	Ion transport defect	Decreased protein synthesis	Decreased half-life of the protein
Main mutations	Gly542X Trp128X Arg553X 621+1G→T	Phe508del Asn1303Lys Ile507del Arg560Thr	Gly551Asp Gly178Arg Gly551Ser Ser549Asn	Arg117His Arg347Pro Arg117Cys Arg334Trp	3849+10kbC→T 2789+5G→A 3120+1G→A 5T	4326delTC Gln1412X 4279insA

Figure 1. Types of mutations in cystic fibrosis [6].

2.1.1. Impact of defective CFTR on the airway

The apical surface of the airway epithelium is covered by a thin layer of fluid, the airway surface liquid (ASL). The volume of fluid, itspH, the presence of ions and nutrients are necessary to the airway's antimicrobial activity and ciliary function [7]. ASL is composed of two layers: the upper mucus layer is more viscous and traps exogenous particles, the lower one is the periciliary layer (PCL), more fluid and allows cilia to beat to eliminate the mucus [7][8]. Furthermore, the presence of antimicrobial peptides produced by epithelium and immune responses like IgA and macrophages prevent microbial colonization [9].

Sphingolipids are a class of lipids made of eighteen carbon amino-alcohol backbones which are synthesized in the ER. Modification of this basic structure gives rise to the large family of sphingolipids that play essential roles in membrane biology and provide metabolites that regulate cell function [10]. Defective CFTR or decreased CFTR expression increases sphingolipid synthesis, resulting in a significantly increased mass of sphingomyelin, sphingosine, and sphinganine, affecting membrane functionality [11][12][13]. Sphingomyelin is subsequently hydrolyzed to ceramide by the acidic, neutral and alkaline sphingomyelinase [14]. Ceramide molecules associate and bind to each other, resulting in the formation of ceramide-enriched membrane microdomains, which tend to cluster in macrodomains called ceramide-enriched membrane platforms [15][16][17]. Ceramide accumulation in bronchial, tracheal and intestinal epithelial cells, causes pulmonary inflammation, susceptibility to infection, peribronchial collagen deposition and cell death, triggering DNA release into the bronchial lumen along with the reduction of mucociliary clearance [14].

In CF lungs with a defective CFTR, the impaired Cl^- ions movement creates an osmotic gradient, which in turn causes water hyper-reabsorption and retention into the cells and

leads to the formation of a thick and sticky ASL with reduced volume, causing an impaired mucociliary clearance and clogging the bronchial tubes [5][18].
The abnormal viscous mucus adheres to the pulmonary epithelium and promotes further mucus retention, infection and inflammation, leading to tissue damage (Fig. 2).

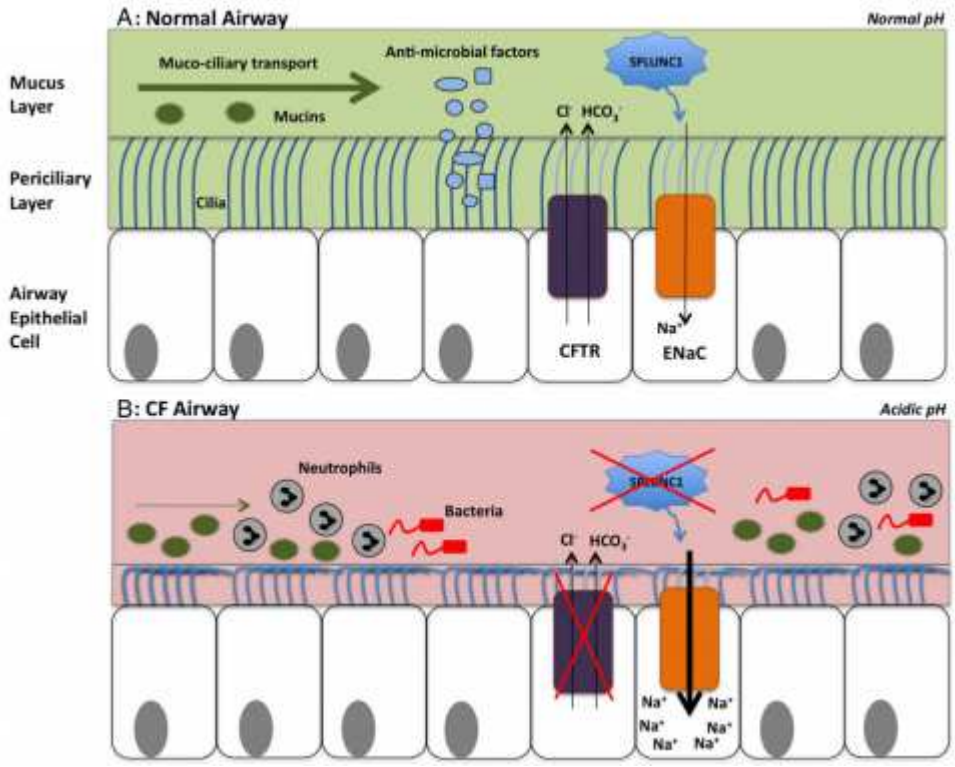

Figure 2. The ASL in CF [19]. (A) the normal airway: the ASL consists of a mucus layer containing large gel-forming mucins that trap inhaled particles for removal by mucociliary clearance. The CFTR transports chloride and bicarbonate into the airway. Sodium is absorbed via the epithelial sodium channel (ENaC), contributing to ASL hydration and mucociliary transport. SPLUNC1 is abundant within the ASL and regulates ASL volume by inhibiting ENaC. The ASL also contains antimicrobial factors, which play a crucial role in innate host defence. (B) the CF airway: defective chloride and bicarbonate transport by abnormal CFTR lead to a dehydrated and acidic ASL. SPLUNC1 fails to regulate ENaC, leading to sodium hyperabsorption and further ASL volume depletion. The acidic environment reduces antimicrobial function and increases mucus viscosity. These mechanisms result in the production of thick secretions and bacterial colonisation. In this dehydrated state, water preferentially moves out of the mucus layer, increasing its concentration. The PCL volume is initially preserved, but eventually, reaches a critical threshold at which water also exits the PCL. The mucus layer subsequently compresses the PCL, compromising ciliary activity and mucociliary clearance.

There is also evidence that mutated CFTR can cause alterations of both innate and adaptive immune systems, leading to compromised bacterial eradication and dysregulated inflammation [5]. Impaired mucociliary clearance and compromised immune response predispose the patients to recurrent bronchopulmonary infections as mucus accumulation in the airways creates a suitable environment for microbial colonization, due to the presence of nutrients for microbial growth [18]. In CF patients morbidity and mortality are caused explicitly by chronic bacterial infection and inflammation of the pulmonary epithelium [20][21]. After an infection is established, its eradication with antibiotic

therapies may be very difficult. Lung infections can cause a progressive decline of the organ functions, respiratory insufficiency and death [18].

2.1.2 Microbiology of CF in the airway

Impaired mucociliary clearance and compromised immune response predispose the patients to recurrent bronchopulmonary infections; mucus accumulation in the airways creates a suitable environment for microbial colonization, due to the presence of many nutrients for microbial growth [18]. In CF patients, morbidity and mortality are specifically caused by chronic bacterial infection and inflammation of the lungs [20][22].
Different microbial communities coexist in the lungs of a CF patient, with the predominant bacterial species being *Pseudomonas aeruginosa, Staphylococcus aureus* and *Haemophilus influenzae* [23]. *Staphylococcus aureus* is the most prevalent pathogen during childhood, and its prevalence decreases over the years to about 40% in the adulthood [21]. *Pseudomonas aeruginosa* is the most common bacterium found in adult patients (prevalence of 60-70%) [23].
The source of the first *P. aeruginosa* strain infecting a CF patient is not entirely clear; although in several patients *P. aeruginosa* infections seem to originate from a nosocomial or social environment, in some cases, the source of the first acquisition appears to be environmental reservoirs [23][24].
Pseudomonas aeruginosa colonization of airways begins with recurrent acute infections eradicable with antibiotic therapies. Over the years the patient can be re-infected with different strains, but in about 25% of cases, the infection is due to strains belonging to the same genotype as the initial colonizer [23]. The re-colonization source can be a reservoir present in the environment or a different niche in the respiratory tract of the patient (e.g., the paranasal sinuses) [23]. Later, usually in patients' mid-twenties, the intermittent acute infections turn into a chronic colonization, currently the factors driving this transition are still not well understood [23].
Other pathogens, such as *Stenotrophomonas maltophilia* or *Achromobacter xylosoxidans* with a prevalence in adult patients of 11% and 7.5% respectively, whilst present are not associated with worse prognosis [25]. The prognosis dramatically worsens after *Burkholderia cepacia* complex (Bcc) colonization [26], however, the prevalence of *Burkholderia* species has decreased from 3.6% to 3.0% in the past 20 years [25] thanks to patient segregation [27]. Colonization and infection of the CF airway by fungi in the late stages of the disease also occur, given the exposure of the population to repeated broad-spectrum antibiotic therapies [28].

2.2. Genomic studies on *Pseudomonas aeruginosa*

The first available *P. aeruginosa* complete genome was the one of the reference strain PAO1 [29]. It is 6,3 Mbp long and contains 5570 open reading frames (ORFs). *Pseudomonas aeruginosa* has a single and supercoiled circular chromosome. PAO1 genome shows a genetic complexity (several genes with unique function) rather than gene duplications. *Pseudomonas aeruginosa* has many paralogous groups (distinct gene families) suggesting that its genome has evolved through genetic expansion [29]. Moreover, 8,4% of *P. aeruginosa* PAO1 genes (521 ORFs) are predicted to be involved in regulation; these, in addition to its remarkable genetic complexity, enable *P. aeruginosa* to

adapt to different environmental conditions and hosts. The bacterium encodes numerous transporters putatively involved in antibiotic resistance, highlighting the significant problems associated with the control of *P. aeruginosa* infections. Several genomic islands were found in *P. aeruginosa* [30]. Genomic islands, differentially distributed among the strains [31], are horizontally acquired segments of DNA and frequently integrated adjacent to tRNA genes, with a G+C content distinct from that of the host core chromosome and containing components of mobile genetic elements [32]. Several genomic islands, also called pathogenicity islands, have been identified and characterized in *P. aeruginosa*. For example, a 49 kb island called *P. aeruginosa* genomic island 1 (PAGI-1) was found in a urinary tract infection strain and subsequently shown to be present in 85% of the clinical isolates tested [33]. The large genomic islands PAGI-2 and PAGI3 were identified by sequencing a hypervariable region of genomic plasticity and an environmental aquatic isolate [34]. *Pseudomonas aeruginosa* pathogenicity island-1 (PAPI-1) represents a large family of genomic islands derived from a pKLC102-like plasmid. pKLC102 is a 103.5 kb plasmid initially described in *P. aeruginosa* clone C strains that exists both as a plasmid or integrated into the chromosome; furthermore, it can excise from the chromosome at a rate of about 10% [35][36].

In *P. aeruginosa* genomes, there is a conserved core component, defined as comprising all genes present in all sequenced genomes of *P. aeruginosa*, and an accessory component, that contains additional strain-specific regions formed by acquisition of clusters of genes by horizontal gene transfer in some strains and deletions of specific chromosomal segments in others [37]. *Pseudomonas aeruginosa* genome is organized as mosaics of conserved regions along with insertions containing blocks of strain-specific genes found in a small number of chromosomal locations called "regions of genomic plasticity" (RGP) [37].

Affordable Next Generation Sequencing (NGS) techniques that have allowed large-scale genomic studies to describe genetic adaptation that occurs in CF lung infections [38]. Several longitudinal studies have reported comparisons among clonally related isolates; these studies focused on mutations that have arisen from the early to the late stages of the infection [39][40][41][42][43][44]. These studies revealed mutations in different functional groups such as virulence, transport, iron acquisition, motility, DNA replication and repair, cell division, transcription and translation, metabolism, and antibiotic resistance. A longitudinal and extensive study on a collection of isolates belonging to a transmissible lineage (DK2), showed that sublineages could appear after the initial colonization and that they can evolve independently in patient's lung by the accumulation of pathoadaptive mutations [40]. It has also been shown that hypermutator and non-hypermutator strains can coexist in the CF lungs [45]. The same group demonstrated that the adaptation process of *P. aeruginosa* in cystic fibrosis infections shows a typical pattern: in a study of 474 longitudinal strains from 34 CF patients, 52 genes were found to be parallelly mutated in all the different lineages [46]. It has been observed in several patients that *P. aeruginosa* improves its ability to uptake iron from haemoglobin towards the late stages of infection [44]. At the earliest stages of infection, *P. aeruginosa* acquires mutations that affect global metabolic regulation, such as mutations in *mucA* and *lasR,* whereas, in the late phases, variations that occur are more specific and have smaller effects [23]. Mutations that lead to pathoadaptation appear to be different among diverse studies,

suggesting that *P. aeruginosa* follows distinct pathoadaptive trajectories [47], in fact, different mutations may lead to similar phenotypes [48].
Despite the trend of *P. aeruginosa* to accumulate loss-of-function mutations throughout the progression of the infection, there are a number of transmissible strains (such as Liverpool Epidemic Strains (LES), Denmark Epidemic Strain (DK2) or Australian Epidemic Strains (AES)) that along with an increased CF lung fitness, show mutations that favour transmission [49][50][51]. These epidemic strains are concerning issues since they often display an MDR phenotype [52]. In a recent study, Lòpez-Causapé et al. [52] analysed a widespread clone (CC274) isolated in Australia and Spain, over an 18-year period. They report the coexistence of two divergent CC274 clonal lineages not split between the two countries; phylogenetic reconstructions and study of mutations leading to multidrug resistance showed an interpatient transmission of mutators. Mutations emerged in over 100 genes involved in antibiotic resistance during the evolution of CC274.

2.3. Adaptation of *Pseudomonas aeruginosa* to the CF airway

During the colonization of the CF airways, *P. aeruginosa* needs to change its nutritional and metabolic properties to survive in this new habitat. The CF airway exposes the bacterium to highly stressful conditions, due to the action of the host immune system, antibiotics therapies, competition with other microorganisms and osmotic stress [23]. All these factors influence *P. aeruginosa* microevolution and adaptation [23].
Young CF patients experience transient pulmonary infections, whereas the lungs become permanently colonized by *P. aeruginosa* in adulthood, and from this point onward the same bacterial lineage can persist in the airway for decades, and its eradication is hardly possible with currently available antibiotic therapies [53]. The characteristics of *P. aeruginosa* isolates present in late CF lung disease differ remarkably from isolates that first colonized the patient years before [23][18].
Chronic respiratory infections by *P. aeruginosa* in cystic fibrosis are associated with genotypic and phenotypic changes [23]. The typical phenotypic changes are development of antibiotic resistance, decreased growth rate, reduced motility, changes in quorum sensing, and modified exopolysaccharides production [54].
Mutations are a significant source of genetic variation that helps bacteria to adapt and survive in a new habitat [39]. Smith et al. [39] sequenced the genome of two *P. aeruginosa* clonal isolates from a single CF patient, the first one isolated after six months from infection, while the second was a clonal descendant, isolated after 96 months. They found a high ratio of nonsynonymous to synonymous mutations, suggesting the occurrence of a positive selection process. About half of the mutations in the two isolates appeared to affect protein functions. In particular, mutations were found in virulence factors and regulators involved in O-antigen biosynthesis, type III secretion, motility, exotoxin A regulation, multidrug efflux, phenazine biosynthesis, quorum sensing, and iron acquisition. The isolate presented a mutation in *mutS*, which encodes a protein involved in the mismatch repair system, the mutation of which results in a hypermutable phenotype favouring bacterial adaptation [39].
Huse et al. studied the expression of a set of 24 genes in three different *P. aeruginosa* lineages and reported similar gene expression patterns. These results suggest the occurrence of convergent evolution in CF airways, i.e. closely related organisms develop

independently the same adaptive traits, in response to the surrounding environment [55]. Despite the convergence of phenotypic changes among clinical isolates, a high level of phenotypic diversity within a single patient and between multiple isolates from the same sputum sample has been reported [23][56]. In general, although most of *P. aeruginosa* infections have a clonal origin, chronic infections are characterized by an adaptive process leading to a marked diversification of the microbial clones into various morphotypes [57]. The adaptive process likely occurs independently in different bacteria of the population, originating subpopulations within the same host [9].

2.4. Antibiotic resistance

Antibiotic resistance is a hallmark of chronic-infection pathogens, especially in those associated with CF infections [58][59][60]. Bacteria acquire and use different resistance mechanisms to protect themselves *in vivo* such as efflux pumps, alterations in membrane permeability and enzymatic modification (i.e. β-lactamases) [61][62][63]. These resistance mechanisms can change during the course of the infection and after the exposure to antimicrobials [58].

Compared to other pathogens, *P. aeruginosa* is difficult to eradicate because of its high intrinsic resistance to a wide range of antibiotics, including aminoglycosides, fluoroquinolones and β-lactams [64]. The most important mechanism underlying this ability is a low outer membrane permeability, which is 12–100 times lower than that of *E. coli* [65]. *Pseudomonas aeruginosa* shows a limited number of large channels of the major porin OprF and small other porins that mediate the passage of other molecules he size of antibiotics, such as OprD and OprB [64]. Different intrinsic mechanisms include rapid efflux [66][67] due to the expression of efflux pumps, like the systems MexAB–OprM and MexXY–OprM [64]. Horizontal gene transfer is a way to acquire antibiotic resistance [64]. For example, aminoglycoside modifying enzymes located on transposons can inactivate aminoglycosides by chemically altering the antimicrobial, lowering its affinity for the 30S ribosomal subunit [68].

Spontaneous mutations are another mechanism by which *P. aeruginosa* acquires antimicrobial resistance [64]. Mutation rate can increase under particular conditions such as in the presence of DNA-damaging agents or during growth in biofilm. For example, the mutation frequency for Meropenem resistance dramatically increased when the culture was preincubated with sub-inhibitory concentrations of ciprofloxacin [69]. Furthermore, a >100-fold increased mutation rate for ciprofloxacin resistance was observed in biofilms rather than free-living cells [70], probably because of a downregulation of antioxidants leading to DNA damage [64]. Mutation frequency considerably increases in hypermutator strains with mutations in genes involved in the repair of DNA replication errors [71]. These strains quickly acquire resistance to different antibiotics. Examples of hypermutators are *mutL* and *mutS*, which are commonly found in CF patients [72].

Critical mutations are those leading to overexpression of efflux pumps, reduced uptake of antimicrobials, overproduction of β-lactamases and altered antibiotic targets [64]. For example, an critical mutational mechanism is the derepression of the efflux pumps MexAB–OprM and MexCD–OprJ caused by mutations in genes encoding *mexR* and *nfxB*, respectively [73].

Mutations in the specific porin OprD reduce the uptake of Imipenem [74], while mutations in either *mexT* or *mexS* reduce the expression of OprD and increase expression of the efflux pump MexEF–OprN leading to multiple antibiotic resistance [75].
Overproduction of β-lactamases is related to mutations in AmpD, an effector of the ampC β-lactamase which directs the activity of the AmpR regulator [64]. Mutations in target enzymes can also result in resistance [76], e.g. mutations in *gyrA* and *gyrB* (gyrase) or *parC* and *parE* (topoisomerase IV). Environment and sub-inhibitory concentrations of antibiotics may lead to changes in gene expression in *P. aeruginosa* and allow the pathogen to cope with following exposures to lethal levels of antibiotics [64].
A relevant adaptive mechanism in *P. aeruginosa* is the induction, caused by pre-exposure to β-lactam antibiotics, of a β-lactamase, encoded by the *ampC* gene, which leads to enzymatic inactivation of several β-lactams [64].
A further resistance mechanism arising from the exposure to sub-inhibitory concentrations of antibiotics is the hyperexpression of genes coding for efflux pumps, such as aminoglycosides, which induce the MexXY efflux pump [77]. These regulatory changes in pump expression lead to a quicker antibiotic efflux, and *P. aeruginosa* becomes more resistant [77].
Recently, mutations were found in genes that had not been fully recognized as antibiotic-related, like *fusA1* and *fusA2*, both encoding elongation factor G (rpoC), which codes for the β-chain of a DNA-directed RNA polymerase [52].

2.5. *Pseudomonas aeruginosa* virulence factors

Pseudomonas aeruginosa presents a multiplicity of regulatory systems allowing it to adapt to the environment [23]. Invasion, dissemination and extensive tissue damage predominate in acute infection. Initial infection may be favoured by the large genome of *P. aeruginosa* and its ability to sense and respond to a broad variety of environmental conditions, while late adaptation may in part result from the selection of clonal lineages containing mutations arising spontaneously [78]. During the transition from acute to chronic infection, the production of several factors of *P. aeruginosa* that exert destructive and immunostimulatory effects is reduced [53]. Virulence factors expression is under the control of complex regulatory circuits and multiple signalling systems. The bacterium produces a broad set of secreted virulence factors, under the control of the quorum sensing system. Accumulation of mutations in *lasR* commonly causes the loss of QS. [38]. *Pseudomonas aeruginosa* adapts by losing most immunogenic traits and acquiring other phenotypical characteristics (e.g., mucoid phenotype and biofilm formation) to escape host immune defences and avoid clearance (Fig. 3) [38].

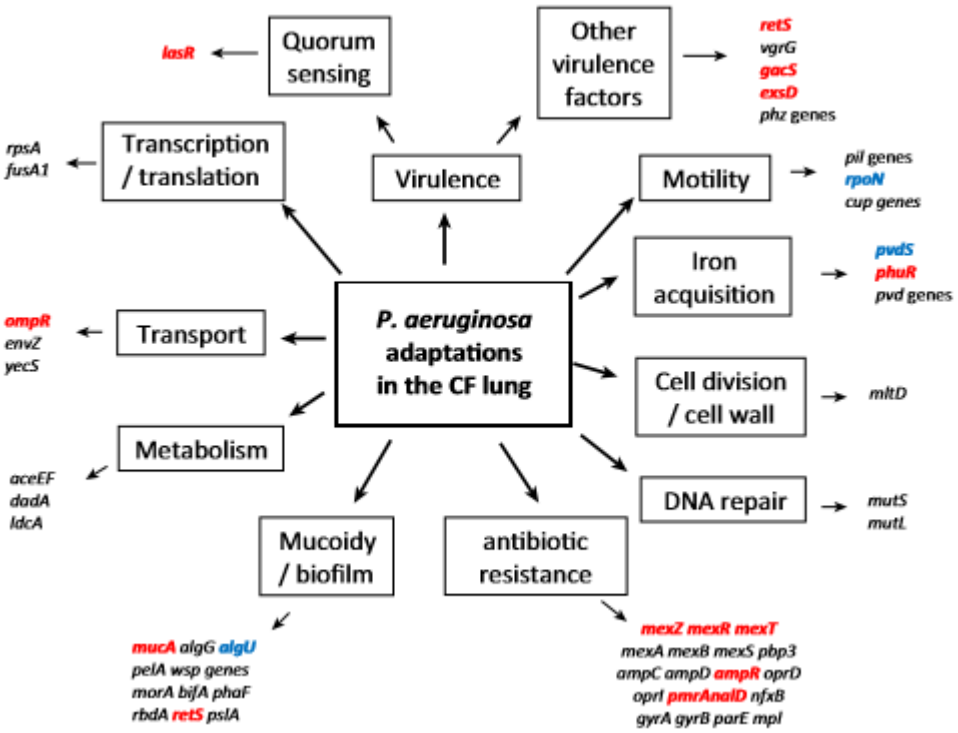

Figure 3. Pathoadaptive mutations in *Pseudomonas aeruginosa*. Genes encoding regulatory proteins are highlighted in red. Genes encoding sigma factors are highlighted in blue [38].

The emergence of mucoid phenotype is a marker for the transition to chronic infection; mucoid *P. aeruginosa* is characterized by the overproduction of alginate, which is a polymer of D-mannuronic and L-glucuronic acid [57][38]. The shift from non-mucoid to mucoid phenotype is mainly due to loss-of-function mutations in *mucA*, which encodes an anti-σ factor that generally represses the expression of the *algD* operon carrying the genes coding for enzymes involved in alginate production [9][57]. Alginate promotes bacterial encapsulation, providing protection against antibiotics and host immune system, especially phagocytosis by macrophages and neutrophils [18]. However, mucoid *P. aeruginosa* triggers a vigorous antibody response, so the presence of mucoid phenotypes is associated with poor prognosis, with tissue damage and decreased lung function [18][57].
Furthermore, the conversion to a mucoid phenotype promotes biofilm formation, which is a key factor for the persistence of *P. aeruginosa* in the CF airways [18]. Biofilm is a community of microorganisms surrounded by an extracellular matrix that protects it. It has a distinct architecture with microcolonies surrounded by fluid-filled channels. Sessile lifestyle may confer antimicrobial resistance [79].
It has been shown that the zone where *P. aeruginosa* grows the most as biofilm is the area comprised between the trachea and terminal bronchioles [80]. Biofilms are an important issue in human disease management, because they lead to a dramatic increase in antibiotic tolerance [81][82].
Biofilm resistance is a result of the combination of different mechanisms, including diminished penetration of antimicrobials through the exopolysaccharide matrix, slow growth rate of bacteria within biofilms due to the reduced availability of nutrients and oxygen, accumulation of metabolic wastes, and quorum-sensing molecules

[83][84][85][86]. The decreased penetration of antibiotics and immunity molecules through the exopolysaccharide matrix represents an essential factor of *P. aeruginosa* persistence [18].
Loss of motility is another feature that *P. aeruginosa* usually acquires during the switch to chronic phenotype. Swarming, swimming and twitching are the three different types of motility, the first two due to the presence of flagella and the last one to the presence of pili, which enable bacteria to adhere to the lung epithelium [57][87]. Several studies have shown that bacteria lacking flagella (e.g. due to mutations in *fliC*, *rpoN*, *vfr*, *fleQ*) are less phagocytized by macrophages and neutrophils, so their loss helps the bacterium evade host immune system and persist in the airway [18][57]. On the other hand, Hassett et al. [88] demonstrated the central role of alginate in bacterial protection against leukocyte killing and phagocytosis. Biofilm also appears to protect sessile communities from antibodies [89] and antibiotics [90].
The presence of pili is necessary for the initial colonization and the translocation of type III exotoxins [57]. The loss of pili could arise from mutations of *pilB*, which encodes an ATPase that enables pili extension and retraction, or from mutations in *pilQ*, required to extrude the pili from the outer membrane [91]. Mutations in *rpoN* lead to loss of both flagella and pili [92].
Lipopolysaccharide (LPS) is a major virulence factor present in the outer membrane of Gram-negative bacteria. It consists of three regions: the hydrophobic lipid A region, a central core oligosaccharide region and a repeating polysaccharide portion, the O-antigen [93]. LPS triggers host immune response by binding to TLR2-4 and CD14; it causes pyrogenicity, platelet aggregation and cytokines production [9][94]. Chronic infections are often characterized by the modification of lipid A and the loss or reduced production of the O-antigen [9]. Lipid A from non-CF *P. aeruginosa* isolates is mainly penta-acylated (contains five acyl groups in the lipid bilayer of the outer membrane), while lipid A from CF isolates contains hexa- and hepta-acylated lipid A [95][96][97]. Loss of O-antigen results from the acquisition of mutations like frameshift deletions or integration of insertion elements in genes responsible for O-antigen production [98][92][99], or from deletion of all or large parts of the locus [100].
Pyocyanine is a blue phenazine that has a redox activity and can cause neutrophils death [101]. Siderophores are secondary metabolites used by bacteria to uptake iron from the environment [102]. Iron is essential for bacterial growth; it is indeed used in respiration processes and as a cofactor for enzymes [102]. *Pseudomonas aeruginosa* uses the yellow-green fluorescent pigment pyoverdine (a siderophore) to seize iron [102].
Proteases are enzymes able to hydrolyse the peptide bonds of proteins; *P. aeruginosa* produces a broad set of proteases such as elastase B, alkaline protease, protease IV and PasP that play an important role in the pathogenic interaction between bacterium and host [103]. Loss of proteases production leads to a decrease in bacterial virulence [103].
The type III secretion system (T3SS) enables *P. aeruginosa* to deliver toxins into the cytoplasm of the host cells and is turned off during chronic infections, resulting in decreased cytotoxicity [104]. The toxins delivered by *P. aeruginosa* T3SS are ExoS and ExoT, which have an ADP-ribosyltransferase activity and decrease macrophage motility and phagocytosis; ExoY, which has an adenylate cyclase activity and affects cell morphology; ExoU, which is a cytotoxin and leads to epithelial cytotoxicity and lung injury

[105]. Patients infected with a strain expressing the T3SS show a higher rate of mortality and an increased incidence of bacteremia compared to the patients carrying *P. aeruginosa* defective of the T3SS [106].
Regulatory pathways associated with the switch from planktonic to sessile lifestyle were shown to be related to RetS and LadS signalling [107][108]. These two proteins modulate the activity of the GacS/GacA two-component system to control levels of sRNAs RsmY and RsmZ [109]. RetS inhibits GacS sensor [110], whereas LadS activates *rsmY* and *rsmZ* expression [109]. In the presence of high level of RsmY and RmsZ, the post-transcriptional regulator RsmA is removed from target transcripts to permit translation [109]. Moreover, RetS/LadS/Gac/Rsm cascade strictly regulates the production of virulence factors: a mutation in *retS* causes a downregulation of T3SS [107], suggesting that RsmA positively influences the expression of T3SS genes [111]. Conversely, the expression of the type VI secretion system (T6SS) was demonstrated to be negatively regulated by RsmA [111]. Therefore, *P. aeruginosa* appears to coordinate the expression of biofilm-related genes with genes coding for T6SS, both of which are related to chronic infection [109].
Along with GacS/GacA signalling cascade, c-di-GMP is known to be an important second messenger for the switch to biofilm lifestyle [112], affecting either polysaccharide production and motility. For example, c-di-GMP showed to influence the production of Pel polysaccharides in *P. aeruginosa* (Fig. 4) [113][114][115]. By measuring intracellular c-di-GMP levels in *retS* mutants, Moscoso et al. [109] (Fig. 4) found that they were much higher compared to wild-type *P. aeruginosa* strains; they also discovered that increased c-di-GMP levels in wild-type strains caused the switch from the expression of T3SS to T6SS, while decreased c-di-GMP levels caused the *retS* mutants switch from T6SS to T3SS. The control of the T3SS and the T6SS by c-di-GMP thus imitates regulation by RetS. The same group discovered how the c-di-GMP-dependent switching from T3SS to T6SS requires Gac/Rsm cascade. Therefore, in *P. aeruginosa* c-di-GMP and sRNAs coordinate together with the switch from T3SS to T6SS [109].

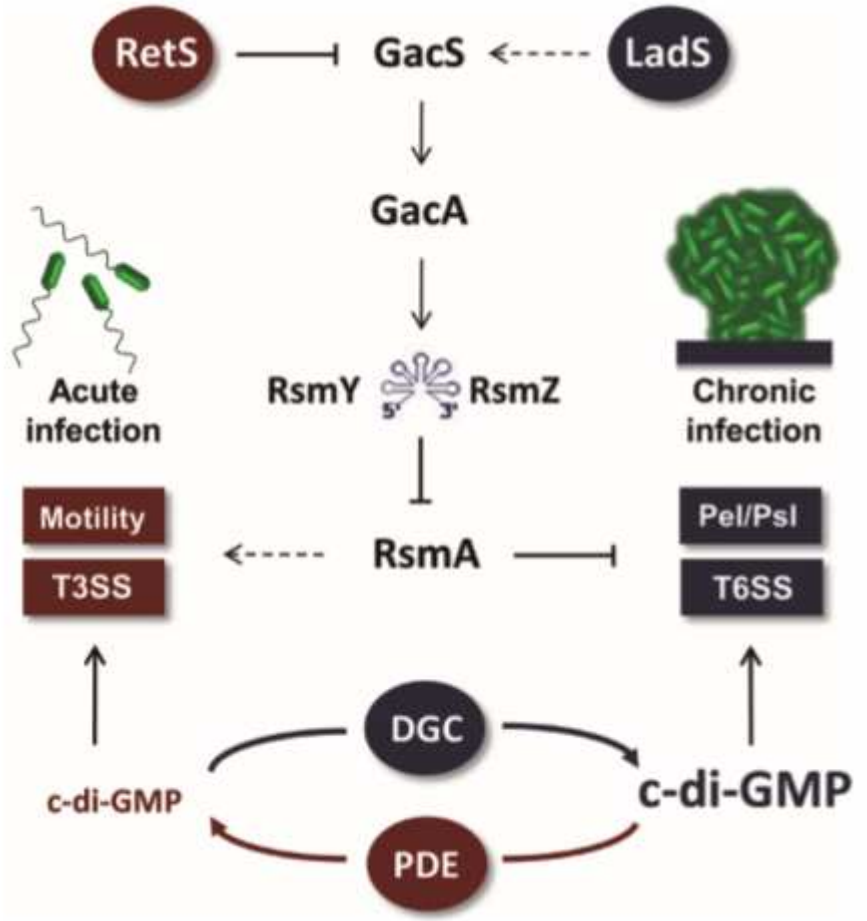

Figure 4. Regulatory networks that switch *P. aeruginosa* lifestyles. The *retS* and c-di-GMP signalling pathways act on the same targets to inversely control functions involved in motility versus biofilm formation, or in acute versus chronic infection. The RetS/LadS signalling network converges on the post-transcriptional regulator RsmA to inversely regulate the T3SS and the T6SS. The same regulation can be achieved by artificially modulating c-di-GMP levels upon overproduction of a diguanylate cyclase (DGC) or a phosphodiesterase (PDE). The dotted arrows indicate an unknown mechanism of action. Figure taken from Moscoso et al. [109].

2.5.1. Role of the T6SS in the progression of infection

The type VI secretion system of Gram-negative bacteria is a nano-machine targeting competitive Gram-negative bacteria in different environments. T6SS injects toxins into cells, and the attacker is protected by cognate immunity proteins that are absent in target cells [116]. These toxins are essential for optimal fitness during host colonization where the pathogen could outcompete host-commensal bacteria [117] or get rid of competitors to establish a niche [118][119].

Genes encoding T6SS components have been found in about 25% of Gram-negative bacteria [120], and *P. aeruginosa* has three T6SS: H1-T6SS, H2-T6SS and H3-T6SS. H1-T6SS is involved in anti-prokaryotic activity [116]. *In vitro*, it secretes two categories of proteins: Hcp (hemolysin coregulated protein) and VgrG (Valine Glycine repeat protein) [121] (Fig. 5). Hcp is believed to be the counterpart of the gp19 protein forming the tail tube of the T4 bacteriophage [122]. VgrG proteins represent the spike at the top of the tube that is sharpened by a proline-alanine-alanine-arginine (PAAR) motif-containing proteins [123]. Tube and spike serve as puncturing tool that allows the injection of toxins into target

cells. The propulsion comes from at least 13 core components called Tss proteins that are associated with the membrane [124]. However, the assembly and the action of the machinery is still poorly understood [125].

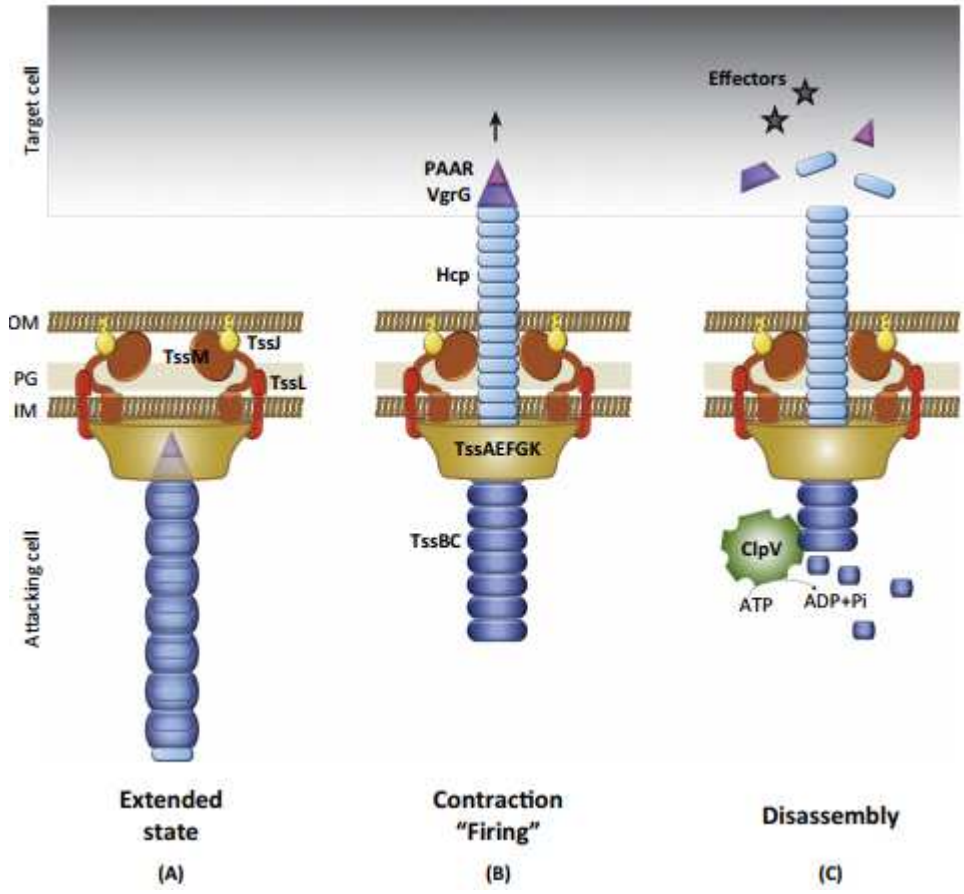

Figure 5. Schematic representation of the structure and mechanism of the Type VI Secretion System [126]**.** (A) The extended machinery is assembled from cytoplasmic and membrane components. The membrane complex, contains TssJ, TssL, and TssM, represented in yellow, red and orange respectively. A putative baseplate-like structure, formed by TssAEFGK and rendered in brown, sits at the cytoplasmic face of the inner membrane. Upon VgrG, within the baseplate, an elongated tubular structure of Hcp hexamers (light blue) is built and extends into the cytoplasm, encompassed in a TssBC sheath (blue). (B) The second step corresponds to sheath contraction and propels the inner tube towards the target cell. PAAR and VgrG, represented in pink and purple triangles respectively, form the puncturing device responsible for membrane perforation prior to effector delivery. (C) Once effectors (grey stars) are delivered into the target cell, the contracted sheath is disassembled by ClpV (green hexamers). Abbreviations: IM, inner membrane; OM, outer membrane; PG, peptidoglycan.

T6SS serves as a gun that injects at least seven effectors (Tse1-7) into other bacteria and produces anti-toxins (Tsi) that protect *P.aeruginosa* from the intrinsic effect of the toxins and the attack from neighbour cells [116].

H1-T6SS was the first type six secretion system to be described, and it explicates antibacterial activity. Tse2, an effector injected via H1-T6SS, was found to cause quiescence in bacterial cells, and its immune cognate Tsi2 interacts with Tse2 in the cytoplasm to counteract its toxic effects [127]. Tse1 and Tse3 exert their activity in the periplasm of target bacterial cells by hydrolysing peptidoglycan [128]. Also, in this case, *P. aeruginosa* presents immunity proteins Tsi1 and Tsi3 to be protected against Tse1 and Tse3 toxicity [128]. In particular, it has been shown how Tsi3 blocks the active site of Tse3

stopping its enzymatic activity [129]. Tse4 and Tse5 (with their immunity cognate Tsi4 and Tsi5, respectively) is a toxic effector that acts at periplasmic level [130]. Tse6 was shown to degrade NAD(+) and NADP(+) causing bacteriostasis in the target cells [131]. All these toxins allow *P. aeruginosa* to outcompete other bacteria in the same niche [132].

Moreover H2- and H3-T6SS show antibacterial activity by injecting the phospholipase D enzymes PldA and PldB into other cells [133][134]. *Pseudomonas aeruginosa* H2-T6SS is responsible for the delivery of Tle5 toxin [133]. Tle5 activity can lead to membrane destabilization, blebbing and depolarization. This activity grants *P. aeruginosa* the capacity to use the enzyme against several different competitors (both eukaryotes and prokaryotes) [133].

PldB is an H3-T6SS-dependent antibacterial effector [134]. PldB targets the periplasm of prokaryotic cells and also facilitates the intracellular invasion of host eukaryotic cells by activation of the PI3K/Akt pathway [134].

Regulators and growth conditions involved in H2- and H3-T6SS expression have been proposed, including quorum sensing and iron limitation [135][136]. Allsopp *et al.* [137] recently displayed H2- and H3-T6SS control by using transposon (Tn) mutagenesis and reporter fusions. They demonstrated that RsmA acts on most known T6SS genes, and showed that AmrZ is another global regulator of the T6SS. They also observed assembly of different T6SSs within a single cell; these results suggest that the three T6SSs are not mutually exclusive [137].

As described above, the T6SS is a contractile tail oriented towards the target cell and attached to the cell envelope by a membrane complex [138][139]. The membrane complex is a 1.7 MDa trans-envelope structure composed of three conserved subunits: the TssJ outer membrane lipoprotein and the TssL and TssM inner membrane proteins [140][141][142][143][125]. In several cases, the membrane complex is inserted and attached to the cell wall by additional proteins with peptidoglycan hydrolysis and peptidoglycan binding properties [141][144][145][146]. The contractile tail consists of an inner tube made of hexamers of the Hcp protein, stacked on each other [122][147], tipped by VgrG, and surrounded by a contractile sheath made of the TssBC proteins [122][147][148]. Polymerization of the tail tube structure is started on an assembly platform called the baseplate and is coordinated by the TssA protein [149][150][151]. Once the T6SS tail is built, the sheath contracts and propels the spike needle complex towards the target cell[152][152][153][154][155]. A recent in vivo study identified five components of the baseplate: TssE, TssF, TssG, TssK and VgrG [150]. T6SS baseplate subcomplexes were isolated in *Serratia marcescens* and uropathogenic *Escherichia coli* (UPEC), including the TssKFG or TssKFGE complexes [149][156]. Furthermore, TssK is a crucial baseplate subunit mediating contacts with the cytoplasmic domains of membrane complex components [151][157][158]. Therefore, TssK is an essential baseplate component connecting the membrane complex, baseplate and tail components. The TssK N-terminal domain attaches to the rest of the T6SS baseplate, and the C-terminal domain binds the membrane complex and has evolved to use the T6SS membrane complex as a receptor that attaches to the baseplate. The flexibility of the TssK C-terminal domain suggests that TssK may establish a flexible link to maintain the anchorage of the baseplate to the T6SS membrane complex [159].

2.6. Aim of the thesis

During my PhD, I have worked to advance our understanding on how *P. aeruginosa* adapts to the cystic fibrosis lung. By performing a longitudinal study of a 40-clonal isolate population, namely applying a series of genotypic and phenotypic analyses, I wanted to gain insights into how the population has evolved over time. Furthermore, by selecting a small number of isolates, I wanted to study in more detail pathoadaptive mutations that have occurred throughout the transition from the early/intermediate-infection strains to the chronic-infection strains.

3. POPULATION STRUCTURE AND MICROEVOLUTION

In the past few years, whole-genome sequencing has significantly triggered the study of clonally related longitudinal isolates to define the genetic basis of the adaptation of *P. aeruginosa* to CF lung. In our study, 40 *P. aeruginosa* isolates isolated from a single cystic fibrosis patient between 2007 and 2014 were sequenced and the genomes were analysed. Furthermore, phenotypic traits of the population were determined.

3.1. Materials and methods

3.1.1. Strains

We obtained 40 *Pseudomonas aeruginosa* isolates from a single cystic fibrosis male patient born in 1983 and followed up by the cystic fibrosis regional centre in Rovereto, Italy. His CFTR mutation profile is ΔF508/G542X. The strains were collected over an eight-year period (2007-2014) (Table 1a).

Table 1a. *Pseudomonas aeruginosa* strains used in this work. Forty isolates came from a longitudinal sampling of sputum from a single cystic fibrosis patient. Along with this collection, an acute-infection strain, VrPa97, was included in the analyses; the isolate derives from a wound swab collected in the intensive care unit at Verona Hospital, Italy.

Isolate name	Isolation date	Sequence type	Source
TNCF_3	13/04/2007	390	CF sputum
TNCF_4M		390	CF sputum
TNCF_6	29/05/2007	390	CF sputum
TNCF_7M		390	CF sputum
TNCF_10	26/07/2007	390	CF sputum
TNCF_10M		390	CF sputum
TNCF_12	04/09/2007	390	CF sputum
TNCF_13	05/09/2007	390	CF sputum
TNCF_14		390	CF sputum
TNCF_16	24/09/2007	1864	CF sputum
TNCF_23	17/10/2007	390	CF sputum
TNCF_23M		390	CF sputum
TNCF_32	23/11/2007	390	CF sputum
TNCF_32M		390	CF sputum
TNCF_42	31/01/2008	390	CF sputum
TNCF_42M		390	CF sputum
TNCF_49M	05/09/2008	390	CF sputum

TNCF_68	02/08/2010	390	CF sputum
TNCF_69	22/03/2010	1863	CF sputum
TNCF_76	09/06/2010	390	CF sputum
TNCF_85	08/11/2010	1864	CF sputum
TNCF_88M	14/12/2010	1864	CF sputum
TNCF_101	30/06/2011	1864	CF sputum
TNCF_105	25/08/2011	390	CF sputum
TNCF_106	16/09/2011	390	CF sputum
TNCF_109	30/09/2011	390	CF sputum
TNCF_130	19/07/2012	390	CF sputum
TNCF_133	14/09/2012	390	CF sputum
TNCF_133_1		1864	CF sputum
TNCF_151	05/04/2013	390	CF sputum
TNCF_151M		1864	CF sputum
TNCF_154	29/04/2013	390	CF sputum
TNCF_155	06/05/2013	390	CF sputum
TNCF_155_1		1923	CF sputum
TNCF_165	23/09/2013	1923	CF sputum
TNCF_167	03/10/2013	390	CF sputum
TNCF_167_1		390	CF sputum
TNCF_174	24/04/2014	390	CF sputum
TNCF_175	23/06/2014	390	CF sputum
TNCF_176	11/08/2014	1923	CF sputum
VrPa97	2007	390	Wound swab (acute infection)

Table 1b. Control strains used in the phenotypic assays.

Assay	Positive control strain	Negative control strain	Supplier
Motility	PAO1 Hannover	PAO1 Δ*pilA*	Craig Winstanley
Protease secretion	PA14 Ausubel	/	Craig Winstanley
Hypermutability	PAO1 *ΔmutS*	PAO1 Hannover	Craig Winstanley

3.1.2. Genome sequencing

All strains were genome-sequenced using Illumina® MiSeq platform (Illumina®, San Diego, CA, USA).

DNA was extracted from overnight cultures in Luria-Bertani (LB) broth (Sigma-Aldrich, Saint-Louis, MO, USA) with DNeasy Blood & Tissue Kit (Qiagen, Düsseldorf, Germany), quantified with Qubit dsDNA HS Assay kit (ThermoFisher Scientific, Waltham, MA, USA) and measured with Qubit 2.0 Fluorometer.

Sample preparation was carried out with Nextera DNA Library Preparation Kit (Illumina), by which DNA was fragmented and tagged at the same time with sequencing adapters in a single step; this step is called "tagmentation" and is the first stage of a library preparation. Subsequently, the fragmented DNA was cleaned-up by removing the Nextera transposon that is likely to interfere with amplification. DNA was amplified and index adapters were added. After the amplification, the amplicons were purified by using AMPure XP Beads. After this stage, a quantification of DNA library templates was required: Qubit dsDNA HS Assay kit was the method of choice. Quality control check was performed with Agilent Technology 2100 Bioanalyzer (Agilent, Santa Clara, CA, USA) to check the size distribution of the library. Right before sequencing, a pooling of libraries in equal volumes was prepared.

Genomes were sequenced on the Illumina MiSeq platform and assembled using SPAdes Genome Assembler version 3.1.0 [160].

Annotation of genomes was performed with Prokka automatic annotation tool v1.11 [161], and analysis of the core and accessory genomes was carried out using Roary with default settings [162]. SNPs were identified using Snippy (available at https://github.com/tseemann/snippy). This software infers polymorphisms at the nucleotide level by aligning the unassembled reads to a reference genome (in this work we used *P. aeruginosa* DK2). In addition, it calls the software SnpEff to annotate and predict the effect for each mutation [163], dividing them into low (e.g. synonym mutations), moderate (e.g. in-frame deletion/insertion) and high (e.g. stop gained).

Genes with multiple SNPs were initially considered to be under non-neutral selection. This statement was further verified by the following procedure: i) the alignment of each homologous gene with reference sequence was exported in FASTA format; ii) the dN/dS ratio was determined using codeml as implemented in PAML package [164] and the likelihood of four different models (two neutral or nearly-neutral, M1a and M7 respectively, and the two corresponding positive selection models M2a and M8) was determined; iii) the likelihood ratio test, using as null model the neutral one, was performed to determine which model better fitted the observed data. This procedure was implemented in a conservative way to detect non-neutral selection in highly similar sequences [165][166].

The occurrence and distribution of genomic islands in the population were inferred using IslandViewer4 [167]. Genbank files, obtained by Prokka, have been uploaded to the web-server, the outputs (both tabular and aminoacidic FASTA sequences) have been downloaded for downstream analysis. All FASTA sequences were concatenated and clustered using CD-HIT [168], with both coverage and identity percentage set at 95%, to

obtain a set of homologous protein clusters (PCs). Coordinates obtained by the tabular output were imported in R, and a genome map of the distribution of the islands was drawn using the package genoplotR. To identify the genomic islands, PCs have been searched on a custom dataset of 23 known genomic islands (nucleotide sequences) using tblastn. Ubiquitous PCs that could not be assigned to any of the known GIs were searched using blastp on the whole nr (restricting the search to *P. aeruginosa*). To determine whether non-ubiquitous PCs distributed according to the phylogenetic structure of the population, we ran the analysis phylo.d (form the r-package caper) [169]. Patterns of gain and loss through time were evaluated using linear models on the presence/absence matrix.
A rooted phylogenetic tree, based on the distribution of SNPs in the core genome, was then obtained using BEAST V1.8 [170].
In silico determination of the O-antigen was performed using the *Pseudomonas aeruginosa* serotypes (PAst) script (https://github.com/Sandramses/PAst).

3.1.3. MLST

In silico MLST analysis was performed with MLST 1.8 (Centre for Biological Sequence Analysis, Technical University of Denmark, Copenhagen). The algorithm eBURST was used to calculate evolutionary closeness among clonal isolates [171][172] (http://eburst.mlst.net/).

3.1.4 Comparative sequence analysis

Genes codifying for factors involved in virulence were extracted from the virulence factor database, VFDB [173]. Gene sequences were compared within the clonal lineage with BioEdit v7.0.5 (http://www.mbio.ncsu.edu/BioEdit/bioedit.html) to determine the occurrence of sequence variants.
Insertions and deletions and single nucleotide substitutions leading to frameshift mutations or premature stop codons were considered relevant for this study.

3.1.5. Phenotypic assays

3.1.5.1. Mucoidy

All 40 strains were inoculated onto PIA (Pseudomonas Isolation Agar) plates (Becton-Dickinson, Franklin Lakes, NJ, USA) and visually inspected for mucoidy (presence/absence of a mucoid phenotype) after 48 hours [174].

3.1.5.2. Motility assay

Swarming and twitching media were prepared using tryptic soy broth (TSB, Oxoid) respectively with 0.5% agar and 1% agar.
Single colonies were picked and inoculated on agar plates and incubated for 15 h at 37° C and for 16 h at 37° C for swarming and twitching test respectively. Twitching plates were additionally incubated at room temperature (RT) for 48 h; motility was indicated by the formation of a halo around the colony [175].

3.1.5.3. Protease production

500 ml of 4% agar containing 8 g of brain heart infusion (BHI) (Sigma-Aldrich) medium was autoclaved at 121° C and subsequently mixed with 500 ml of 20% skim milk solution (pre-autoclaved at 118° C for 10 minutes) (Sigma-Aldrich)for a final content of 2% agar and 10% milk in BHI. After thorough mixing, the medium was poured into 150 x 15 mm Petri dishes. Bacteria were inoculated onto the agar surface and incubated at 37° C for 24 hours. The diameter of milk turbidity clearing surrounding each colony was measured [176].

3.1.5.4. Biofilm formation assay

Biofilm formation was assessed by the crystal violet staining assay with minor modifications [177]. Briefly: isolates were grown on LB ON at 37° C. Pellets were collected by centrifugation and re-suspended in M63 liquid medium (Amresco, Solon, OH, USA) to a final OD_{600} of 0.05. Ten µl of the cultures were then added to 90 µl of the M63 medium in a 96-well U-bottom microtiter plate (Costar, Washington, DC, USA). After 24 h of static incubation at 37° C, supernatants were removed and OD_{600} was measured to determine the cell density of planktonic bacteria.

Cells attached to the microtiter wells through biofilm were washed twice with H2O Milli-Q to remove unattached and dead cells and then stained with 150 µl of an aqueous solution of 0.1% crystal violet (Sigma-Aldrich) for 15 min. Biofilm was washed again with H_2O Milli-Q, dried, resuspended in 125 µl of 30% acetic acid and incubated for 15 min. OD_{550} of resuspended biofilm was determined and normalized to the OD_{600} of corresponding planktonic cells. The assay was repeated at least three times per isolate.

3.1.5.5. Mutation frequency

A single *P. aeruginosa* colony was grown in 5 ml of LB ON at 37°C. Aliquots from serial dilutions were then plated on LBA plates with and without rifampicin (300 µg/ml) (Sigma-Aldrich) and counted after 36 h at 37°C. The mutation frequencies on rifampicin were determined relative to the total count of viable organisms plated according to previously established criteria [72]. The assay was repeated in triplicate for each isolate.

3.1.6. Antibiotic susceptibility

Sensititre GRAM™ Negative Plate Format (Thermo Scientific, Waltham, MA, USA) panels were used to assess resistance/susceptibility for Amikacin, Cefepime, Ceftazidime, Ciprofloxacin, Colistin, Doripenem, Fosfomycin, Gentamycin, Imipenem, Levofloxacin, Meropenem, Piperacillin/Tazobactam.

3.1.7. Statistical analysis

In the phenotypic assays, Spearman's correlation coefficient was used to study the correlation between the phenotypes and the time of isolation of the samples, and the correlation between phenotypes.

The R function used is cor.test and the script is:

```
>cor.test(as.numeric(phenotypes$Isolation_date), phenotypes$#Phenotype,
method="spearman").
```

Phenotypic data were plotted as a function of the isolation time. Graphics were drawn using the ggplot function within the ggplot2 package of R [178]:
>ggplot(phenotypes, aes(Isolation.date, #Phenotype)) + geom_point() + geom_smooth()
+ geom_text(aes(label=rownames(phenotypes)), hjust=0, vjust=0)
This scrip returns a scatter plot with a trend line calculated on the bases of a smoothed conditional mean.
Significance of changes over time of protease production, biofilm formation and swarming motility were also evaluated with Wilcox test.

3.2. Results

3.2.1. Whole Genome Sequencing

Longitudinal studies are a key tool to understand pathoadaptive evolution of *Pseudomonas aeruginosa* in CF lung. In our study, 40 *P. aeruginosa* isolates isolated from a single cystic fibrosis male patient were sequenced on the Illumina MiSeq platform and assembled using SPAdes version 3.1.0.
The number of contigs per genome ranged from 53 for TNCF_151 to 356 for TNCF_6. Mean draft genome size was 6.6 Mb, with slight variations from 6.545 Mb to 6.653 Mb in TNCF_12 and TNCF_101, respectively, with a mean GC content of 66.28%. The N50 of the draft genomes was in average 179.843 bp, ranging from 30.645 in TNCF_6 to 378.317 bp in TNCF_151 (Table 2).
Genomes encoded for an average of 6151 putative ORFs with an SD of 29 (from 6052 to 6219 in TNCF_12 and TNCF_6, respectively), with about 713 of them carrying a signal peptide; the average number of tRNA per genome was 60 (SD 4), and only one tmRNA per genome was identified.
O-antigen in silico serotyping revealed that all the isolates belonged to the serotype O6, one of the most commonly found among CF isolates.
Genome sequence data for all the 40 isolates were deposited and publicly released [179].

Table 2. Genome statistics of the 40 *P. aeruginosa* CF isolates. N50 is the length of the shortest contig which, along with the larger contigs, contains half of the genome sequences.

Accession no.	Isolate name	Yr of isolation	Sequence type	No. of contigs	Genome size (kb)	N_{50} (kb)	G+C content (%)
MAUO00000000	TNCF_3	2007	390	139	6,636	92	66.28
MAUP00000000	TNCF_4M	2007	390	161	6,630	78	66.29
MAUQ00000000	TNCF_6	2007	390	356	6,618	31	66.28
MAUR00000000	TNCF_7M	2007	390	259	6,623	47	66.28
MAUS00000000	TNCF_10	2007	390	101	6,643	143	66.28
MAUT00000000	TNCF_10M	2007	390	107	6,633	111	66.29
MAZG00000000	TNCF_12	2007	390	102	6,545	177	66.36
MAZI00000000	TNCF_13	2007	390	75	6,637	195	66.27
MAZH00000000	TNCF_14	2007	390	89	6,633	158	66.28
MAKL00000000	TNCF_16	2007	1864	59	6,638	269	66.28
MAZJ00000000	TNCF_23	2007	390	71	6,635	228	66.28
MAZK00000000	TNCF_23M	2007	390	64	6,636	228	66.28
MAKM00000000	TNCF_32	2007	390	67	6,639	229	66.28
MAZL00000000	TNCF_32M	2007	390	138	6,627	93	66.28
MAZM00000000	TNCF_42	2008	390	70	6,639	228	66.28
MAZN00000000	TNCF_42M	2008	390	71	6,640	228	66.28
MAZO00000000	TNCF_49M	2008	390	76	6,635	177	66.29
MAZP00000000	TNCF_68	2010	390	82	6,633	162	66.28
MAZQ00000000	TNCF_69	2010	1863	88	6,639	150	66.28
MAZR00000000	TNCF_76	2010	390	61	6,634	281	66.28
MAZS00000000	TNCF_85	2010	1864	101	6,644	124	66.29
MAZT00000000	TNCF_88M	2010	1864	65	6,636	229	66.28
MAZU00000000	TNCF_101	2011	1864	142	6,653	92	66.28
MAZV00000000	TNCF_105	2011	390	92	6,644	191	66.28
MAZW00000000	TNCF_106	2011	390	77	6,634	205	66.28
MAZX00000000	TNCF_109	2011	390	69	6,634	205	66.28
MAZD00000000	TNCF_130	2012	390	157	6,625	76	66.28
MAZF00000000	TNCF_133	2012	390	82	6,637	154	66.29
MAZE00000000	TNCF_133_1	2012	1864	87	6,641	269	66.28
MAKK00000000	TNCF_151	2013	390	53	6,629	378	66.28
MBMI00000000	TNCF_151M	2013	1864	103	6,636	143	66.28
MBMJ00000000	TNCF_154	2013	390	86	6,635	177	66.28
MBMK00000000	TNCF_155	2013	390	62	6,634	339	66.28
MBML00000000	TNCF_155_1	2013	1923	71	6,635	221	66.28
MBMM00000000	TNCF_165	2013	1923	119	6,634	135	66.28
MBMN00000000	TNCF_167	2013	390	73	6,634	191	66.27
MBMO00000000	TNCF_167_1	2013	390	91	6,628	143	66.28
MBMP00000000	TNCF_174	2014	390	111	6,645	143	66.29
MBMQ00000000	TNCF_175	2014	390	118	6,642	124	66.28
MBMR00000000	TNCF_176	2014	1923	61	6,637	354	66.28

3.2.1.1. *In Silico* MLST Genotyping

To understand clonal relationship among isolates, *in silico* MLST analysis, performed with MLST 1.8, revealed a characteristic single clonal population dominated by a previously characterized sequence type (ST390, 36 isolates), and a small number of new, closely related ST variants: ST1864 (six isolates: TNCF_16, TNCF_85, TNCF_88M, TNCF_101, TNCF_133_1, TNCF_151M), ST1923 (three isolates: TNCF_155_1, TNCF_165, TNCF_176) and ST1863 (one isolate: TNCF_69). The novel variants were deposited in the PubMLST database (https://pubmlst.org/). Eburst analysis of the sequence types indicated that strain 390 was the founder, while 1863, 1864, and 1923 directly descended from 390 and differed from it at a single locus (Fig. 6).

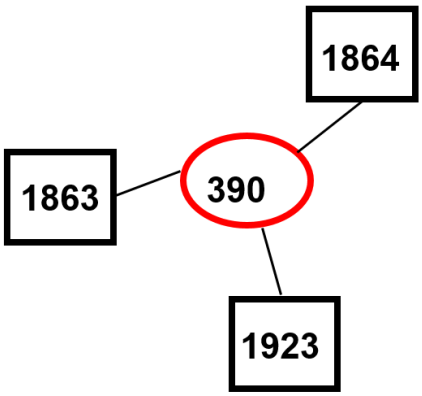

Figure 6a. E-burst analyses. Strain 390 was identified as founder; 1863, 1864 and 1923 directly descended from 390 and differed from it at a single locus.

3.2.1.2. Phylogenetic analyses

The distribution of SNPs in the core genome was analysed using BEAST to reconstruct the evolutionary history of the lineage and to examine the relationships between the isolates. The tree topology indicates that the population is composed by two main clusters: the first one comprised nearly all the early clones (13 out of a total of 17 strains isolates sampled between 2007 and 2008), whereas the majority of the late isolates branched within the second cluster (17 out of a total of 23 isolates sampled between 2010 and 2014). The six ST1864 isolates fall in the cluster with ST390 early isolates, while the three ST1923 isolates and the ST1863 one group in the cluster with the late ST390 isolates sampled between 2010 and 2014 (Fig. 6b).

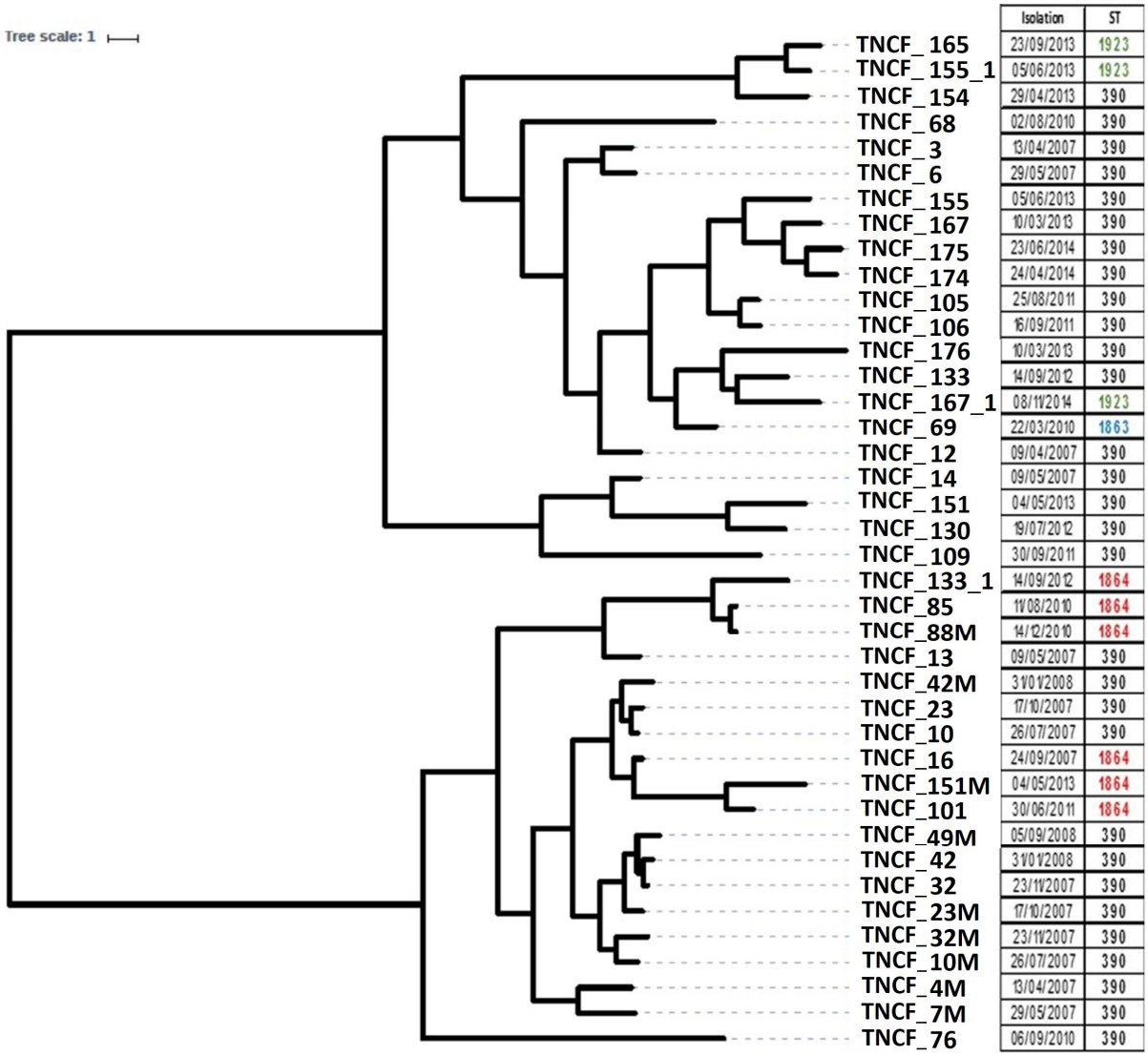

Figure 6b. Rooted phylogeny of the *P. aeruginosa* population. The tree was built on core genome SNPs obtained using BEAST V1.8 with ten independent runs of 10^9 steps using the relaxed clock model. The right panel reports the date of sampling and the Sequence Type of each isolate.

3.2.1.3. Core and accessory genome analyses

Previous studies have shown that the genomes of *P. aeruginosa* isolates are usually highly conserved, with a small accessory genome containing about 10% of total coding sequences [180][181].

The pangenome of our population comprised 7035 genes, with nearly 85% of the genes shared between all the isolates (5972 genes). Among these, 5608 were core genes present in 39-40 isolates, and 364 were soft core genes found in at least 38 isolates (Fig. 7). A total of 1063 genes (15%) belonged to the accessory genome. Among these, 264 were shell genes present in at least six isolates, and 787 were cloud genes identified in less than six strains. Among the latter genes, 555 were found to be present only in one isolate. The average number of accessory genes per genome was 516, with TNCF_12 being the isolate with the minor portion of the accessory genome (415 genes) and TNCF_6 the one with the largest accessory genome (583 genes), consistent with the higher length of its genome.

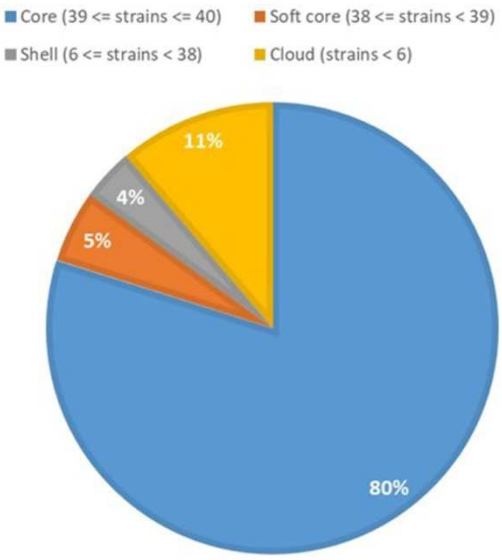

Figure 7. Core and accessory genome proportions in the *P. aeruginosa* population. Genomic portions present in 38 or 39 isolates out of 40 (soft core) were considered as core genes in the text due to the draft assembly of the genomes.

Tree topology of Figure 8 shows wide collapse at the root, and the presence of three major lineages: a lineage includes 31 out of 40 isolates (the bulk of the population), a second lineage with the isolates TNCF_23, TNCF_10 and TNCF_42M, monophyletic also in the SNP-based tree, and a third lineage comprises TNCF_16, TNCF_7M, TNCF_4M, TNCF_10M, TNCF_32M, TNCF_151M. TNCF_6 also resulted to be the strain with the most diverse accessory genome, in agreement with its high number of unique regions.

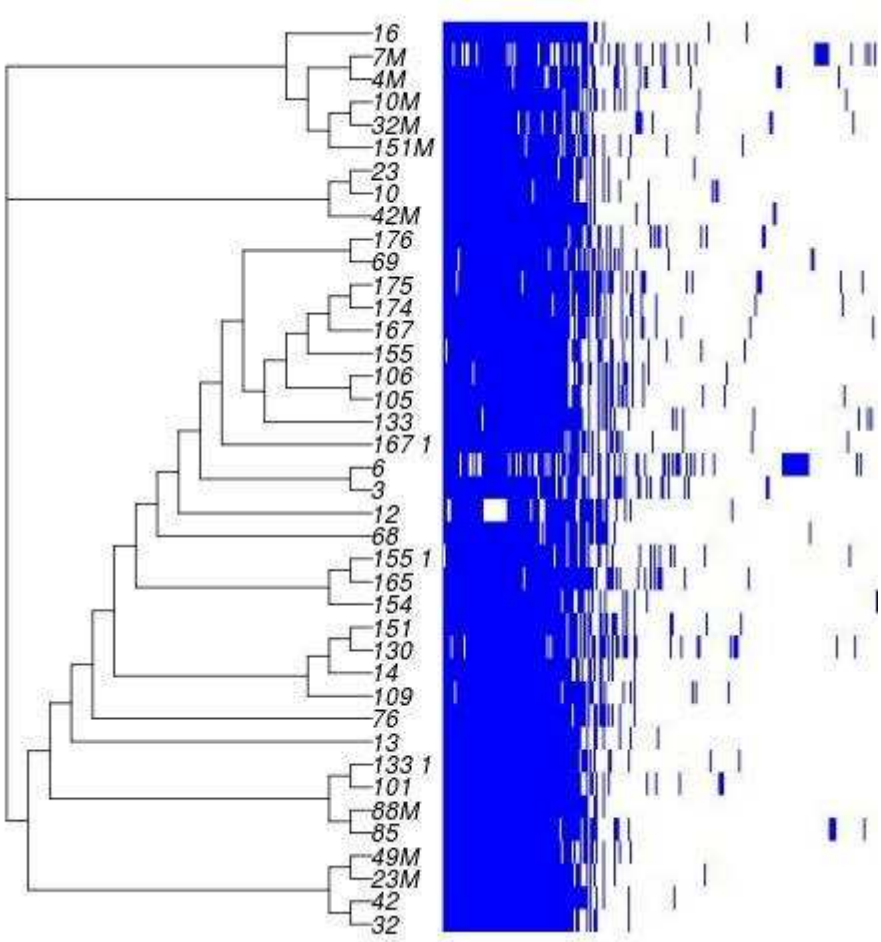

Figure 8. Phylogenetic tree based on the distribution of accessory genes in the *P. aeruginosa* population. The analysis was performed using the hclust() function from the base R package; core genes have been removed from the analysis to improve the resolution of the picture.

Clustering of isolates based on the composition of the accessory genome (Fig. 9) revealed a group of 11 highly similar genomes comprising both early and late isolates, eight belonging to the dominant ST390 type (TNCF_10, TNCF_13, TNCF_23, TNCF_23M, TNCF_32, TNCF_42, TNCF_42M, TNCF_49M) and three belonging to the derived ST1864 (TNCF_16, TNCF_88M and TNCF_133_1). Accordingly, the number of accessory genes in each genome of this cluster was remarkably homogeneous, ranging from 488 to 511 genes in TNCF_16 and TNCF_10, respectively.

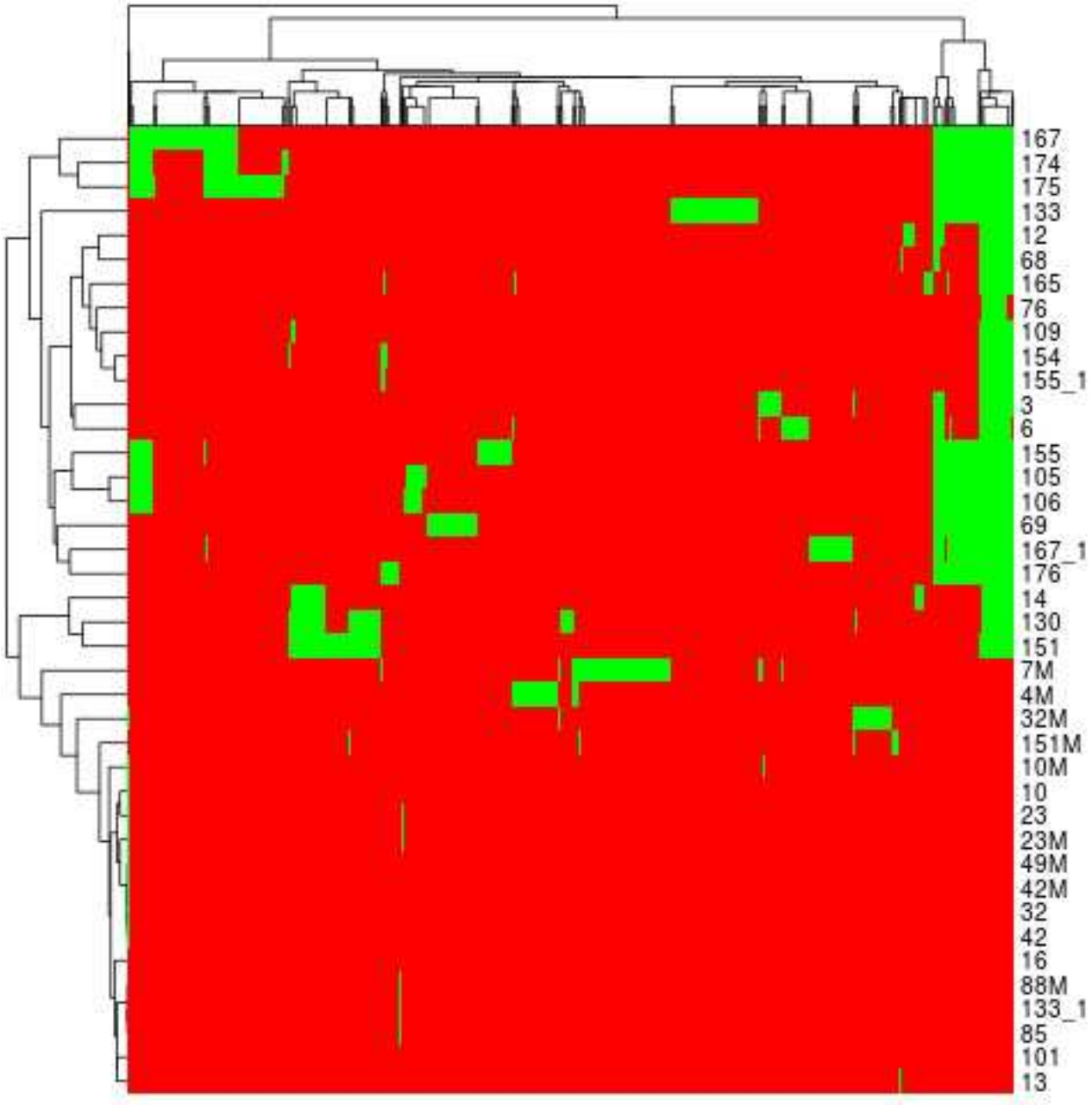

Figure 9: Heatmap derived from the presence/absence matrix of accessory genes within the population.

3.2.1.3. Identification of genomic islands

Several comparative genomic studies of *P. aeruginosa* have shown that most inter-strain diversity is due to the presence of regions of genomic plasticity (RGPs) or genomic islands (GIs) often acquired by horizontal gene transfer [182][183][37].

The distribution of Protein Clusters (PCs) was very skewed towards the two extremes, that is PCs were either ubiquitous or isolate-specific; 87 PCs, belonging to six genomic islands, were ubiquitous in the population (Fig. 10). The analysis done with tblastn on our custom dataset of known GIs detected four PCs (with identity > 80% and low e-value < 4.7 e80) putatively belonging to the island LESGI-1 [49], two PCs (id > 85%, e-value < 1.7 e46) were assigned to LESGI-3 [184], while three PCs (id > 90%, e-value < 5.3 e80) were assigned to

the island PAGI-2 [50]. Twenty-one ubiquity PCs, belonging to the three unidentified genomic islands were searched, using blastp, in the non-redundant NCBI database restricting the search to *P. aeruginosa*. Most PCs found matches with hypothetical proteins, only six PCs found matched with the following annotated proteins: YqaJ-like viral recombinase domain cl09232 (WP_031641785), recombination protein RecT (WP_019682741), Resolvase (EJY58266), serine recombinase (WP_070330427), DNA ligase (NAD(+)) LigA (WP_003114675), N-acetyltransferase (WP_003096122).

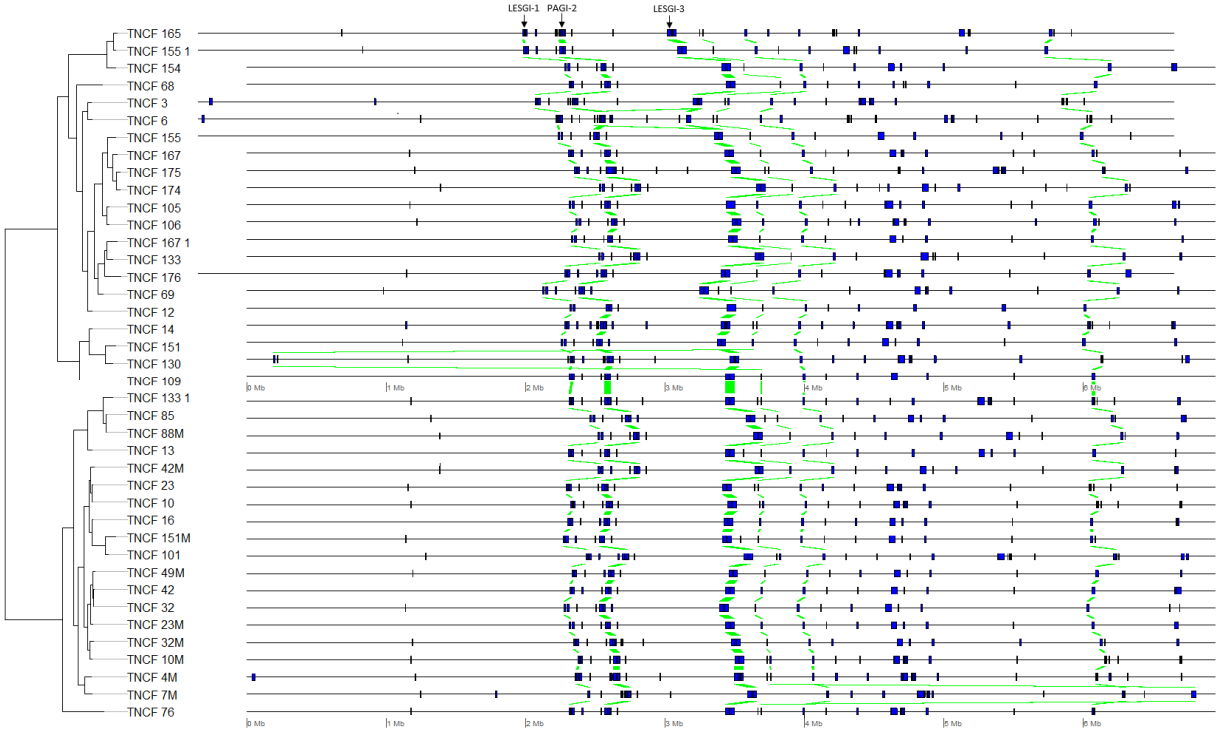

Figure 10: Genomic map showing the position of each genomic island on each genome. Homologous regions are highlighted in green.

3.2.1.4. Variants and SNPs analysis

We then looked at the distribution of variants in the core genome of the population. Data relative to insertions/deletions were not considered as the draft nature of the genomes could bias the output of the program. Each isolate contained a total of 27,249 ± 3,300 single nucleotide variations. In particular, variants per genome ranged from 12,983 to 29,744 in the isolates TNCF_7M and TNCF_165, respectively, with a median number of 28,668 nucleotide variations per genome (as in TNCF_23M and TNCF_32) (Table 3).

Table 3. Analysis of SNPs in the population.

Genome accession number	Isolate name	Year of isolation	Sequence type	Number of contigs	Genome size (Kbp)	N50 (Kbp)	%GC	Total SNPs	High impact variants	Moderate impact variants
MAUO00000000	TNCF_3	2007	390	139	6.636	92	66.28	23926	1	258
MAUP00000000	TNCF_4M	2007	390	161	6.630	78	66.29	18451	0	186
MAUQ00000000	TNCF_6	2007	390	356	6.618	31	66.28	16917	0	243
MAUR00000000	TNCF_7M	2007	390	259	6.623	47	66.28	12983	0	132
MAUS00000000	TNCF_10	2007	390	101	6.643	143	66.28	28588	0	231
MAUT00000000	TNCF_10M	2007	390	107	6.633	111	66.29	27377	0	227
MAZG00000000	TNCF_12	2007	390	102	6.545	177	66.36	27551	0	280
MAZI00000000	TNCF_13	2007	390	75	6.637	195	66.27	28381	0	231
MAZH00000000	TNCF_14	2007	390	89	6.633	158	66.28	28893	1	297
MAKL00000000	TNCF_16	2007	1864	59	6.638	269	66.28	28697	0	230
MAZJ00000000	TNCF_23	2007	390	71	6.635	228	66.28	28430	0	232
MAZK00000000	TNCF_23M	2007	390	64	6.636	228	66.28	28668	0	231
MAKM00000000	TNCF_32	2007	390	67	6.639	229	66.28	28668	0	230
MAZL00000000	TNCF_32M	2007	390	138	6.627	93	66.28	21302	0	194
MAZM00000000	TNCF_42	2008	390	70	6.639	228	66.28	28682	0	230
MAZN00000000	TNCF_42M	2008	390	71	6.640	228	66.28	28691	0	230
MAZO00000000	TNCF_49M	2008	390	76	6.635	177	66.29	28187	0	230
MAZP00000000	TNCF_68	2010	390	82	6.633	162	66.28	28277	0	269
MAZQ00000000	TNCF_69	2010	1863	88	6.639	150	66.28	29398	0	344
MAZR00000000	TNCF_76	2010	390	61	6.634	281	66.28	28793	0	251
MAZS00000000	TNCF_85	2010	1864	101	6.644	124	66.29	28605	0	231
MAZT00000000	TNCF_88M	2010	1864	65	6.636	229	66.28	28678	0	231
MAZU00000000	TNCF_101	2011	1864	142	6.653	92	66.28	28541	0	229
MAZV00000000	TNCF_105	2011	390	92	6.644	191	66.28	29525	0	338
MAZW00000000	TNCF_106	2011	390	77	6.634	205	66.28	29346	0	336
MAZX00000000	TNCF_109	2011	390	69	6.634	205	66.28	28808	0	264
MAZD00000000	TNCF_130	2012	390	157	6.625	76	66.28	24731	1	312
MAZF00000000	TNCF_133	2012	390	82	6.637	154	66.29	29356	2	374
MAZE00000000	TNCF_133_1	2012	1864	87	6.641	269	66.28	28687	0	231
MAKK00000000	TNCF_151	2013	390	53	6.629	378	66.28	29377	1	340
MBMI00000000	TNCF_151M	2013	1864	103	6.636	143	66.28	26177	0	221
MBMJ00000000	TNCF_154	2013	390	86	6.635	177	66.28	27323	0	254
MBMK00000000	TNCF_155	2013	390	62	6.634	339	66.28	29744	0	353
MBML00000000	TNCF_155_1	2013	1923	71	6.635	221	66.28	28689	0	255
MBMM00000000	TNCF_165	2013	1923	119	6.634	135	66.28	26654	0	260
MBMN00000000	TNCF_167	2013	390	73	6.634	191	66.27	29024	2	392
MBMO00000000	TNCF_167_1	2013	390	91	6.628	143	66.28	27629	0	335
MBMP00000000	TNCF_174	2014	390	111	6.645	143	66.29	29317	1	353
MBMQ00000000	TNCF_175	2014	390	118	6.642	124	66.28	29582	1	393
MBMR00000000	TNCF_176	2014	1923	61	6.637	354	66.28	29299	0	304

To investigate polymorphisms that presumably have an impact on the adaptive process of the isolates, we extracted non-synonymous polymorphisms classified as high impact variants (i.e. variants resulting in protein truncation, loss of function or triggering nonsense-mediated decay). The number of high impact variations, based on the complete genome sequence of the isolates (both core and accessory genome), considerably varied in the population, ranging from 6 in the early isolate TNCF_7M to 167 in the late isolate TNCF_175 (Table 4).

Table 4. High impact variations in the population.

gene name	omega (M1a)	omega (M2a)	LogL H0 (M1a)	LogL H1	Likelihood Ratio Test (2*(l1-l0)) with 2 df (>5,991)	under selective pressure	omega (M7)	omega (M8)	LogL H0 (M7)	LogL H1	Likelihood Ratio Test (2*(l1-l0)) with 2 df	under selective pressure	Tajima's D
aruF		0,402	0,402	-1.291,9725	-1.291,9740	-0,0030	no	0,402	0,402	-1.291,9725	-1.291,9728	-0,0006	no
cbrA		1	1,12	-883,3932	-883,3882	0,0101	no	1	1,12	-883,3932	-883,3882	0,0101	no
chpA	0,77	1,417	-10.486,4352	-10.474,7069	23,4566	yes	1	1,417	-10.486,6790	-10.474,7078	23,9424	yes	-1,93
ftsJ		1	1,12	-883,3932	-883,3882	0,0101	no	1	1,12	-883,3932	-883,3882	0,0101	no
gidA	0,501	2,241	-2.696,9706	-2.688,2459	17,4495	yes	0,5	2,241	-2.696,9707	-2.688,2462	17,4490	yes	-1,65
glnE	1	1	-4.164,6365	-4.164,6365	0,0000	no	1	1,318	-4.164,6365	-4.164,5473	0,1785	no	-1,98
gltB	0,618	2,179	-6.159,6129	-6.149,4395	20,3468	yes	0,4	2,986	-6.168,9490	-6.150,0270	37,8441	yes	-1,36
gyrB	1	13,00	-3.380,5391	-3.370,0833	20,9115	yes	1	13,49	-3.380,5392	-3.370,9076	19,2631	yes	-0,06
nagE	1	38,787	-2.484,3199	-2.473,3311	21,9775	yes	1	38,78	-2.484,3188	-2.473,3298	21,9780	yes	-2,26
ParE	1	24	-2.655,0258	-2.645,9685	18,1145	yes	1	24,4	-2.655,0265	-2.645,9685	18,1159	yes	-0,66
PmrB	1	2,16	-2.005,4163	-2.005,1474	0,5378	no	1	2,1611	-2.005,4163	-2.005,1543	0,5240	no	-0,8
pvdL	\	\	\	\	\	\	\	\	\	\	\	\	N/A
15595416 *	0,486	0,486	-2.140,5747	-2.140,5747	0,0000	no	0,485	0,486	-2.140,5749	-2.140,5749	0,0000	no	-2,33
15595440 *	1	1,573	-942,6485	-942,5663	0,1642	no	1	1,573	-942,6488	-942,5659	0,1658	no	-1,87
15595766 *		1	80,768	-655,5545	-654,6594	1,7902	no	1	998	-655,5546	-654,6460	1,8172	no
15596248 *	1	3,5	-1.940,2519	-1.937,2854	5,9331	no	1	3,5	-1.940,2519	-1.937,2854	5,9331	no	-2,03
15596746 *	0,522	2,042	-3.438,3693	-3.427,6205	21,4976	yes	0,5	2,034	-3.438,3685	-3.427,6870	21,3631	yes	-1,61
15597414 *	1	999	-1.542,2655	-1.540,7609	3,0093	no	1	998	-1.542,2655	-1.540,7609	3,0093	no	-1,64
15597654 *	0,2320	2,19	-1.560,9988	-1.544,3529	33,2918	yes	0,3	2,191	-1.561,0650	-1.544,3530	33,4240	yes	-1,4
15599121 *	0,5361	1,7982	-1.683,4464	-1.676,3017	14,2893	yes	1	1,7355	-1.683,8311	-1.676,3156	15,0312	yes	-1,7

We performed a Cluster of Orthologous Groups (COG) analysis wherein we assigned the genes in which high-impact variants were found to their respective COG categories to determine whether the majority of variants fell into few functional categories or were randomly distributed among all of them. The percentage of genes assigned to each COG is shown in Figure 11. Mutations occurred primarily (8%) in genes involved in transcription, followed by the following COG categories: amino acid transport and metabolism, inorganic ion transport and metabolism, signal transduction mechanisms and general functions (7% each). A large proportion of genes (28%) were not assigned to any COG category but were classified as genes with unknown function. The remaining genes were distributed into all the functional categories, with proportions reflecting those found in the analysis of whole genomes.

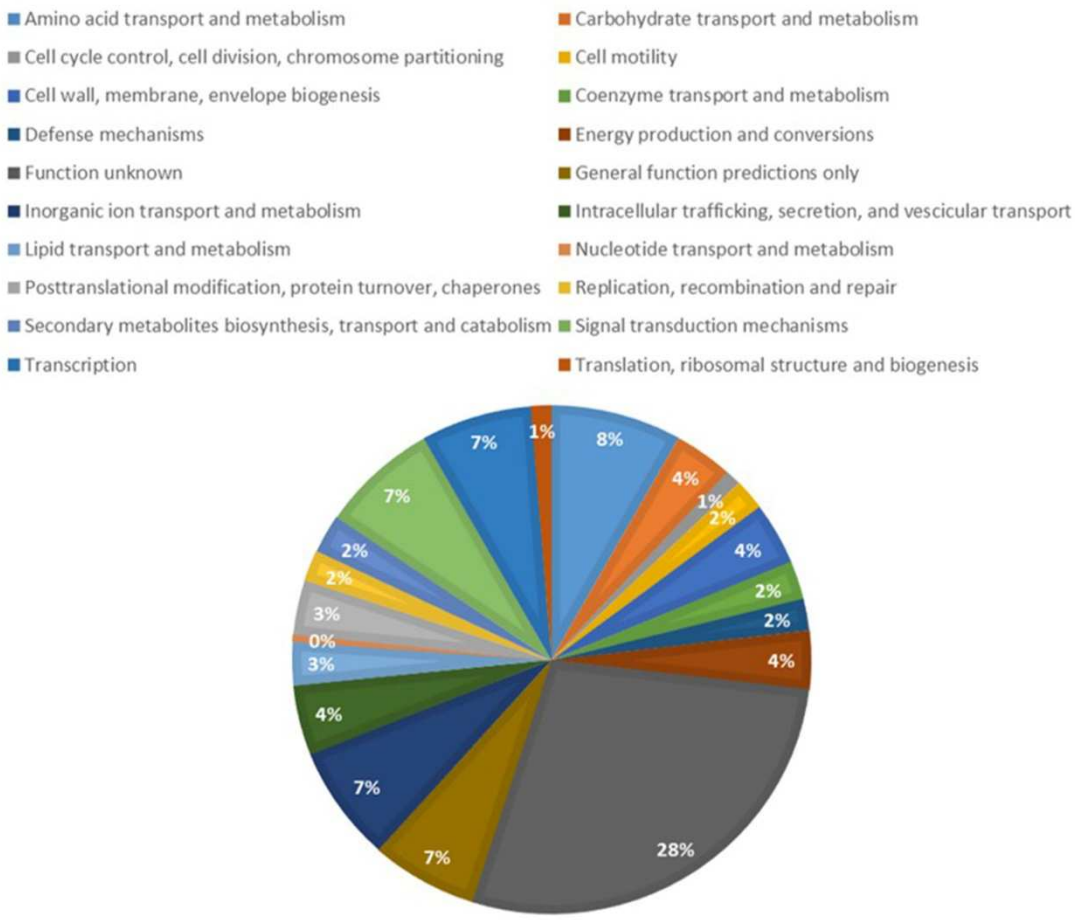

Figure 11. Percentages of genes assigned to each COG.

3.2.1.5. Polymorphisms in the core genome of the population

We then extended the analysis to variants in the core genome with high and moderate impact (non-disruptive variants that might change protein effectiveness). These ranged from 132 (TNCF_7M) to 394 (TNCF_167, TNCF_175) per genome, with a mean of 270 (Table 3). Moreover, an analysis of the distribution of variants in the population (Fig. 12) revealed a cluster of 13 isolates (TNCF_10, TNCF_13, TNCF_16, TNCF_23, TNCF_23M, TNCF_32, TNCF_42, TNCF_42M, TNCF_49M, TNCF_85, TNCF_88M, TNCF_101, TNCF_133_1) with a high similarity in their variants pattern. One isolate, TNCF_7M, stands out in the distance matrix, probably due to the lowest number of SNPs present in the genome.

Eight genes belonging to the core genome carried high-impact variants (Table 4). Interestingly, four of them have unknown function, while the known ones were: *nail, lspA, aaltP, pcoA*.

Within the whole population, a total of 675 different genes carried mutations with moderate impact within the core genome (Table 4). The distribution of these variants was consistent with population structure (Fig. 12). Focusing on the moderate impact polymorphisms in the core genome of the population, we found 20 genes with three or more of such variations in the population (Table 5), which might be indicative of loci under selective pressure.

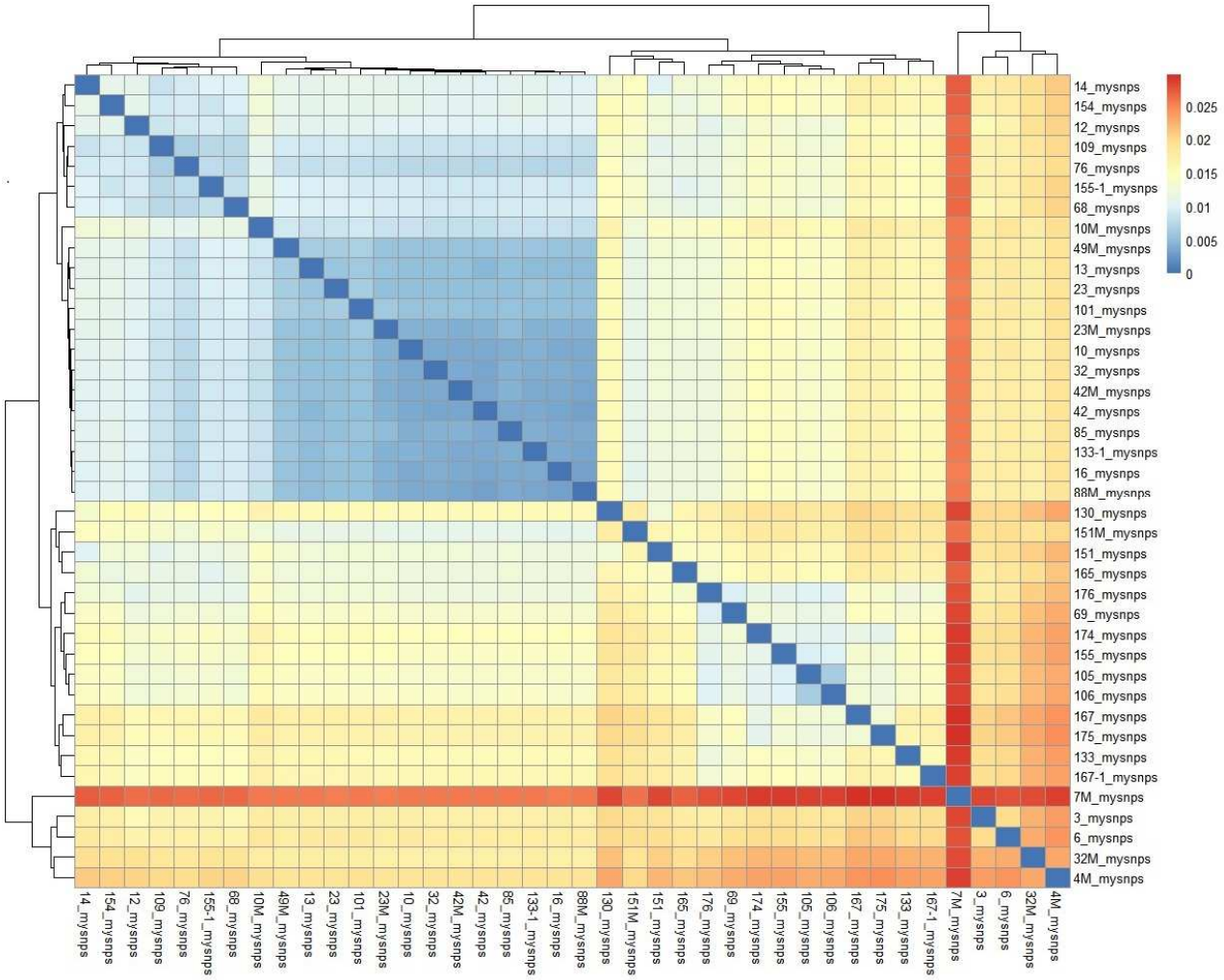

Figure 12. Analysis of the distribution of variants in the population.

Table 5. Core genes with the highest number of SNPs in the population.

Gene name	Product name	Variations (n.)
gyrB	**DNA gyrase subunit B**	**5**
pvdL	non-ribosomal peptide synthase, pyoverdine biosynthesis	5
15595766 *	hypothetical protein	4
aruF	subunit I of arginine N2-succinyltransferase = ornithine N2-succinyltransferase	3
ftsJ	cell division protein FtsJ	3
chpA	**component of chemotactic signal transduction system**	**3**
gidA	**glucose-inhibited division protein A**	**3**
glnE	glutamate-ammonia-ligase adenylyltransferase	3
gltB	**glutamate synthase subunit alpha**	**3**
nagE	**N-Acetyl-D-Glucosamine phosphotransferase system transporter**	**3**
parE	**DNA topoisomerase IV subunit B**	**3**
pmrB	two-component regulator system signal sensor kinase PmrB	3
cbrA	two-component sensor CbrA	3
15595416 *	probable aldehyde dehydrogenase	3
15595440 *	probable transcriptional regulator	3
15596248 *	probable transporter	3
15596746 *	**probable cation-transporting P-type ATPase**	**3**
15597654 *	**hypothetical protein**	**3**
15599121 *	**probable major facilitator superfamily (MFS) transporter**	**3**
15597414 *	hypothetical protein	3

The 20 genes listed above belong to the core genome and have at least three different polymorphisms with a moderate impact on the encoded protein according to Snippy analysis [185]. Genes under non-neutral pressure are in bold. * Corresponding gene accession number in the reference strain PAO1, when the gene name does not exist.

3.2.2. Phenotypic and genotypic characterization

Cystic fibrosis *P. aeruginosa* strains undergo phenotypic and genotypic changes during the switch from acute to chronic lung infection but the relative roles of these changes in pathogenesis and persistence are still not entirely understood [186]. These adaptations likely occur in response to the host airway environment, immune system components, and antibiotics [23].

We have therefore analysed our collection for several phenotypic traits. In the phenotypic analyses, an extra strain was included, VrPa97: this isolate was an acute-infection strain coming from a wound swab and it was isolated from a patient at Verona hospital; the strain was genotypically closely related to our patients' isolates, since it belonged to the Sequence Type ST390. This isolate predictably showed all the characteristics of acute-infection strain.

3.2.2.1. Antibiotic resistance profiles

Susceptibility to 12 antibiotics was tested for all isolates of the population (Table 6). All isolates were susceptible to Colistin, and nearly all the early isolates were susceptible to almost all the antibiotics tested. On the other hand, multidrug-resistant phenotypes dramatically increased over time in the persistent population. Among early strains isolated in 2007 and 2008, TNCF_4M was found to be susceptible to all antibiotics, while TNCF_7M, TNCF_10, TNCF_10M and TNCF_42M had an intermediate resistance profile only to Cefepime. Four early strains were found to have an MDR phenotype: TNCF_3, TNCF_6, TNCF_12, TNCF_14 were resistant to all the antibiotics tested with the exception of Colistin. Among 23 strains isolated between 2010 and 2014, only two of them, TNCF_88M and TNCF_151M, both belonging to ST1864, did not show an MDR phenotype: TNCF_88M, isolated in December 2010, was susceptible to eight antibiotics, with an intermediate profile to Cefepime and resistant to Ciprofloxacin, Levofloxacin, Fosfomycin and Piperacillin/Tazobactam, whereas TNCF_151M, isolated in May 2013, was found to be susceptible to 10 antibiotics, with an intermediate profile for Cefepime, and was resistant only to Amikacin.

Table 6. Antibiotic susceptibility profiles of the *P. aeruginosa* population. Resistance is highlighted in red, susceptibility in green, and intermediate profile in yellow. Resistance and susceptibility were determined according to the EUCAST clinical breakpoint tables. Resistant, intermediate and susceptible isolates are highlighted in red, yellow, and green, respectively. Acronyms are: AMI, Amikacin; GEN, Gentamicin; IPM, Imipenem; MEM, Meropenem; DOR, Doripenem; CAZ, Cefepime; FEP, Ceftazidime; CIP, Ciprofloxacin; LVX, Levofloxacin; FOS, Fosfomycin; CST, Colistin; TZP, Piperacillin/Tazobactam.

Isolate	AMI	GEN	IPM	MEM	DOR	CAZ	FEP	CIP	LVX	FOS	CST	TZP
TNCF_3												
TNCF_4M												
TNCF_6												
TNCF_7M												
TNCF_10												
TNCF_10M												
TNCF_12												
TNCF_13												
TNCF_14												
TNCF_16												
TNCF_23												
TNCF_23M												
TNCF_32												
TNCF_32M												
TNCF_42												
TNCF_42M												
TNCF_49M												
TNCF_68												
TNCF_69												
TNCF_76												
TNCF_85												
TNCF_88M												
TNCF_101												
TNCF_105												
TNCF_106												
TNCF_109												
TNCF_130												
TNCF_133												
TNCF_133_1												
TNCF_151												
TNCF_151M												
TNCF_154												
TNCF_155												
TNCF_155_1												
TNCF_165												
TNCF_167												
TNCF_167_1												
TNCF_174												
TNCF_175												
TNCF_176												
VrPa97												

Genomic analyses of the population showed a correlation between the evolution of antibiotic resistance profiles, MLST sequence types, and phylogenetic relationships (Fig. 13). We further investigated the MDR isolates in comparison to the susceptible ones, looking specifically at *P. aeruginosa* genes involved in antibiotic resistance and susceptibility. Non-synonymous mutations were found in *gyrB*, *mexG*, *parC*, *parE* and *pmrB*, while a deletion, ΔC_{437}, was found in *oprD* (Table 7).

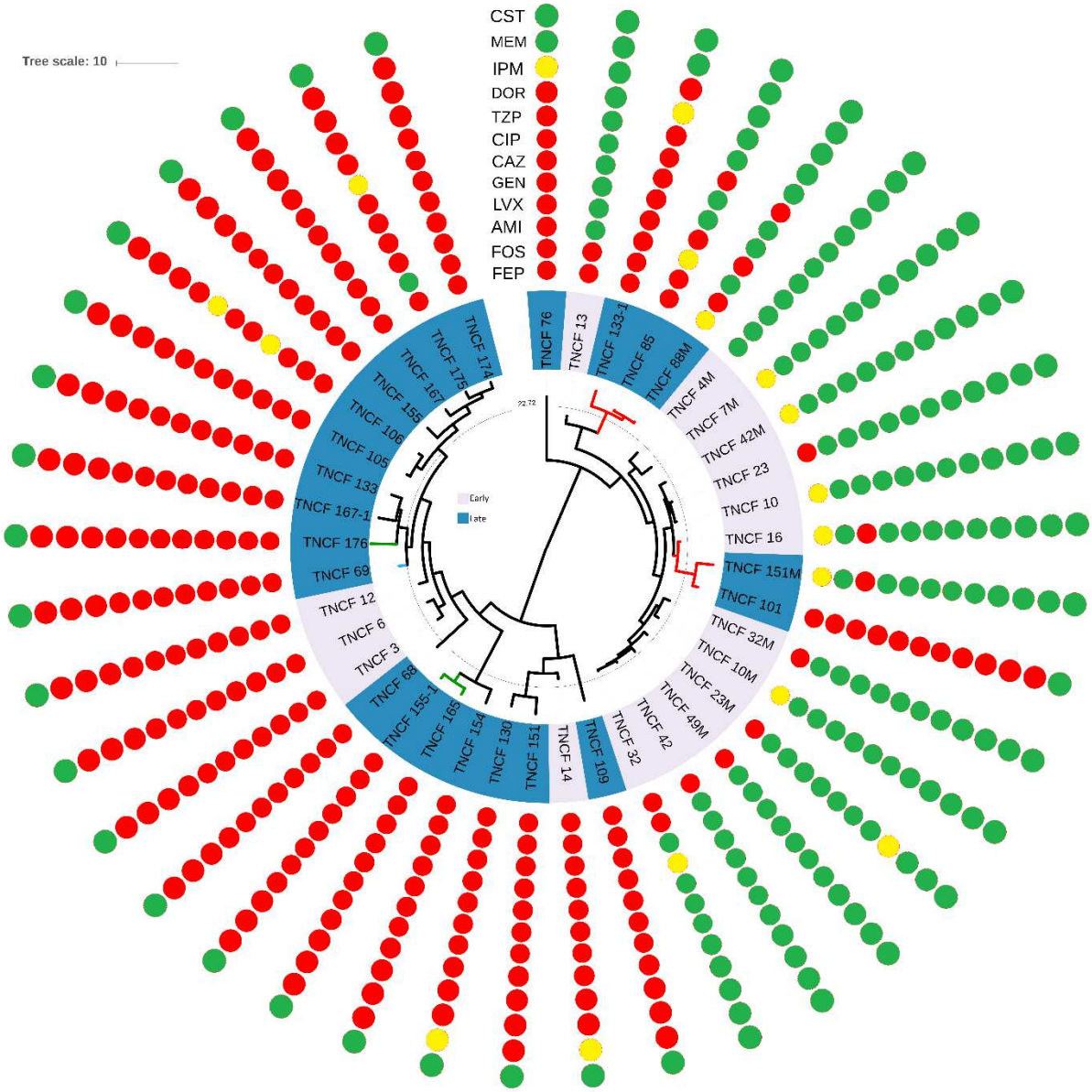

Figure 13: Comparison of population structure with antibiotic susceptibility profiles. The tree topology is the same as shown in Fig. 6b. The inner part of the figure represents the phylogenetic tree with demarcation line between early and late strains. Early strains are highlighted in grey, whereas late isolates are highlighted in blue. Black branches of the tree, ST390; red, ST1864; green, ST1923; blue, ST1863. Antibiograms are reported as follows: red dots, resistance to the antibiotic considered; green dots, susceptibility; yellow dots, intermediate susceptibility phenotype.

Table 7. Variations in genes involved in antibiotic resistance.

Gene	Nt mutation	Variation	Isolates
gyrB	G_{1404}-T	E_{468}-D	TNCF_3, TNCF_6, TNCF_12, TNCF_13, TNCF_14, TNCF_68, TNCF_69, TNCF_76, TNCF_85, TNCF_88M, TNCF_101, TNCF_105, TNCF_106, TNCF_109, TNCF_130, TNCF_133_1, TNCF_151, TNCF_155, TNCF_165, TNCF_167, TNCF_167_1, TNCF_174, TNCF_175, TNCF_176
	T_{2245}-C	S_{749}-P	TNCF_10, TNCF_10M, TNCF_23, TNCF_23M, TNCF_32, TNCF_32M, TNCF_42, TNCF_42M, TNCF_49M
mexG	C_{151}-T	P_{51}-S	TNCF_3, TNCF_12, TNCF_68, TNCF_76, TNCF_85, TNCF_88M, TNCF_105, TNCF_106, TNCF_109, TNCF_130, TNCF_133, TNCF_151, TNCF_155, TNCF_165, TNCF_167, TNCF_167_1, TNCF_174, TNCF_175, TNCF_176
oprD	ΔC_{437}	frameshift	TNCF_3, TNCF_6, TNCF_12, TNCF_68, TNCF_69, TNCF_101, TNCF_105, TNCF_106, TNCF_133, TNCF_155, TNCF_165, TNCF_167, TNCF_167_1, TNCF_174, TNCF_175, TNCF_176
parC	A_{509}-G	N_{170}-S	TNCF_3, TNCF_12, TNCF_14, TNCF_68, TNCF_76, TNCF_101, TNCF_105, TNCF_106, TNCF_109, TNCF_130, TNCF_151, TNCF_155, TNCF_165, TNCF_167, TNCF_167_1, TNCF_174, TNCF_175, TNCF_176
parE	T_{88}-C	R_{30}-C	TNCF_69, TNCF_105, TNCF_106, TNCF_133, TNCF_155, TNCF_155_1, TNCF_165, TNCF_167, TNCF_167_1, TNCF_174, TNCF_175, TNCF_176
	G_{176}-A	H_{59}-R	TNCF_69, TNCF_105, TNCF_106, TNCF_133, TNCF_155, TNCF_155_1, TNCF_165, TNCF_167, TNCF_167_1, TNCF_174, TNCF_175, TNCF_176

The variations listed above are present only in the MDR isolates and are, therefore, putatively involved in the acquisition of the MDR phenotype. Nt, nucleotidic.

3.2.2.2. Functional phenotypic assays and their associated genes.

To assess how *Pseudomonas aeruginosa* virulence traits eventually changed over time in the course of chronic infection, a number of phenotypic assays were performed, including swarming and twitching motility, mucoidy, protease secretion, and biofilm production.

Twelve isolates (30%) produced alginate and had a mucoid phenotype; eight isolates (20%) showed swarming motility and no one twitching motility; protease secretion was observed in 4 isolates (10%); 17 isolates (42.5%) produced a detectable amount of biofilm; 23 isolates (57.5%) were hypermutable (Table 8). These analyses served as a basis for the selection of few strains for further characterization: TNCF_23, one of the earliest isolates, showed all typical acute-infection related phenotypic features (except for twitching motility) and was susceptible to all the antibiotics tested with the exception of Cefepime. The late isolate TNCF_175 showed instead all typical characteristics of a chronic-infection strain, and it was resistant to most antibiotics.

Sequences of the virulent genes associated with the screened phenotypes were examined to tentatively associate the variations observed in the phenotypes with mutations in the genomes. Sequence analysis revealed both synonymous and nonsynonymous single nucleotide polymorphisms (data not shown), non-synonymous mutations leading to the insertion of stop codons, frameshift mutations and deletions of single genes or entire operons. Main genotypic differences between strains TNCF_23 and TNCF_175 are presented in Table 9.

Table 8. Phenotypic assays. Qualitative assessment of mucoid phenotype is reported, as well as quantitative measurements of swarming, twitching, protease production and biofilm formation assays. Positive phenotypes are in green.

Isolate	Date of isolation	ST	Mucoidy	Swarming (cm)		Twitching	Protease secretion (cm)		Biofilm production (OD 695/600)		Hypermutability
				Mean	SD		Mean	SD	Mean	SD	
TNCF_3	13/04/2007	390	NO	0	0	0	0	0	0.2538	0.2767	YES
TNCF_4M		390	YES	2.5333	0.4933	0	0	0	0.0266	0.0392	NO
TNCF_6	29/05/2007	390	NO	0	0	0	0	0	0.1719	0.1415	YES
TNCF_7M		390	YES	0	0	0	0	0	0.0185	0.0163	NO
TNCF_10	26/07/2007	390	NO	0	0	0	8.3333	0.5774	0.0059	0.0098	NO
TNCF_10M		390	YES	0	0	0	0	0	0.0132	0.0187	NO
TNCF_12	04/09/2007	390	NO	0	0	0	0	0	0.0563	0.0381	YES
TNCF_13	05/09/2007	390	YES	1.1667	0.3786	0	0	0	0.0049	0.0075	NO
TNCF_14		390	NO	0	0	0	0	0	1.1492	1.4577	YES
TNCF_16	24/09/2007	1864	YES	0.9900	0.4278	0	0	0	0.0232	0.0246	NO
TNCF_23	17/10/2007	390	NO	0	0	0	7.3333	0.5774	0.0056	0.0092	NO
TNCF_23M		390	YES	0	0	0	0	0	0.0046	0.0074	NO
TNCF_32	23/11/2007	390	NO	0	0	0	0	0	0.0294	0.0641	NO
TNCF_32M		380	YES	0	0	0	0	0	0.0040	0.0072	NO
TNCF_42	31/01/2008	390	NO	3.3333	0.2887	0	5.3333	0.5774	0.0032	0.0051	NO
TNCF_42M		390	YES	0.8667	0.1155	0	3.0000	0	0.0035	0.0042	NO
TNCF_49M	05/09/2008	390	YES	0	0	0	0	0	0.0136	0.0236	NO
TNCF_68	02/08/2010	390	NO	3.200	0.2000	0	0	0	0.1404	0.0860	YES
TNCF_69	22/03/2010	1863	NO	0	0	0	0	0	0.3606	0.2108	YES
TNCF_76	09/06/2010	390	NO	0	0	0	0	0	53.8531	16.8565	YES
TNCF_85	08/11/2010	1864	YES	2.0000	0.2000	0	0	0	0.0649	0.0783	NO
TNCF_88M	14/12/2010	1864	YES	0.9167	0.3488	0	0	0	0.0177	0.0188	NO
TNCF_101	30/06/2011	1864	NO	0	0	0	0	0	0.1535	0.0999	YES
TNCF_105	25/08/2011	390	NO	0	0	0	0	0	2.3635	2.2542	YES
TNCF_106	15/09/2011	390	NO	0	0	0	0	0	0.7177	0.5608	YES
TNCF_109	30/09/2011	390	NO	0	0	0	0	0	1.2620	1.6300	YES
TNCF_130	19/07/2012	390	NO	0	0	0	0	0	1.4477	1.3660	YES
TNCF_133	14/09/2012	390	NO	0	0	0	0	0	0.0336	0.0598	YES
TNCF_133_1		1864	NO	0	0	0	0	0	0.0086	0.0119	NO
TNCF_151	05/04/2013	390	NO	0	0	0	0	0	4.4742	2.2776	YES
TNCF_151M		1864	YES	0	0	0	0	0	0.0176	0.0087	NO
TNCF_154	29/04/2013	390	NO	0	0	0	0	0	0.1406	0.1426	YES
TNCF_155	06/05/2013	390	NO	0	0	0	0	0	0.0046	0.0124	YES
TNCF_155_1		1923	NO	0	0	0	0	0	0.9051	1.1274	YES
TNCF_165	23/09/2013	1923	NO	0	0	0	0	0	0.0113	0.0257	YES
TNCF_167	03/10/2013	390	NO	0	0	0	0	0	0.1702	0.2495	YES
TNCF_167_1		390	NO	0	0	0	0	0	19.7247	19.1355	YES
TNCF_174	24/04/2014	390	NO	0	0	0	0	0	0.0892	0.1629	YES
TNCF_175	23/06/2014	390	NO	0	0	0	0	0	0.2394	0.3112	YES
TNCF_176	11/08/2014	1923	NO	0	0	0	0	0	0	0	YES

Table 9. Genotypic differences between TNCF_23 and TNCF_175 and related phenotypic effects.

GENE	TNCF_23	TNCF_175	MUTATION EFFECT
mucA	Deletion in C34	Wild-type	Mucoid phenotype
algQ	Wild-type	ΔG40	Dysregulation of Pyoverdine genes; changes in quorum sensing
oprD	Wild-type	ΔC436	Acquisition of resistance to carbapenems
pscG	Wild-type	InsG170	Effector protein of Type 3 Secretion System
Piv	Wild-type	InsC200	Changes in protease IV activity
tssK3	Wild-type	C958T →Q320STOP	Baseplate component of Type 6 Secretion System
fliR		C382T	Motility
flhA		C2116T	Motility
pvdL		T7837C	Iron uptake
prpL	Wild type	insC205	Secretion system and toxins
pscG	Wild-type	insG160	Secretion system and toxins

3.2.2.3. Analysis of phenotype correlation

Correlation among the different phenotypes and relationship between phenotypes and time of isolation of the strains were examined. The analyses were performed calculating the Spearman's correlation coefficient (rho). To visualize the variation of the phenotype as a function of time, phenotypic data were plotted with the isolation date of the samples. In figures 14a-e, each dot represents a *P. aeruginosa* isolate, and the colour of the dot corresponds to its ST. The blue trend line represents the smoothed conditional mean of the phenotypic values, while the shaded area highlights the confidence interval around the smoothed line.

The Spearman's correlation test indicates that the mucoid phenotype (Fig. 14a) has a significant inverse correlation (rho = -0.407, p = 0.009); mucoid isolates were indeed concentrated mainly in the first half of the plot, except for TNCF_151M.

Although swarming motility (Fig. 14b) was observed mainly in early isolates, there was no significant correlation between swarming motility and time of sampling (rho = -0.272, p = 0.090).

Only a few of the earliest strains showed secreted proteolytic activity (Fig. 14c). However, the regression line didn't show a marked trend. In fact, there wasn't any significant correlation between the two parameters studied (rho = -0.251, p = 0.118).

An increasing biofilm formation trait occurred from 2011 to the first half of 2013, but after that, biofilm formation decreased. Spearman's coefficient indicated no significant correlation (rho = 0.202, p = 0.211) between biofilm formation and time of sampling (Fig. 14d).

Hypermutable phenotype showed a significant correlation (rho = 0.500, p = 0.001) with the time of isolation (Fig. 14e); this trait was present mainly in late isolates.

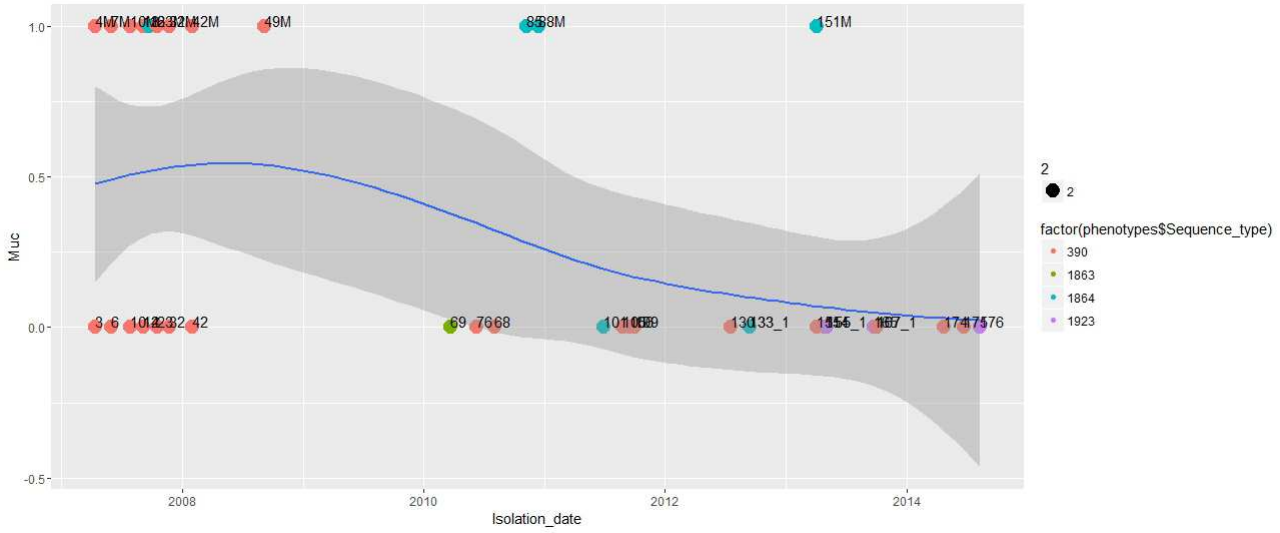

Figure 14a. Evolution of mucoid phenotype as a function of time of isolation. The plot was drawn using the R-package ggplot2. The function geom_smooth() was used with all default parameters. Blue line, regression line fitting the data; grey shaded area, 95% confidence interval. Orange dots, ST390 isolates; green, ST1863; blue, ST1864; purple, ST1923.

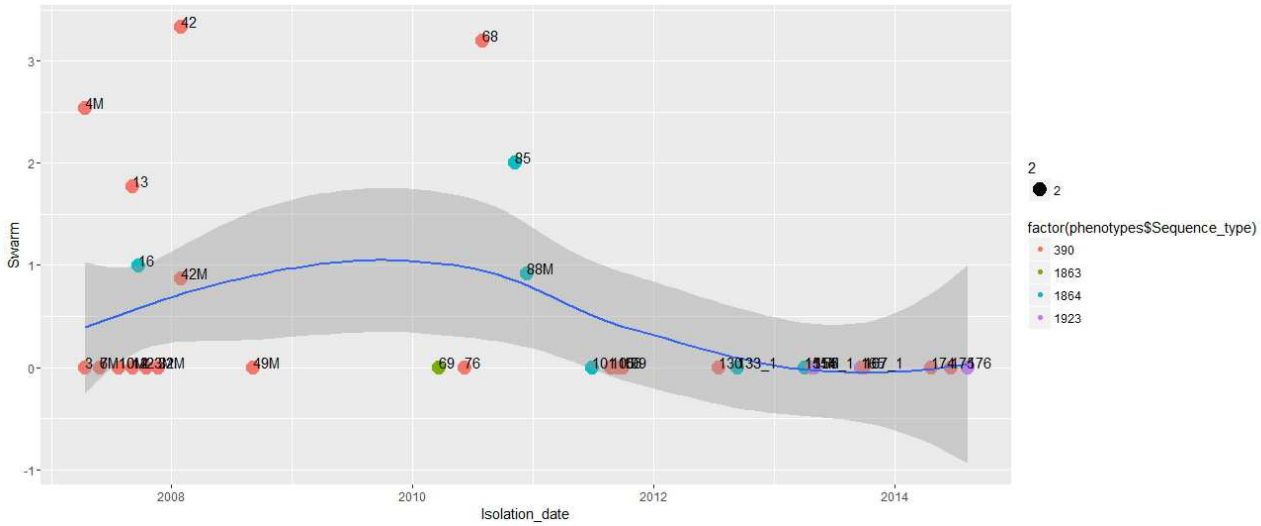

Figure 14b. Evolution of swarming phenotype as a function of time of isolation.

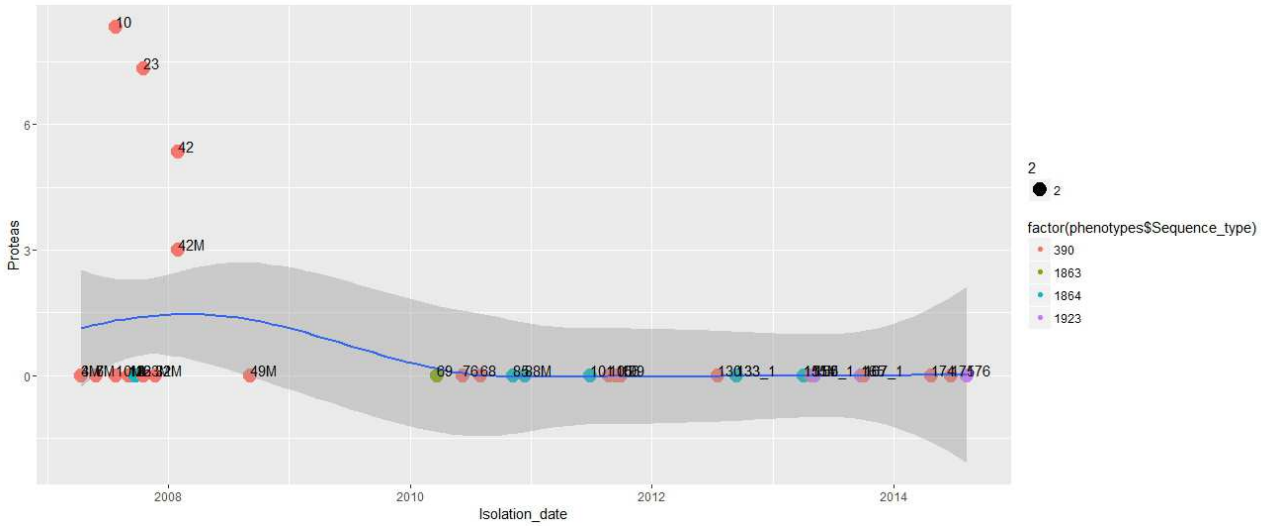

Figure 14c. Evolution of protease secretion phenotype as a function of time of isolation.

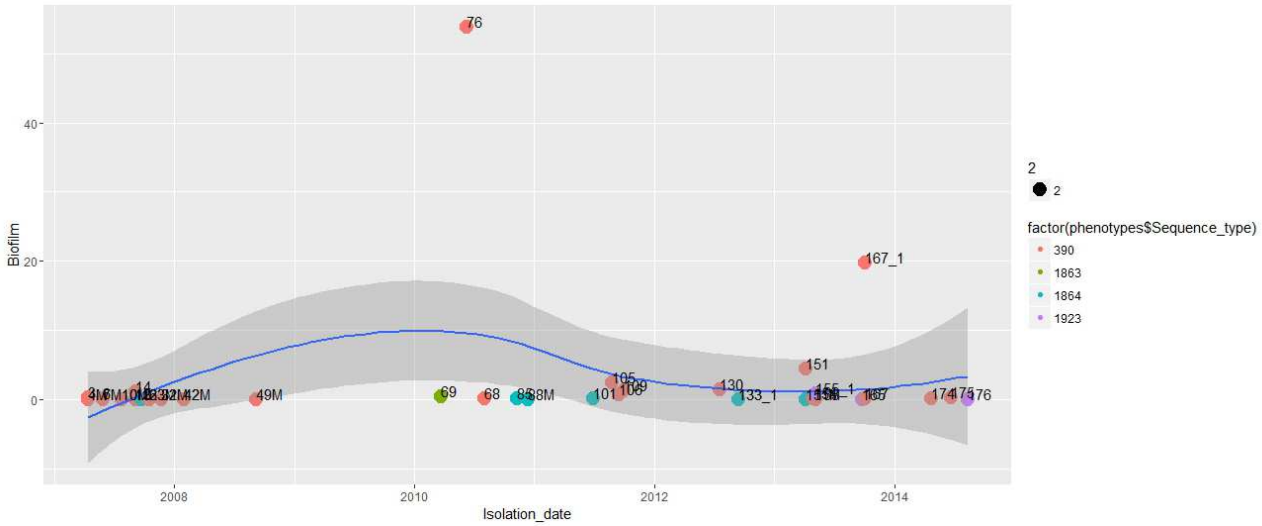

Figure 14d: Evolution of biofilm formation phenotype as a function of time of isolation.

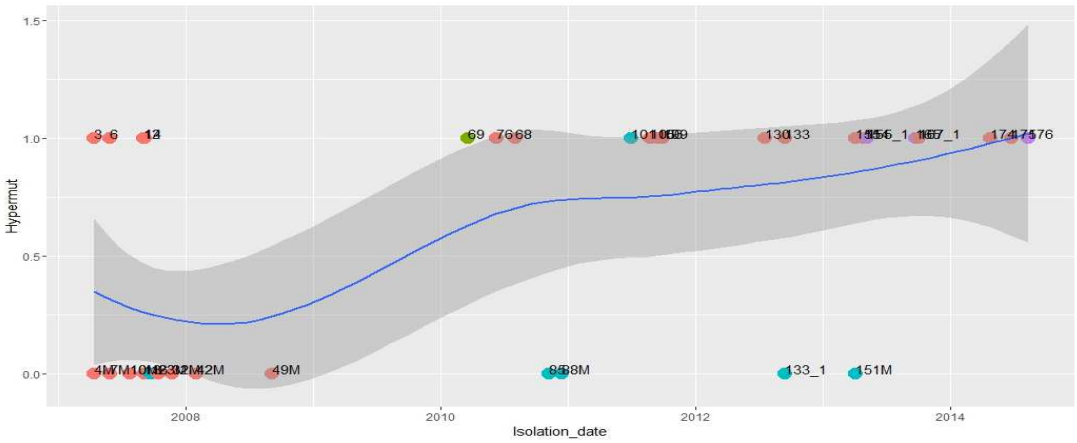

Figure 14e: Evolution of hypermutability phenotype as a function of time of isolation.

To compare early against late isolates, a Wilcox analysis was performed on quantitative phenotypes, namely protease production, swarming motility and biofilm formation. Significative results were obtained for biofilm formation and protease secretion: later strains produced significantly more biofilm than the early isolates, and only four samples out of 40 (all early) showed proteolytic activity. Eight isolates out of 40 presented swarming motility, among which three late strains and five early isolates; nevertheless, the test performed on swarming motility did not reveal a significant trend (Figs. 15a-c).

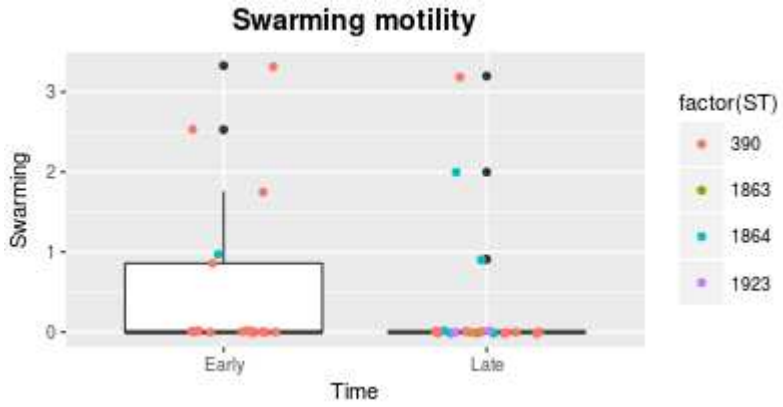

Figure 15a. Wilcox test on swarming motility data.

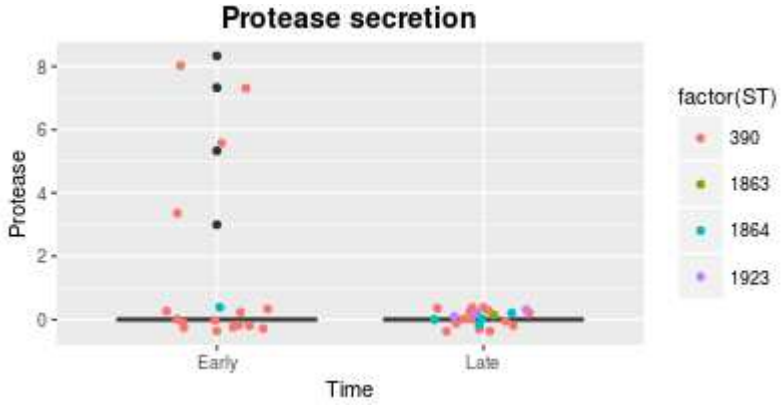

Figure 15b. Wilcox test on protease secretion data.

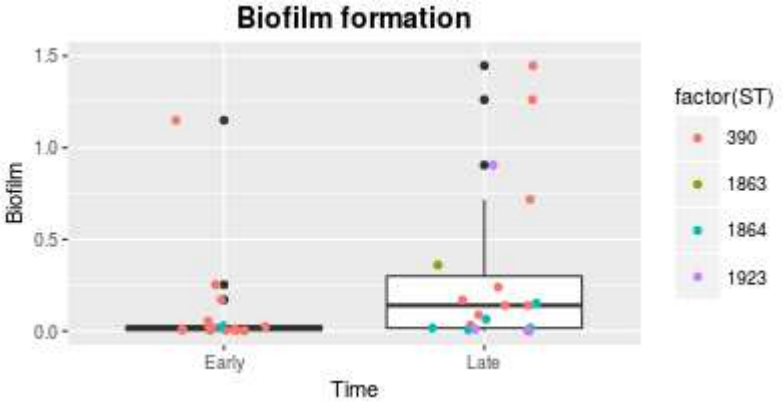

Figure 15c. Wilcox test on biofilm formation data.

3.2.2.4. Correlation of patient data with *P. aeruginosa* phenotypes

The exacerbation of lung conditions seems to correlate with the time of predominance of MDR, hypermutable, biofilm-forming isolates (Fig. 16, Tables 6 and 8). From January 2010 onwards, the patient started enduring a progressive and inexorable decline in lung

function. In the latest stages of infection, the selected antibiotic therapy consisted of a combination of glycopeptides, aminoglycosides, and carbapenems. Most of the isolates isolated between 2010 and 2014 show resistance to aminoglycosides and carbapenems.

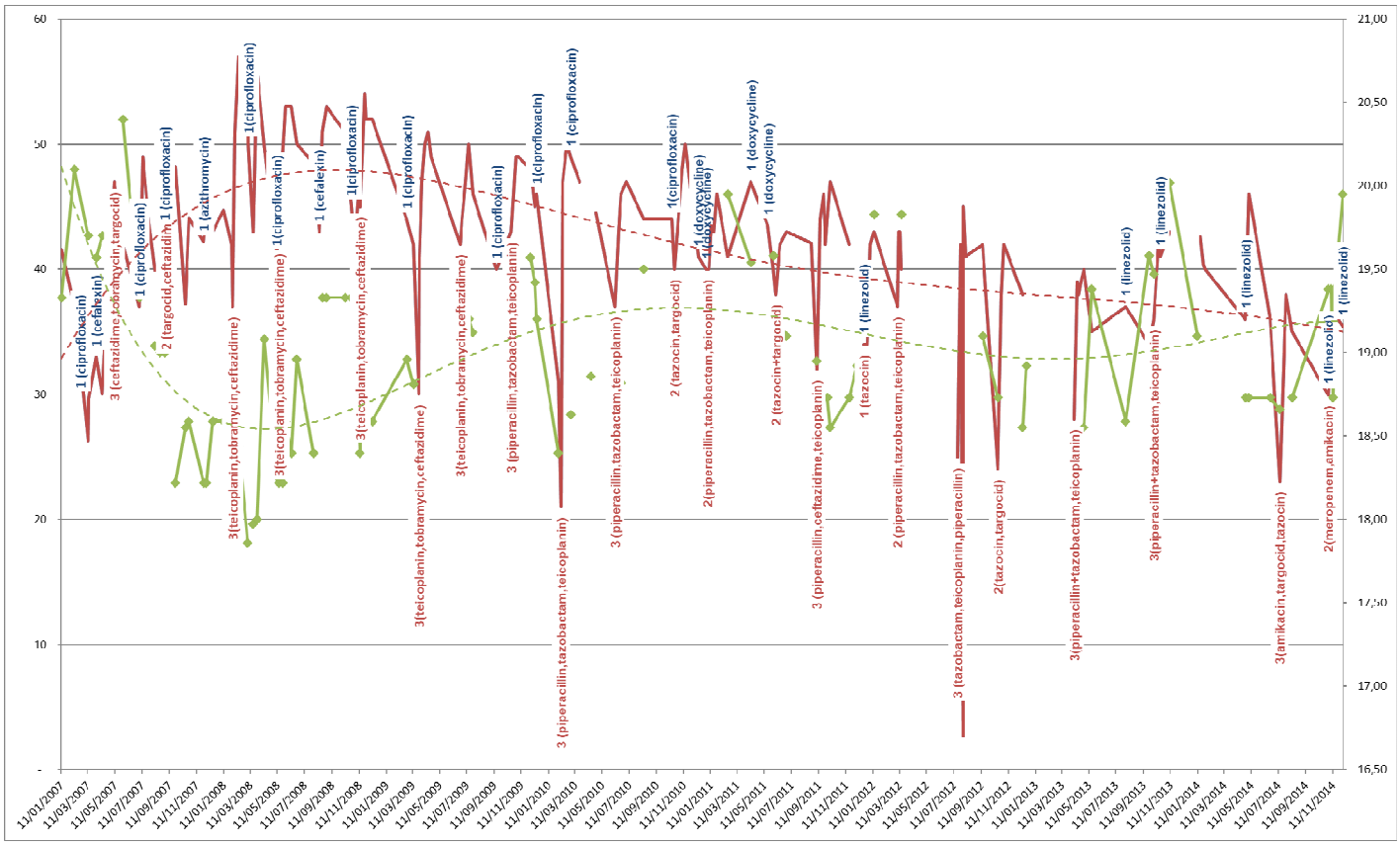

Figure 16: Time course of FEV1 (Forced Expiratory Volume in the 1st second), BMI (Body Mass Index) and antibiotic therapy. Intravenously administered antibiotics are shown in orange while orally administered drugs are indicated in blue. Trendlines of FEV1 (red) and BMI (green) time courses are shown.

4. FUNCTIONAL STUDIES ON SPECIFIC STRAINS

To get further insights into changes that have occurred in our population over the years, two strains were chosen for further characterization:

- one early CF isolate (TNCF_23 isolated in 2007) with phenotypic traits typically observed at the initial stage of adaptation, including susceptibility to most antibiotics;
- one late CF isolate (TNCF_175 isolated in 2014), clonal to TNCF_23, with traits typically observed in CF-adapted strains, including a multidrug-resistant phenotype.

A third strain was included in the analyses: an acute isolate (VrPa97) isolated from a non-CF patient, but belonging to the same Sequence Type as the two CF isolates (ST390).
The aim was to identify additional phenotypic and functional variations within isolates with a very homogeneous genomic background but remarkably different phenotype, to possibly find new pathoadaptive mutations occurring during the course of chronic infection.

4.1. Materials and methods

4.1.1. Cell cultures and invasion assay

A549 (human type II pneumocytes) cell line was purchased from American Type Culture Collection CCL-185 and cultured in DMEM (Gibco, Carlsbas, CA, USA), 10% FBS (fetal bovine serum) (Gibco), 2 mm l-glutamine (Gibco), 100 U/ml penicillin (Gibco), 100 mg/ml streptomycin (Gibco). Bacterial invasion assay was performed by using Polymixin B protection assay with minor modifications [187]. *Pseudomonas aeruginosa* strains were grown in TSB until mid-exponential phase (OD_{600} of 0.5–0.6). Cells were harvested at 4°C, washed twice with PBS and diluted in the tissue culture serum-free medium. The cell suspension was used to infect cell monolayers (approximately 80% confluence) in 24-well tissue culture plates at a multiplicity of infection (MOI) of 100:1 (2.5x107 bacteria per 2.5x105 cultured cells). The infected monolayers were centrifugated (800 g per 5 min) and incubated at 37°C in 5% CO2 for 2h to allow bacterial entry. The monolayers were then washed three times with PBS, and tissue culture medium containing 100 μg/ml Polymixin B (Sigma-Aldrich) was added. After 2 h of incubation, the cell monolayers were washed and lysed with H_2Odd. Intracellular bacteria were quantified by plating serial dilutions of the lysates and the supernatants on TSB agar plates. All quantitative invasion assays were performed in triplicate.

4.1.2. IL-8 secretion

IL-8 was determined in supernatants collected from the cell cultures described above using an ELISA kit (Merck Millipore, Billerica, MA, USA). According to the manufacturer, the minimum detectable concentration of IL-8 is 4.4 pg/mL.

4.1.3. Deletion of *tssK3* in *P.aeruginosa* and complementation

As shown in Table 9, *tssK3*, which encodes a structural protein of T6SS, is one of the genetic differences between TNCF_175 and TNCF_23. Specifically, TNCF_175 has a mutation in *tssK3* that gives rise a premature stop codon (C958T →Q320STOP). By impairing

the function of the *tssK3* gene in PAO1 and PA14, the aim was to explore and explain phenotypic differences that have been observed between the two isolates.

4.1.3.1. Creation of a mutator fragment

Briefly, to create a clean *tssK3* deletion on the chromosome of *P. aeruginosa*, a fragment of approximately 500bp on either side of the gene of interest was amplified. The 3' primer of the upstream fragment (primer no.2) and the 5' primer of the downstream fragment (primer no.3) contained a few bases of the gene, including the start and stop codons.
The two fragments were joined by overlapping PCR to create a mutator fragment, which was cloned into pKNG101 [188], a *Pseudomonas* suicide vector. Subsequently, pKNG101 was conjugated into PAO1 and PA14.
Primer 1 (OAL4076): located 706 bp upstream *tssK3*. A BamHI restriction site was added, which is compatible with pKNG101, plus three random base-pairs, for a total of 30 bp.
Primer 2 (OAL4077): located at the 5' end of *tssK3*, it contains the start codon of the gene + 18 *tssK3* bp + 9 bp of the 3' end of the gene that will match with primer 3, for a total of 29 bp.
Primer 3 (OAL4078): located at the 3' end of *tssK3*, it contains 18 bp of the gene of interest and includes stop codon + five bp downstream *tssK3* + 9 bp of primer 2, for a total of 32 bp.
Primer 4 (OAL4079): located 620 bp downstream *tssK3*. A SpeI restriction site was added, which is compatible with pKNG101, plus three random bp, for a total of 29 bp
Primer 5 (OAL4080): located 96 bp upstream of primer 1; it is 20 bp long, and it is used to check if mutator fragment is integrated into the chromosome. It is 20 bp long.
Primer 6: 108 bp downstream primer 4; it is 20 bp long, and it is used to check if mutator fragment is integrated into the chromosome. In is 20 bp long.
All primers are described in Table 10.

Table 10. Primers used in this study.

Primer	Sequence	Purpose	Source
OAL4076	3'-AAAGGATCCAGGTGTCCGATACCGCTCATC-5'	Primer 1 for the creation of *tssK3* mutator fragment and screening	This study
OAL4077	3'-CTGCCTGACGGCAGCGACAACACCTAGAC-5'	Primer 2 for the creation of *tssK3* mutator fragment	This study
OAL4078	3'-GTCGCTGCCGTCAGGCAGAACACTCATACGAC-5'	Primer 3 for the creation of *tssK3* mutator fragment	This study
OAL4079	3'-TATACTAGTGAACCTGTCCTTGGCGATCC-5'	Primer 4 for the creation of *tssK3* mutator fragment and screening	This study
OAL4080	3'-AACCAGCATGAACAGGGTCG-5'	Primer 5 for insertion screening	This study
OAL4081	3'-CTTGTGCTGCGTACTCTCGG-5'	Primer 6 for insertion screening	This study
OAL4069	3'-ATGGAATTCACGTCGAAGGGGAGTCGTAT-5'	*TssK3* complementation	This study
OAL4070	3'-	*TssK3*	This study

	CTACTCGAGGGATCCCTAGGTGTTGTCGCTGCCG-5’	complementation	
Upkn	3’-CCCTGGATTTCACTGATGAG-5’	pKNG101 screening primer	[189]
Rpkn	3’-CATATCACAACGTGCGTGGA-5’	pKNG101 screening primer	[189]
M13F	3’-TGTAAAACGACGGCCAGT-5’	pBBR1MCS-4 screening primer	[190]
M13R	3’-CAGGAAACAGCTATGACC-5’	pBBR1MCS-4 screening primer	[190]

First, genomic DNA from TNCF_23 was extracted. Upstream and downstream fragments were amplified using primers 1 and 2, and 3 and 4, respectively. PCR products were checked on a 1% agarose gel and subsequently purified with Qiagen PCR purification kit, following manufacturer's instructions. PCR products were diluted 1:20 and 1.5 µl of each were used for the overlapping PCR using primers 1 and 4.
After this step, PCR product was checked on an agarose gel. Mutator fragment was then digested using BamHI and SpeI. Mutator fragment concentration was determined with a Nanodrop spectrophotomer (Thermo Scientific).
To ligate the product into pKNG101 (Fig. 17 and Table 11), a digestion of the plasmid with the same restriction enzymes was performed. Digestion product was checked on an agarose gel, and the linearized plasmid of the right size was gel-extracted. After determining its concentration, ligation was performed, using a vector:insert ratio of 1:3. pKNG101-*tssK3* was then transformed into Chemically Competent CC118λ*pir* with heat shock. Transformants were selected on Streptomycin 50 µg/ml LB upkn agar and a colony PCR with primers 1 and 4 was carried out to assess the presence of vector and insert.

Figure 17. pKNG101-Δ*tssK3*. *tssK3* mutator fragment is located between the sequences of the primers OAL_4076 ("Primer 1") and OAL_4079 ("Primer 4"), which contain the restriction sites BamHI and SpeI, respectively. The plasmid also contains the sequences of its specific screening primers, Upkn and Rpkn, a Streptomycin resistance cassette, sacB cassette and R6K origin of replication.

4.1.3.2. tssK3 deletion in PA14 and PAO1

On the first day, overnight cultures in LB of receiver strains (PA14 and PAO1), helper strain (*E.coli* 1047 pRK2013) and donor strain (CC118λ*pir*) were inoculated. The following steps were performed in parallel for both PAO1 and PA14 as receiver strains.

On the second day, 500 µl of receiver overnight culture was incubated for 2 hours at 43°C. This step inactivates *P. aeruginosa* restriction-modification system. 20 µl spots of the helper strain were placed on top of 20 µl of the donor strain onto an LB plate and incubated for 2 hours at 37°C. After the 2 hours of incubation, 40 µl of the receiver strain was placed on top of one donor + helper spot (Fig. 18). Single donor, helper and receiver spots were also plated and incubated as controls.

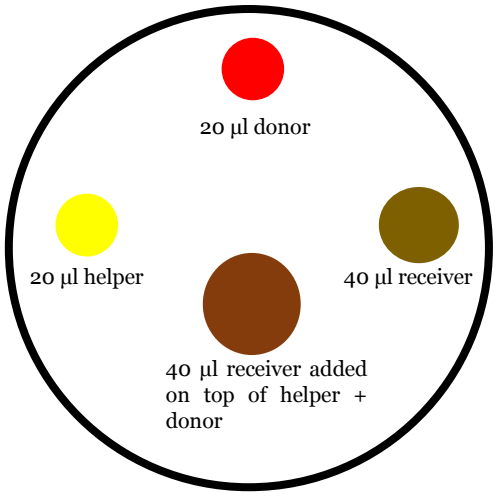

Figure 18. Scheme of conjugation plate.

After 4 hours, each patch was collected and resuspended in 500 µl TSB and subsequently grown for one hour at 37°. All of the donor, helper and receiver 500 µl TSB cultures were plated as negative controls on Vogel-Bonner Medium (VBM) with streptomycin 2000 µg/ml (these should not grow on VBM + antibiotic). 100 and 400 µL of donor + helper + receiver spot were plated on two VBM plates with streptomycin. Plates were incubated for 36 h at 30 °C.

On day four conjugant colonies were patched onto LB agar 20% sucrose, and then on LB agar Sm_{2000}. Plates were incubated for 48h at room temperature. On day six we looked for no or considerably reduced growth on sucrose and normal growth on Sm_{2000}. This 1st event of recombination was screened by colony PCR with the following primer pairs: Rpkn + primer 4, and Upkn + primer 1. 10ml LB with one upstream, and one downstream recombinant 1st event clone were inoculated and incubated with shaking at 30°C for around 4h, when the slightest amount of turbidity was visible. 100 µl of the cultures were then plated on LB agar 20% sucrose and incubated for 24-72h at room temperature until colonies appeared.

On day 7, colonies were patched on LB agar Sm_{2000}, PIA and LB agar in that order, and incubated at 37°C overnight. On day eight we looked for Sm_{2000}-sensitive (no growth) clones, which instead grew on PIA and LB agar. This second event was screened from an LB agar plate with internal (primer 1+4) and external (5+6) primers. A couple of positive clones were streaked onto LB Sm_{2000} and LB agar in that order to confirm expulsion of the plasmid. Plates were then incubated at 37°C overnight. On day nine a colony PCR was done on single colonies from streaked out clones that didn't grow on LB Sm_{2000}. A positive clone single colony was inoculated overnight in TSB and stocked on day 10.

4.1.3.3. Complementation of tssK3 in PA14 and PAO1

The following primers for *tssK3* complementation were designed (Table 10):

- OAL4069: forward primer, composed by ATG + EcoRI site + 18 bp + 2 bp at the beginning of *tssK3*, for a total of 29 bp;
- OAL4070: reverse primer, made of 3 bp + BamHI site + XhoI site + 19 bp at the end of *tssK3,* for a total of 34 bp.

After PCR amplification and purification of the fragment, this was digested with EcoRI and BamHI, as well as the plasmid pBBR1MCS-4 (Table 11), which was then gel-extracted; the following step was a ligation between digested plasmid and *tssK3*, using the same proportions used for *tssK3* deletion (vector:insert=1:3). The vector with the gene was then transformed into XL-1 Blue Competent Cells, and the presence of the gene was assessed by colony PCR using screening primers M13F and M13R. Positive colonies were inoculated overnight. The following day a Miniprep (Qiagen) was performed on the cultures, and one plasmid was chosen to be sequenced. Sequencing confirmed the presence of *tssK3* in pBBR1MCS-4 (Fig. 19).

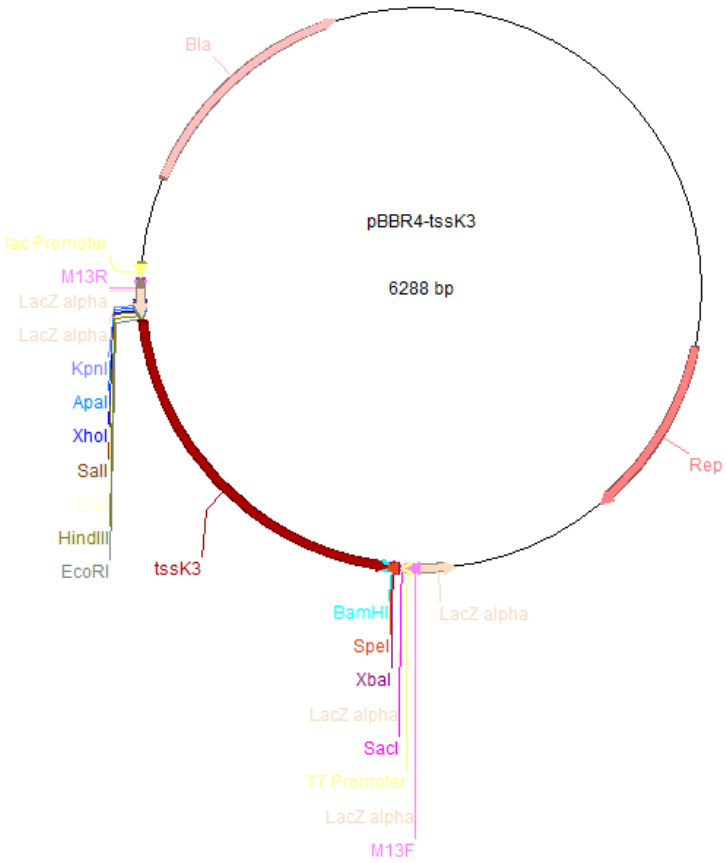

Figure 19. pBBR1MCS-4-*tssK3*. Along with *tssK3*, the plasmid presents several restriction sites, a LacZ alpha fragment, a bla cassette, and the sequences of the screening primers M13F and M13R upstream and downstream of *tssK3* gene.

To insert the plasmid into PAO1 and PA14, a similar procedure as the one used to insert pKNG101-Δ*tssK3* was followed: On day 1, overnight cultures in LB of PA14, PAO1, helper strain (*E.coli* 1047 pRK2013) and donor strain (XL1-Blue) were inoculated. On day 2, 500 µl of receiver overnight culture was incubated for 2 hours at 43°C. 20 µl spots of the helper were placed on top of 20 µl of the donor strain onto an LB plate and incubated for 2 hours at 37°C. After the 2 hours of incubation, 40 µl of the receiver strain was placed on top of one donor + helper spot. Single donor, helper and receiver spots were also plated and incubated as controls. After 4 hours, each patch was collected and resuspended in 500 µl TSB and subsequently grown for one hour at 37°. All of the donor, helper and receiver 500 µl TSB cultures were plated as negative controls on to Vogel-Bonner Medium (VBM) with Carbenicillin 250 µg/ml. 100 and 400 µL of donor + helper + receiver spot were plated on

two VBM plates with Carbenicillin. Plates were incubated for 36 h at 30 °C. Colonies were screened for the presence of pBBR1MCS-4 + *tssK3*, and positive colonies were inoculated overnight. The following morning stocks of complemented strains were made.

Table 11. Plasmids used in this study.

Plasmid	Purpose	Source
pKNG101	*tssK3* deletion	[188]
pBBR1MCS-4	*tssK3* complementation	[190]

4.1.4. Artificial Sputum Medium

The media mimics the patient lung environment and is rich in amino acids, free DNA and mucin [191]. Therefore, by using ASM it was possible to see how CF strains grow in an environment that resembles cystic fibrosis lungs and to check if any differences between early and late isolates occur.

4.1.4.1. ASM recipe

Four grams of DNA from fish sperm (Sigma-Aldrich) were slowly added to 250 ml of deionized water, kept on stirrer and let dissolve; five grams of mucin (Sigma-Aldrich) were gradually added to 250 ml water, kept on stirrer and let dissolve; 250 mg of each aminoacid (Sigma-Aldrich), except cysteine and tyrosine, were added to 100 ml water, kept on stirrer and let dissolve; 250 mg cysteine was dissolved in 25 ml water, while 250 mg tyrosine was dissolved in 25 ml KOH 0.5M; 5.9 mg DTPA, 5 g NaCl and 2.2 g KCl were dissolved in 250 ml water. Solutions were mixed all together and 5 ml Egg Yolk emulsion (Sigma-Aldrich) were added. pH was adjusted to 6.9 using Tris pH 8. The mix was filled up to 1 l volume with sterile water. Five aliquots of 200 ml each were obtained out of 1 l, and the medium was autoclaved and then stored at 4°C until use.

4.1.4.2. ASM assays

Single assay: overnight LB cultures of *P. aeruginosa* were diluted to OD_{600}=0.05. The 0.05 OD_{600} cultures were diluted in ASM 1:100. ASM + *P. aeruginosa* were transferred into a 24-well plate (Fig. 11). Once a day, 2 ml from three wells were collected and dissolved in 2 ml Sputasol (Thermo Scientific). Seven 10-fold dilutions were performed from the diluted cultures. From each dilution, 10 µl were taken and plated onto LB agar as spots (Fig. 21). At each time point, day 0 (T0), day 1 (T1), day 2 (T2), day 3 (T3), day 5 (T5), day 7 (T7), colonies were counted and CFU concentration was calculated.

Competitive assay: the same procedure was adopted as for the single assay, but using two strains at the same time: for each strain the overnight cultures were diluted to OD_{600}=0.05, and these were subsequently diluted as following: strain 1: ASM = 1:200; strain 2: ASM = 1:200 (both strains were inoculated in the same ASM flask). Culture obtained in this way was placed in a 24-well dish (Fig. 20). Every day, 2 ml from three wells were collected and dissolved in 2 ml Sputasol (Thermo Scientific). From the diluted cultures, seven 10-fold dilutions were made. From each dilution, 10 µl were taken and plated onto LB agar and LB agar + appropriate antibiotic: in this work, Ampicillin was used to select for TNCF_175 against TNCF_23, and for VrPa97 against TNCF_23; Meropenem was used to select for

TNCF_175 against VrPa97; Imipenem was used to select for VrPa97 against PA14, PA14Δ*tssK3*, PA14Δ*tssK3*p*tssK3*, PAO1, PAO1Δ*tssK3* and PAO1Δ*tssK3*p*tssK3*.
At each time point, day 0 (T0), day 1 (T1), day 2 (T2), day 3 (T3), day 5 (T5), day 7 (T7), CFU were counted. Antibiotic-free plates were used to infer the total amount of CFU from both strains; to calculate CFU from the isolate that had been previously selected against on the selective plate, the formula (number of colonies on antibiotic-free plate – number of colonies on selective plate) was applied.

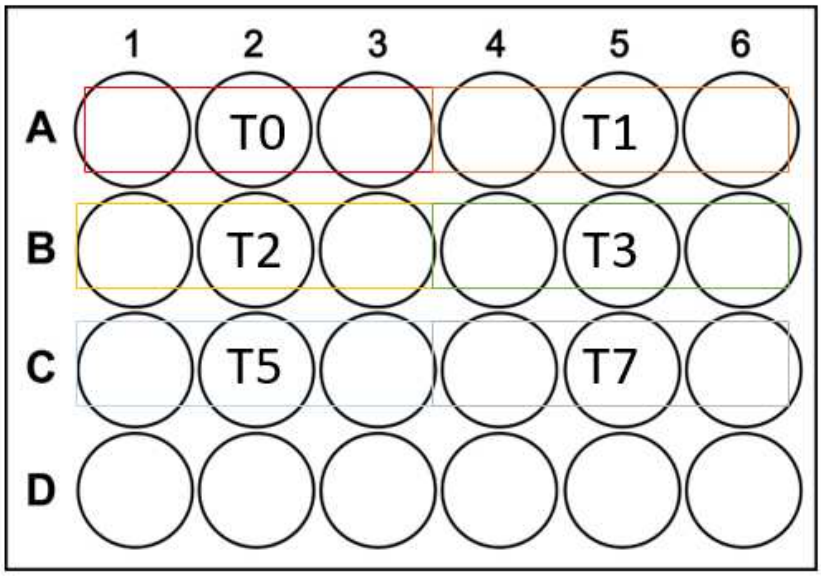

Figure 20. Scheme of ASM culture in a 24-well plate. T0=day 0; T1=day 1; T2=day 2; T3=day 3; T5=day 5; T7=day 7. The experiment was performed in triplicates, and each day cultures from three wells were analysed (coloured rectangles).

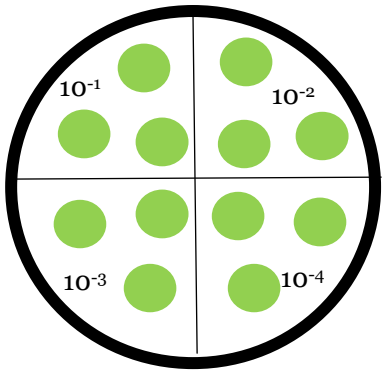

Figure 21. Example of the scheme of 10 µl spots on a culture plate. Each quadrant corresponds to a dilution, and each spot corresponds to a single well.

4.1.5. T6SS-mediated bacterial competition

An *Escherichia coli* recipient cell was engineered by transforming *E.coli* DH5α cells with pBluescript KS(+) allowing the a-complementation of the *lacZ* gene. The transformed cells were plated on LB agar plates containing 5-bromo-4-chloro-indolyl-β-D-galactopyranoside

(X-gal) at 40 µg/ml final concentration and Ampicillin at 100 µg/ml. Plates were incubated at 37 °C. The *P. aeruginosa* donor cells were grown on LBA overnight at 37 °C. The next day, an overnight liquid culture in aerated flask was prepared by inoculating a blue colony among the *E. coli* transformants in 5 ml of TSB supplemented ampicillin and incubated under agitation at 37°C. Single colonies of donor strains were inoculated too.
As described by Hachani et al. [192], with minor modifications, after overnight growth, a cell density of 1 OD_{600} of each strain was harvested in a 1.5 ml tube and centrifuged at 13.000 rpm for 1 minute. The pellets were resuspended in 100 µl of fresh TSB by gentle pipetting and 10 µl of each corresponding strain as a single spot were inoculated. 30 µl of donor and 30 µl of recipient *E. coli* were mixed. 20 µl of the mixes were plated as individual spots on an LBA plate. A bacterial killing occurred after 5 hours incubation at 37°C.
Readout assay was performed on LBA plates containing 40 µg/ml X-gal. Individual bacterial spots were collected with a sterile loop and resuspended in distinct 1.5 ml tubes containing 1 ml of TSB. For every strain, series of 7 times 3 tubes containing 900 µl of TSB were prepared and each spot was resuspended to 10-fold serial dilutions up to 10^{-7}. These dilutions were spotted on LBA plates containing 40 µg/ml X-gal. For reproducibility of the results, 20 µl were spotted in triplicate within a quadrant (Fig. 22).

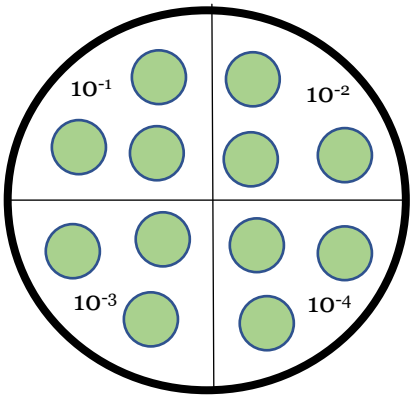

Figure 22. Example of the scheme of the readout plate. Each quadrant corresponds to a dilution spotted in triplicate.

For a quantification of the competition assay, 100 µl of the dilutions wear spread on LBA plates containing 40 µg/ml X-gal. The dilution plates were incubated in a 37 °C incubator overnight.
For a qualitative assay, plates were placed in a 37 °C incubator overnight. Pictures were taken for the analysis: spots remaining predominantly blue indicated that *E. coli* had not been killed by *P. aeruginosa*. This happens when *E. coli* is co-cultured with a T6SS-defective *P. aeruginosa* strain. A positive and a negative controls were included in this study: PAK*Δret* (positive for T6SS) and PAK*Δret*ΔH1-T6SS (defective in T6SS) [192].

4.1.6. *Caenorhabditis elegans* slow killing assay

4.1.6.1. Nematode Growth Medium

Caenorhabditis elegans was maintained on Nematode Growth Medium agar [41]. For NGM preparation and general maintenance procedures, protocols described by Stiernagle *et al.* were followed with minor modifications [193]. 23 g of Nematode Growth Medium (NGM) powder (US Biological, Salem, MA, USA) were dissolved in 1 L of Milli-Q water and the solution was autoclaved for 15 min at 121° C. The flask was cooled in a 55° C water bath for 15 min. Previously sterilized solutions were then added: 1 mL of 1 M CaCl2, 1 mL of 1 M MgSO4 and 25 mL of KPO4 buffer (108.3 g of KH2PO4, 35.6 g of K2HPO4, H2O to 1 L). Finally, 22 mL of complete medium were dispensed into Petri plates (100 mm diameter). Plates were left 2-3 days at room temperature (RT).

4.1.6.2. Conservation of *C. elegans*

100 µL of an *E. coli* OP50 liquid culture in LB-grown overnight at 37° C at 180 rpm were spread onto NGM plates and then incubated overnight at 37° C to allow formation of a thin layer. Worms were transferred onto NGM plates with OP50 using the "chunking" method [193]. Briefly, a sterile scalpel was used to move a chunk of agar from an old plate to a fresh plate. Stocks were maintained at 20° C.

4.1.6.3. Killing assay plates preparation

5-Fluorodeoxyuridine or Floxuridine (FUdR) is an inhibitor of DNA synthesis which prevents *C. elegans* reproduction, without interfering with nematode development and ageing. The use of FUdR is therefore essential to avoid errors in worms lifespan evaluation. FUdR (Sigma-Aldrich) was added to NGM to a final concentration of 160 µM and 10 mL of medium were poured into 60x15mm Petri dishes.

For each CF strain, OD_{600} of overnight liquid cultures was measured and subsequently diluted to a concentration of 1 OD/ml; 36 µL of the diluted cultures were added onto an NGM+FUDR plate. As a control, one plate was spread with 36 µL of a 1 OD/ml *E. coli* OP50 culture. Plates were incubated overnight at 37°C.

4.1.6.4. Synchronization of *C. elegans*

To synchronize worms at the first larval stage (L1) the bleaching technique was used [194]. The principle of this method is that adult worms are sensitive to bleach (5% solution of sodium hypochlorite, NaClO) and therefore die rapidly, while the eggshell protects embryos from dissolution.

About 7 mL of M9 medium (Sigma-Aldrich) were poured onto NGM plates with *C. elegans*. M9 was aspirated and transferred to a 15-mL tube. This step was repeated twice. After a 1-minute centrifugation at 1500g the supernatant was discarded. Other additional washes with M9 were performed until the liquid was clear. After elimination of the supernatant, 3.5 mL of M9, 500 µL of 5 M NaOH and 1 mL of bleach were added. After vigorous shaking, bleach started to kill adult worms. To not damage embryos, bleach-induced death was observed by using a stereomicroscope to verify the dissolution of adult worms that normally occurs within 4 minutes. Bleach was inactivated by adding M9 to a final volume of 15 mL. The supernatant was discarded, and M9 was added to a final volume of 15 mL.

Tubes were centrifugated for 2 minutes at 1500g, and supernatant was discarded. This step was performed five times. After the last wash, the supernatant was discarded and about 6 mL of M9 were added. The content of tubes was split onto 3 NGM plates.

4.1.6.5. Slow killing assay

50 worms at the L4 stage were individually transferred from an NGM plate onto an NGM+FUDR+bacterial strain plate using a sterilized platinum wire with the aid of a stereomicroscope. Plates were incubated at 20°C and the number of live nematodes was counted every day over a period of 20 days. A worm was considered dead when it no longer responded to touch. The experiment was repeated three times for each CF strain.

4.1.7. *Galleria mellonella* killing assay

The virulence potential of *P. aeruginosa* TNCF_23, TNCF_175 and VrPa97 strains was evaluated in *Galleria mellonella* larvae, according to Betts et al. [195], with minor modifications. Briefly, overnight cultures of *P. aeruginosa* grown in Trypticase Soy broth were washed and resuspended in PBS. Each strain was tested at doses of 10^3, 10^4, 10^5, and 10^6 CFU/larva. Ten microliters of the bacterial suspension were injected directly into the hemocoel of the wax moth via the right proleg using 10 µl Hamilton syringe (Hamilton Co., Nevada, USA). Bacterial colony counts on Trypticase Soy agar plates were used to confirm inoculum size of bacterial suspensions. Control larvae were injected with 10 µl of PBS to measure any potential lethal effects of the injection process. An additional control group had no manipulation. Each experimental group consisted of 20 *G. mellonella* larvae, with each experiment repeated 3 times. After exposure, larvae were incubated in the dark at 37°C and checked daily for survival until 96 h. Larvae were considered dead if they failed to respond to touch.

4.1.8. Statistical analysis

Results of all assays were plotted and analysed with GraphPad Prism version 6.0 for Windows (GraphPad Software, San Diego, CA, USA)[196].

For the invasion assay and the IL-8 secretion assay, Mann-Whitney test [197] and unpaired t-test with Welch's correction [198] were applied.

For the T6SS-mediated bacterial competition test, unpaired t-test with Welch's correction and Mann-Whitney test were applied.

For the *C. elegans* slow killing assay, survival curves of *C. elegans* were plotted showing survival rate as a function of time and were compared with the non-parametric Log-rank (Mantel-Cox) statistical test [199].

For the *G. mellonella* killing assay, survival curves were plotted and differences in survival were calculated using the Log-rank (Mantel-Cox) test. LD50 values of *P. aeruginosa* strains were calculated by the generalized linear model, and differences were tested for significance by Student-t-test. P values less than 0.05 were considered as statistically significant.

4.2. Results

4.2.1. Phenotypic characterization

4.2.1.1. Internalization assay in A549 human cells

During the course of chronic infection, the bacterium tends to internalize more compared to non-chronic strains, and this could benefit bacterial survival through evasion of host phagocytic- and antibody/complement-mediated killing mechanism [200]. An invasion assay was therefore performed using A549 epithelial lung cells. TNCF_175 seemed to internalize more than TNCF_23 and VrPa97, with a mean value of 3.5x10^3 bacteria/ml, while TNCF_23 showed a mean value of 2.5x10^3, and VrPa97 2.2x10^3 (Fig. 23). Despite a clear tendency of TNCF_175 to be more invasive than VrPa97 and TNCF_23, neither Mann-Whitney test nor unpaired t-test with Welch's correction showed data significance; this is probably due to the low number of replicates (3).

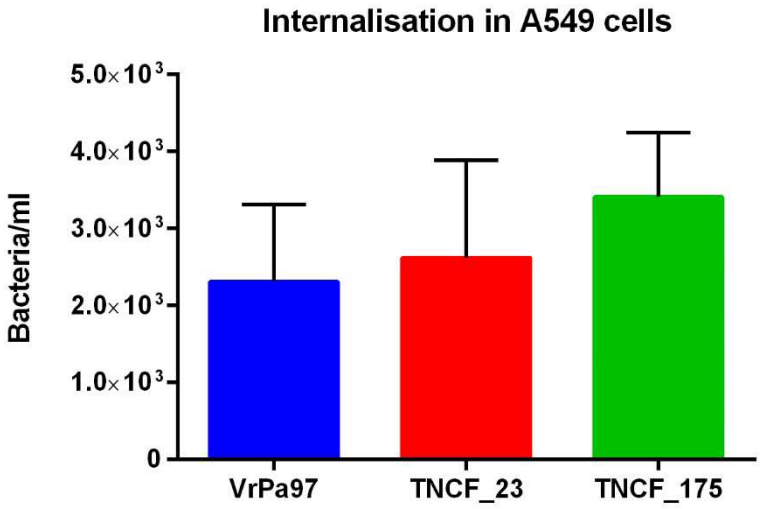

Figure 23. Internalization of *P. aeruginosa* in A549 cells. Concentration of invading bacterial cells in A549 type II pneumocytes after 2 hours of stimulation with strains VrPa97, TNCF_23 and TNCF_175. Measurements were performed in triplicate.

4.2.1.2. Inflammation assay in A549 human cells

Pseudomonas aeruginosa possesses a number of virulence factors (such as pilin, flagellin, proteases) that have been shown to increase secretion of the chemokines such as IL-8 by human airway epithelial cells [201][202][203]. To assess the capability of *P. aeruginosa* to induce IL-8 secretion, A549 epithelial lung cells were used. Mean values of IL-8 production by A549 cells were 187.5 pg/ml when infected with VrPa97, 212.5 pg/ml in the presence of TNCF_23, and 81.3 pg/ml when infected with TNCF_175 (Fig. 24). Despite an apparent tendency of TNCF_175 to be less immunostimulatory than VrPa97 and TNCF_23, neither Mann-Whitney test nor unpaired t-test with Welch's correction showed statistical significance; this is probably due to the low number of replicates (3).

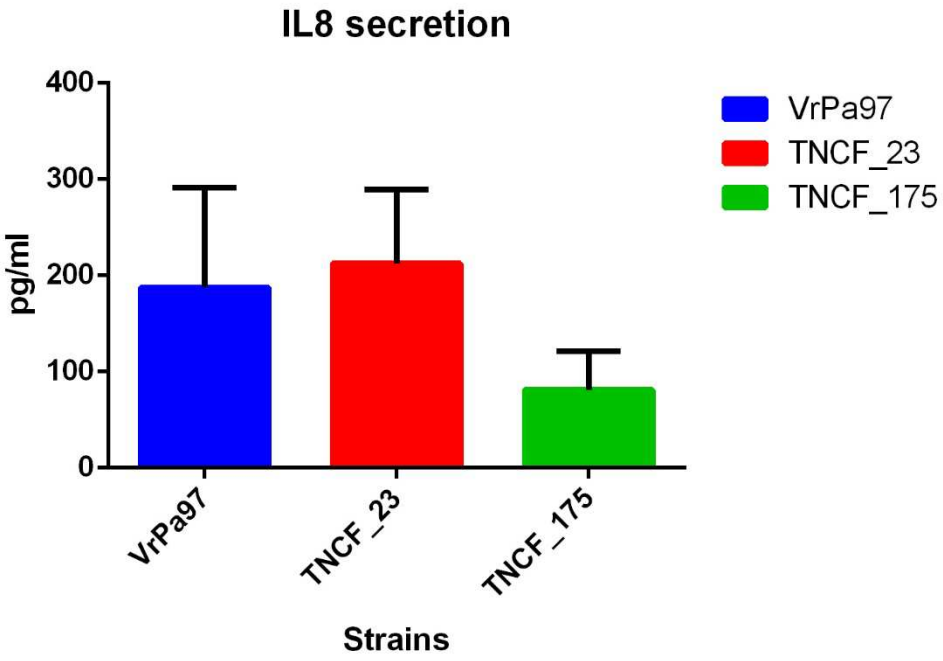

Figure 24. Levels of IL-8 production in A549 epithelial cells infected by *P. aeruginosa*. Interleukin-8 production was quantified by ELISA after stimulation with VrPa97, TNCF_23 and TNCF_175 for 2 hours. Measurements were performed in triplicate.

4.2.2. Construction of clean mutants in *tssK3* and *tssK3* complementation

By analysing the genome of TNCF_175, a stop-mutation in *tssk3* was found. The gene encodes a T6SS structural protein that has not been characterized in depth to date. To get further insights on the role of the protein, clean mutants in *tssK3* in the backgrounds of PAO1 and PA14 have been constructed.

By conjugation, clean mutants in *tssK3* and complemented strains with a plasmid containing constitutively expressed *tssK3* were created, in the background of the reference laboratory strains PAO1 and PA14 (Figs. 25-26).

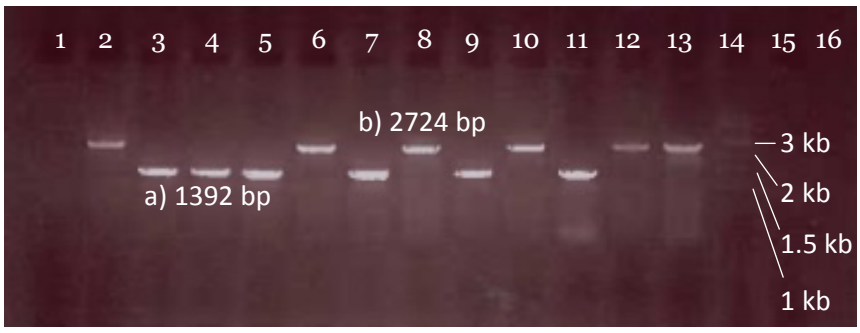

Figure 25. PCR amplification confirming that the second recombination event has occurred to create a) mutants or b) wild-type PA14 and PAO1 strains. Well 1: Negative control; wells 2, 6: PA14*ΔtssK3*; wells 3-5: PA14; wells 7, 9, 11: PAO1; wells 8, 10, 12: PAO1*ΔtssK3*; well 13: PA14 wt used as control.

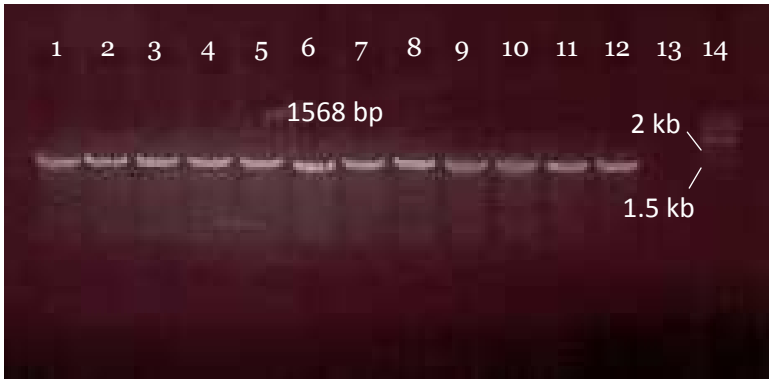

Figure 26. PCR amplification confirming the insertion of the plasmid pBBR-4-*tssK3*.Wells 1-6: PA14*ΔtssK3*p*tssK3*; wells 7-12: PAO1*ΔtssK3*p*tssK3*.

4.2.3. Artificial Sputum Medium (ASM) assays

4.2.3.1. Bacterial growth in ASM

To evaluate how CF strains grow in Artificial Sputum Medium, a particular medium which reproduces environmental conditions that are present in cystic fibrosis patients' lungs, *P. aeruginosa* isolates were grown for seven days and growth was assessed on day 0, day 1, day 2, day 3, day 5 and day 7. The isolates that were grown in ASM are TNCF_23, TNCF_175, VrPa97, PA14, PA14Δ*tssK3*, PA14Δ*tssK3*p*tssK3*, PAO1, PAO1Δ*tssK3* and PAO1Δ*tssK3*p*tssK3* (Fig. 27). They all showed a similar growth pattern when they were cultured alone in ASM. Interestingly, TNCF_23 and TNCF_175, namely the strains isolated from CF patient, appeared to grow slightly faster than other strains.

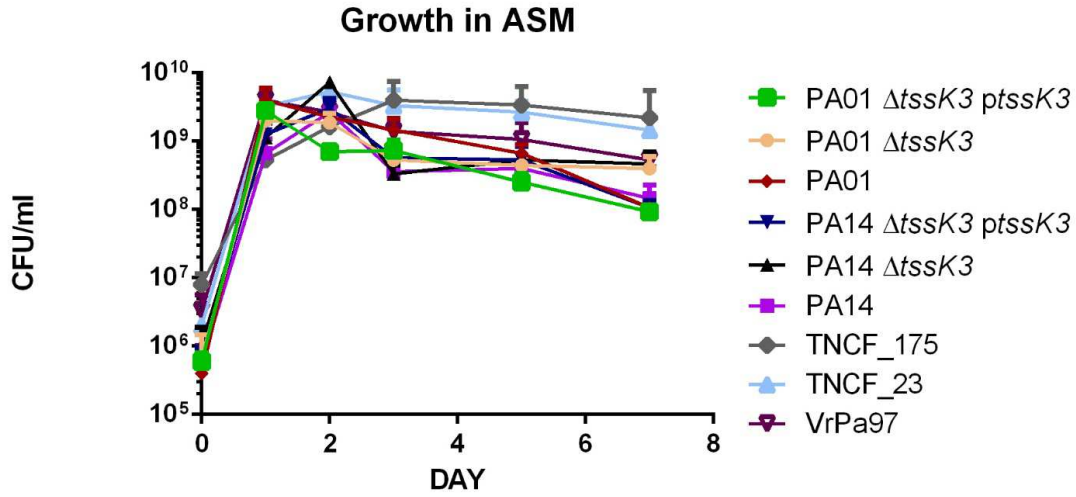

Figure 27. Growth of *Pseudomonas aeruginosa* in Artificial Sputum Medium. Single culture growth curves are represented.

4.2.3.2. Bacterial competition in ASM

To evaluate bacterial competition, isolates were subsequently co-cultured in pairs in ASM and studied at the same time-points as they were assessed when cultured alone. This implied diluting cultures in a 10-fold series and plating on selective agar plates to calculate the number of CFU.

The first series of competitive ASM assays (Fig. 28) included:

- TNCF_23 vs TNCF_175, in which TNCF_23 appeared to outcompete TNCF_175;
- TNCF_175 vs VrPa97, in which VrPa97 dramatically outcompeted TNCF_175, leading the late chronic strain near to elimination;
- TNCF_23 vs VrPa97, where instead the presence of another isolate in the culture didn't affect growth compared to pure culture.

Based on these results, to check for the presence of any secreted factors that could lead to bacterial toxicity, further analyses were performed. TNCF_175 growth in ASM was assessed in the presence of supernatants derived from: a) a TNCF_23 overnight culture; b) an overnight co-culture of TNCF_23 and TNCF_175; c) a VrPa97 overnight culture, and d) an overnight co-culture of VrPa97 and TNCF_175 (Fig. 29). No supernatant turned out to have any toxic effect on TNCF_175. These results suggested that growth inhibition observed in the competitive ASM assay is due to cell-cell interaction.

To study a possible role of *tssK3* impairment in this mechanism, a second series of competitive ASM assays (Fig. 30) was carried out; at this stage, six strain pairs were analysed:

- VrPa97 vs PA14;
- VrPa97 vs PA14Δ*tssK3*;
- VrPa97 vs PA14Δ*tssK3*p*tssK3*;
- VrPa97 vs PAO1;
- VrPa97 vs PAO1Δ*tssK3*;
- VrPa97 vs PAO1Δ*tssK3*p*tssK3*.

In no cases VrPa97 significantly affected growth and survival of the other isolates.

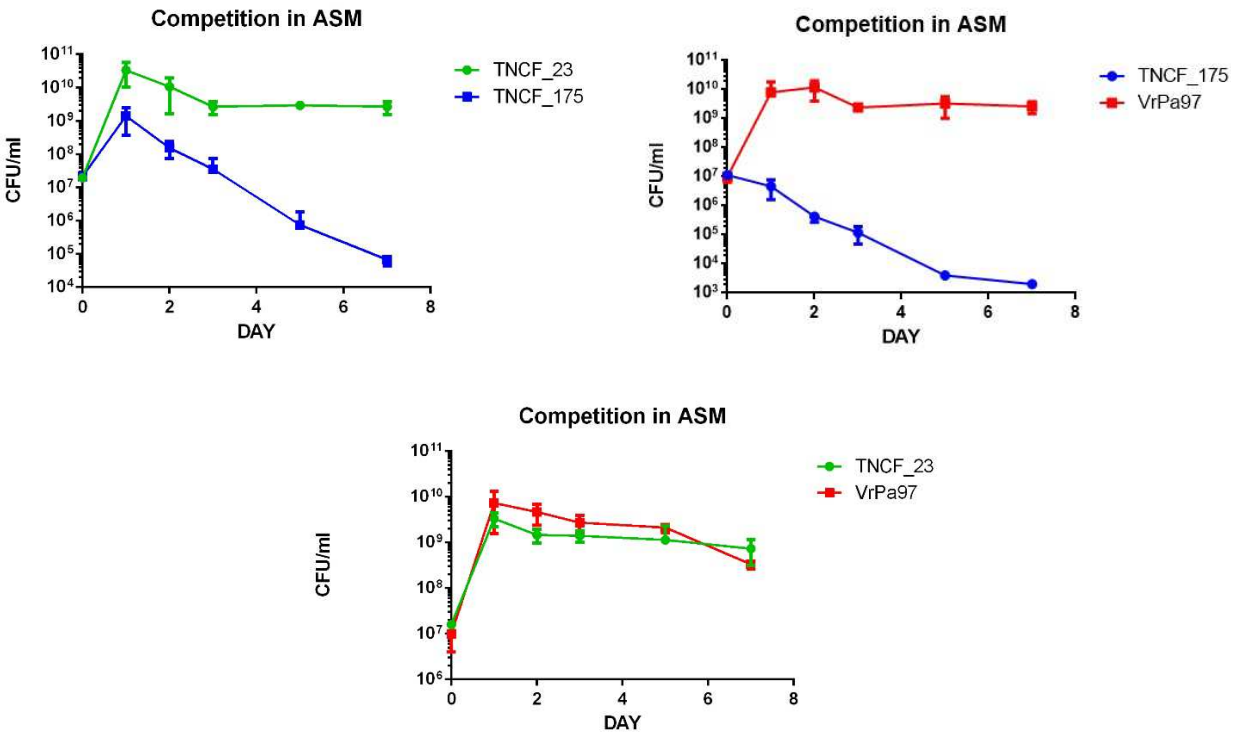

Figure 28. ASM competition assay. In-pairs culture growth curves in ASM are represented. Clockwise, TNCF_23 vs. TNCF_175, TNCF_175 vs. VrPa97 and TNCF_23 vs. VrPa97.

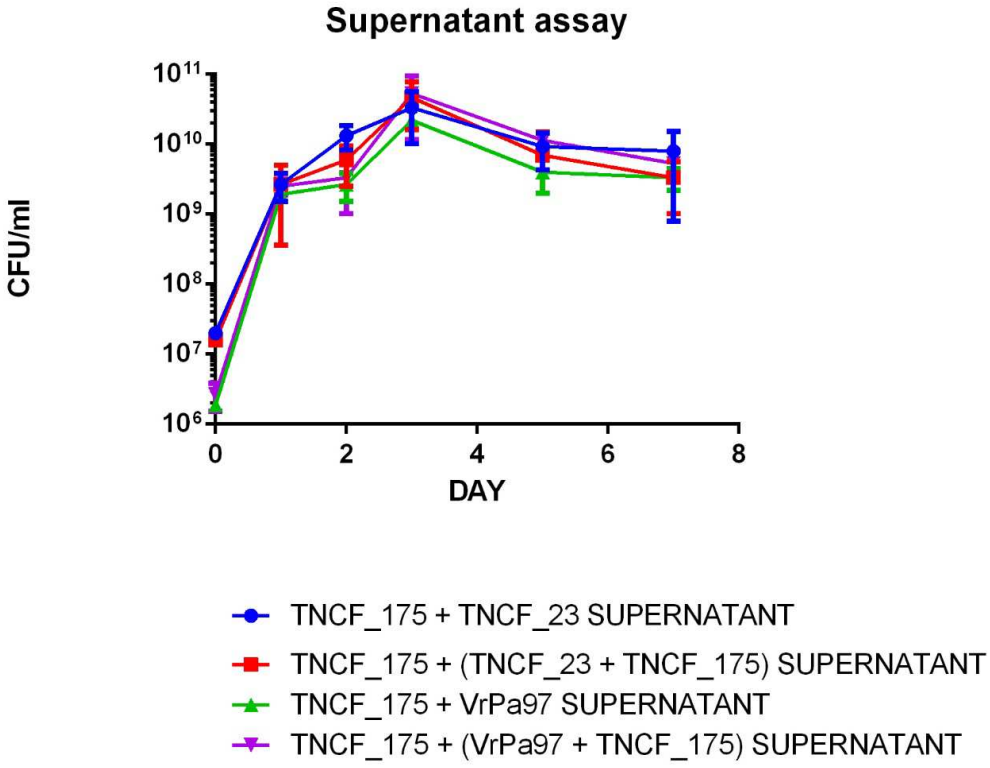

Figure 29. ASM assay performed on TNCF_175 in the presence of TNCF_23 and VrPa97 cultures supernatants.

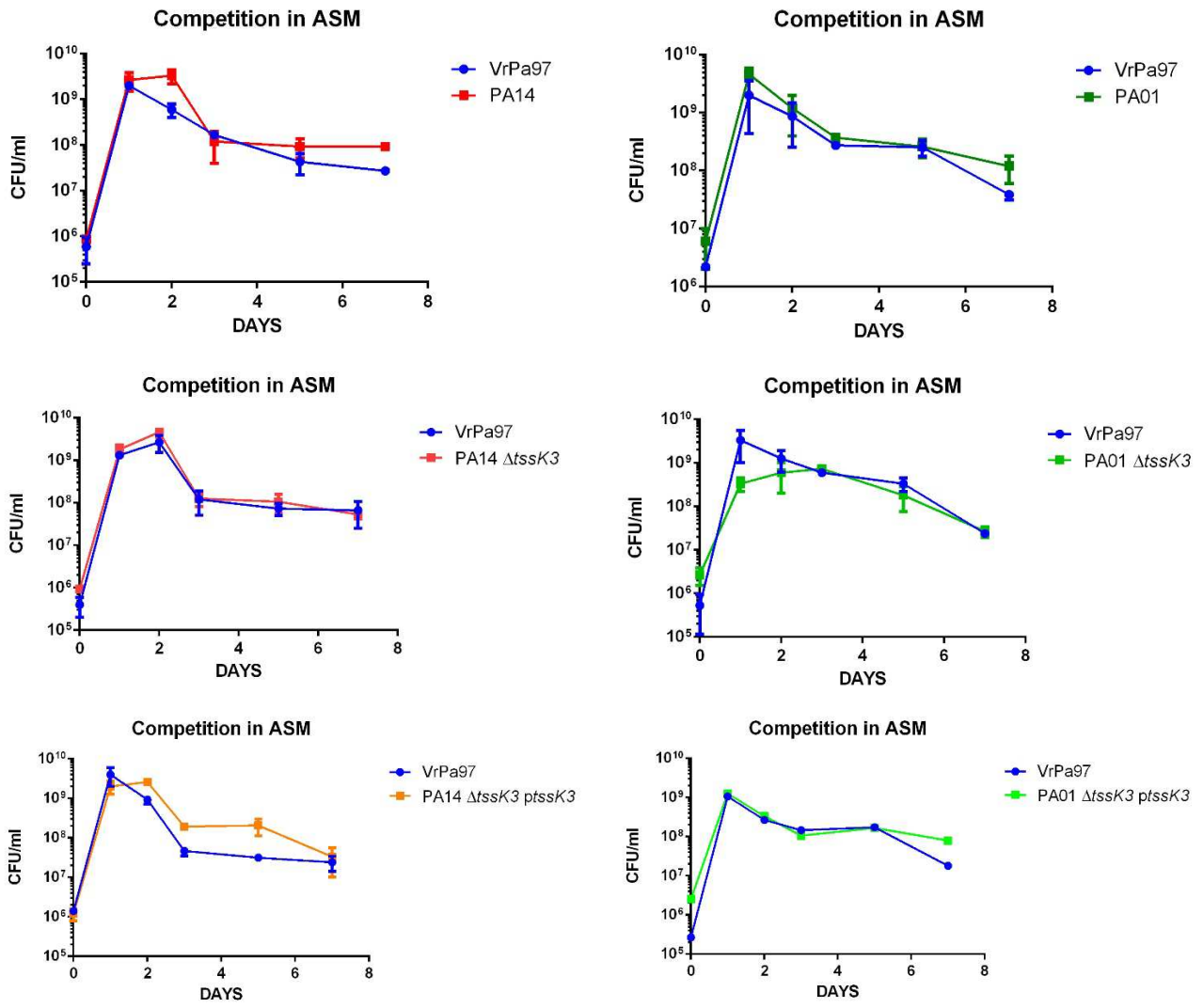

Figure 30. ASM competition assay. In-pairs culture growth curves in ASM are represented. In the left part of the panel, VrPa97 vs PA14, VrPa97 vs PA14Δ*tssK3* and VrPa97 vs PA14Δ*tssK3*p*tssK3* competitive growth in ASM is reported; in the right part of the panel, VrPa97 vs PAO1, VrPa97 vs PAO1Δ*tssK3* and VrPa97 vs PAO1Δ*tssK3*p*tssK3* competitive growth in ASM is represented.

4.2.4. T6SS-mediated bacterial competition

The type VI secretion system is a weapon that bacteria use to outcompete non-sister bacterial cells [154] by the direct injection of toxins. Based on data obtained with competitive ASM assays, an assay aimed at testing the functionality of T6SS was performed. The assay involves the *E. coli* strain MH5α as a target of the T6SS machinery [192].

Plates were checked after an overnight incubation by a qualitative evaluation based on the observation of colour intensity of blue colonies (*E.coli* DH5α); the more blue are the colonies, the less active *Pseudomonas aeruginosa* strain T6SS is. The highest intensity of blue spots was observed for TNCF_175, followed by the negative control PAK*Δret*ΔH1-T6SS. TNCF_23 and the positive control PAK*Δret* showed a similar pattern in the

distribution of blue shades in the spots. VrPa97, PA14, PA14*ΔtssK3,* PA14*ΔtssK3*p*tssK3,* PAO1, PAO1*ΔtssK3* and PAO1*ΔtssK3*p*tssK3* showed no blue shades in the qualitative analysis.
A quantitative analysis was performed using the same assay, by plating 100 µl of the mixed cultures in a Petri dish and counting blue colonies. Results are reported in figure 31: TNCF_175 appeared to be the least aggressive against DH5α, even less than the negative control PAK*Δret*ΔH1-T6SS (with inactive T6SS), while its clonally related strain TNCF_23 and genotypically related VrPa97 seemed to have a very active T6SS, more than PAK*Δret* (positive control). PA14, PA14*ΔtssK3* and PA14*ΔtssK3*p*tssK3* appeared as the most aggressive towards DH5α, although differences could be observed within the three strains: a trend in decreasing DH5α killing could be spotted in PA14*ΔtssK3* compared with PA14. PA14*ΔtssK3*p*tssK3* seemed to gain back the original killing ability. However, no statistically significant difference could be calculated between these three isolates. PAO1 and its relative mutants (PAO1*ΔtssK3* and PAO1*ΔtssK3*p*tssK3*) showed a similar trend: PAO1*ΔtssK3* showed a slightly weaker killing activity compared to PAO1 and trend as PAO1*ΔtssK3*p*tssK3*, although a statistical significance difference was found only between PAO1*ΔtssK3* and PAO1*ΔtssK3*p*tssK3,* and not between PAO1 and PAO1*ΔtssK3 (*unpaired t-test with Welch's correction and Mann-Whitney test were applied).

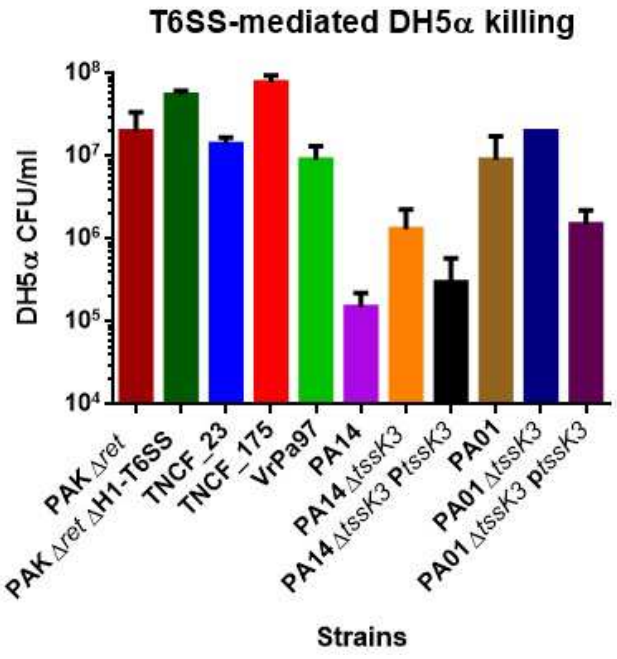

Figure 31. Quantitative analysis of T6SS-mediated DH5α killing by *Pseudomonas aeruginosa* isolates. Number of colonies of DH5α in the presence of bacterial strains are represented.

4.2.5. Slow killing assay in *Caenorhabditis elegans*

Caenorhabditis elegans has been used for numerous studies as an infection host for *P. aeruginosa* and many other bacteria [204]. To verify a possible role of T6SS, and particularly of *tssK3*, a slow killing assay was performed. TNCF_23 and VrPa97 showed a marked virulence against *C. elegans* (Fig. 32): Both strains provoked the death of all worms within six days. TNCF_175 showed a mild virulence: all 50 *C. elegans* individuals

died after 15 days. Mantel-Cox test showed that curves representing survival rates of *C. elegans* in the presence of TNCF_23 and VrPa97 were not significantly different (P-value 0.6619), whereas *C. elegans* survival rate in the presence of TNCF_175 was remarkably different from both TNCF_23 curve (P-value 0.0006) and VrPa97 curve (P-value 0.0004). All curves strikingly differed from *C. elegans* survival rate with OP50 (P-value <0.0001 with VrPa97 and TNCF_23, and 0.0010 with TNCF_175).

PA14, PA14Δ*tssK3* and PA14Δ*tssK3*p*tssK3* show a remarkably high killing activity in *C. elegans* (Fig. 33). Death of all 50 worms occurred within 7 days with both PA14 and PA14Δ*tssK3*, and within 8 days with PA14Δ*tssK3*p*tssK3*. Comparison of the three survival curves did not show any relevant differences. The same curves were all significantly different from OP50 curve: P-value <0.0001 in all three cases.

PAO1 and PAO1Δ*tssK3* showed a comparable pattern in the killing of *C. elegans*: in both cases, all worms died within 18 days. PAO1Δ*tssK3*p*tssK3* appears to be slightly more virulent than the other two, with a total killing of worms occurring after 13 days, although survival rates were not significantly different between PAO1 and PAO1Δ*tssK3*p*tssK3*, and between PAO1Δ*tssK3* and PAO1Δ*tssK3*p*tssK3* (P-value 0.8341 and 0.2118 respectively). Only the survival curve obtained with PAO1Δ*tssK3*p*tssK3* appeared to be significantly different from the curve obtained with OP50, with a P value of 0.0153 (Fig. 34).

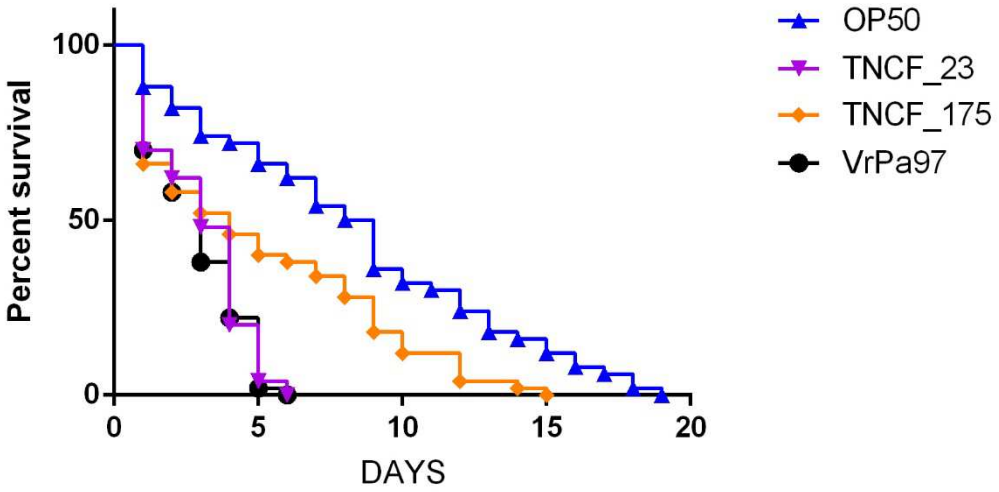

Figure 32. Survival rate of *C. elegans* in the presence of TNCF_23, TNCF_175 and VrPa97.

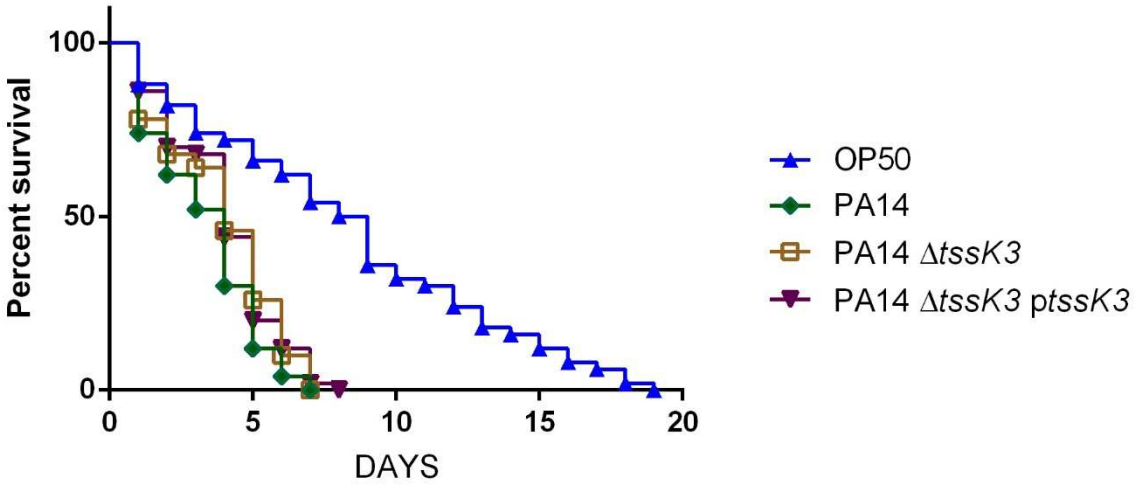

Figure 33. Survival rate of *C. elegans* in presence of PA14, PA14Δ*tssK3* and PA14Δ*tssK3*p*tssK3*.

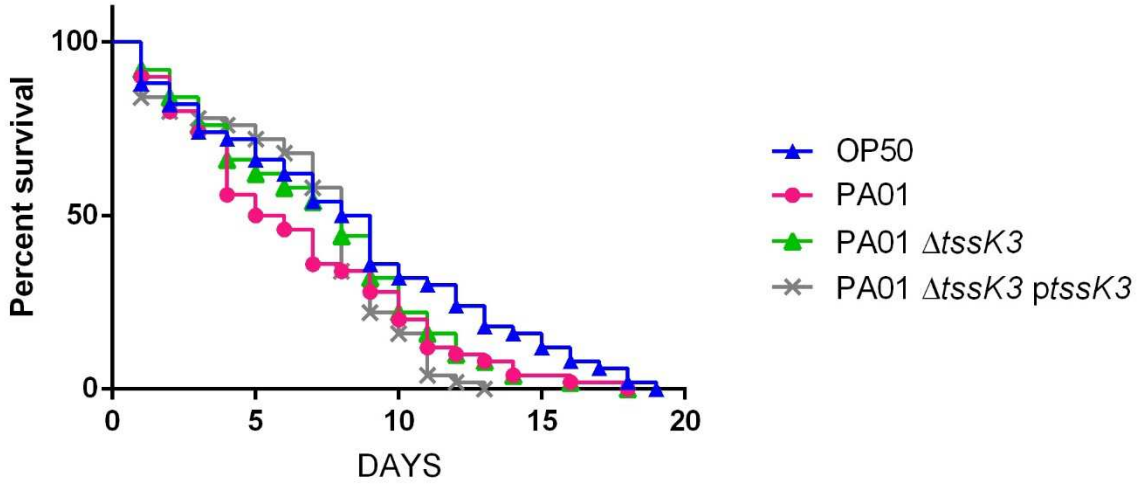

Figure 34. Survival rate of *C.elegans* in the presence of PAO1, PAO1Δ*tssK3* and PAO1Δ*tssK3*p*tssK3*.
Each curve represents survival rate of *C.elegans* with respect to bacterial strain given.

4.2.6. Virulence in *Galleria mellonella*

The greater wax moth caterpillar, *Galleria mellonella,* has been used in several studies as a useful model for investigating the pathogenesis of many bacterial and fungal pathogens [205][206][207]. The larvae were injected, on three different occasions, with a range of inoculum doses to determine the mortality rates caused by each isolate. VrPa97 strain was found to be significantly more virulent towards *G. mellonella* than TNCF_23 and TNCF_175 strains. Curve comparison showed significant differences ($p<0.0001$) for each strain, although the survival outcome of the tested strains varied. VrPa97 strain showed the highest virulence, causing higher mortality rates, compared to TNCF_23 and TNCF_175, and killed all the larvae already at a lower dose (10^2 CFU) after 24h-incubation. The killing rate exhibited by both TNCF_23 and TNCF_175 strains was positively correlated with both incubation time and dose. However, TNCF_175 strain was more virulent compared to TNCF_23 (Figs. 35-37). Non-infected larvae showed no mortality.

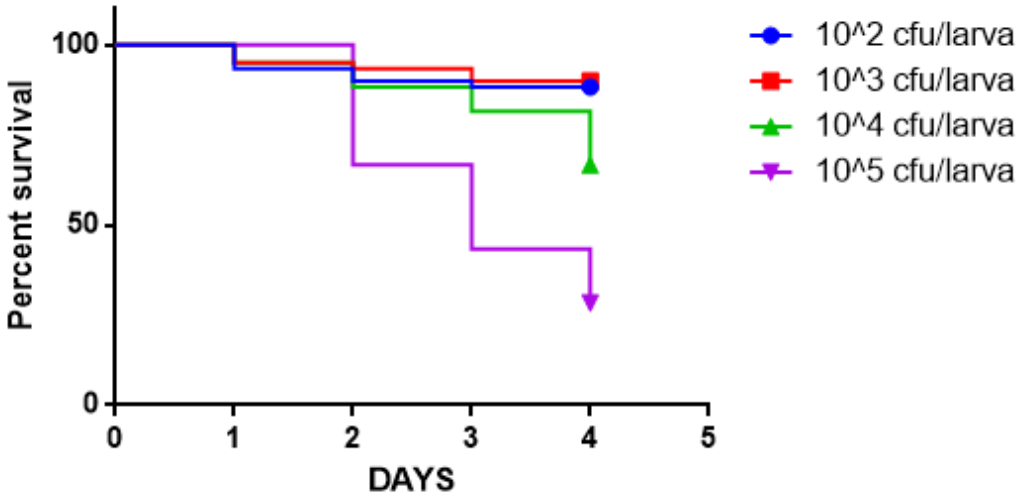

Figure 35. Survival curves of *Galleria mellonella* larvae following injection of different doses of *P. aeruginosa* TNCF_23. Data presented are the mean + SD of three independent assays (n=30 larvae/assay) with TNCF_23. PBS-injected larvae were used as controls and showed no mortality.

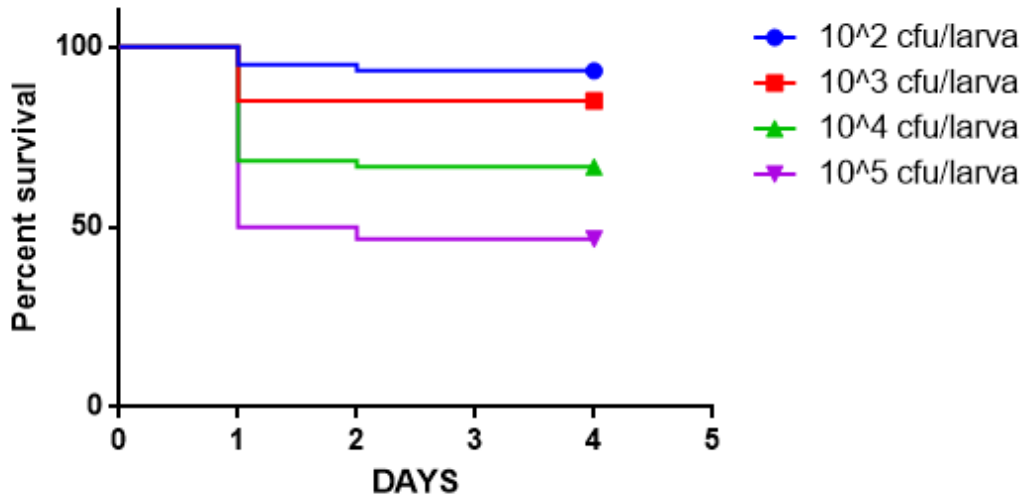

Figure 36. Survival curves of *Galleria mellonella* larvae following injection of different concentrations of *P. aeruginosa* TNCF_175. Data presented are the mean + SD of three independent assays (n=30 larvae/assay) with TNCF_175.

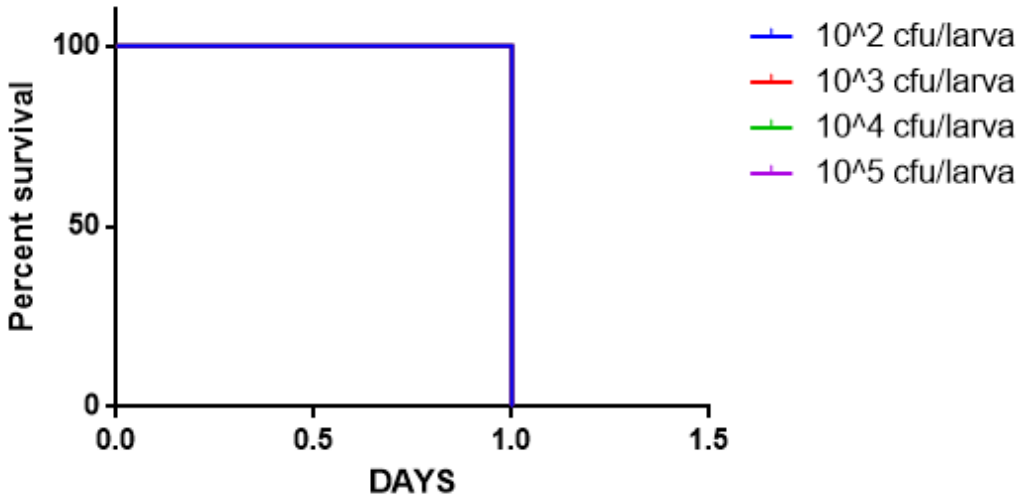

Figure 37. Survival curves of *Galleria mellonella* larvae following injection of different concentrations of *P. aeruginosa* VrPa97. Data presented are the mean + SD of three independent assays (n=30 larvae/assay) with VrPa97.

5. DISCUSSION

Pseudomonas aeruginosa undergoes a characteristic evolutionary adaptation during chronic infection of CF lung [38]. Infection of CF patients occurs via primary colonization of the airway with subsequent accumulation of adaptive mutations in the bacterial genome related to an increased fitness in the lung environment, resulting in chronicization [23]. Adaptation to the airway of *P. aeruginosa* is a crucial aspect in the progression of CF lung disease and *P. aeruginosa* chronic isolates are known to express different phenotypic traits compared to acute infection isolates, including biofilm formation, loss of motility, and hypermutability [208][209][210][72]. Genomic studies have revealed extensive strain genetic variability within patients [38], and selection within CF lung appears to play a key role for *P. aeruginosa* diversification [38].

Population structure and microevolution. We obtained genome sequences from 40 *P. aeruginosa* isolates from a single CF patient collected over an eight-year period (2007-2014). Interestingly, Eburst analysis of the sequence types revealed that the collection consisted of a single clonal population dominated by ST390 plus three novel variants, with variations only at a single locus each, indicating that all isolates belonged to the same clonal lineage and likely evolved from a single ancestral colonizing strain. This is in contrast with what has been previously reported in other CF patients, in which either different lineages coexist [211][212][180] or a first infecting lineage is replaced by a new one [213][214]. In this patient, a single dominant clonal lineage apparently persisted in the airways for at least eight years, allowing a detailed study of the microevolution and adaptive process of the bacterium in the course of chronic infection. However, within this population, we could observe the presence of two sublineages that have evolved in parallel, with one of them being the most prevalent in the latest stage of the infection; not surprisingly, this sublineage comprised most multi-drug resistant isolates. In a retrospective analysis of serial isolate collections from CF patients starting at the onset of airways colonization over a 30-year period from 51 CF centres in Hannover and Copenhagen, Cramer et al. [215] provided a unique opportunity to understand the molecular evolution of *P. aeruginosa* in the course of chronic infection. Genotyping revealed that the *P. aeruginosa* population was dominated by a few ubiquitous clones. On the other hand, these authors also noticed a site-specific expansion of clones. Similarly to our findings, In Hannover, the clonal distribution resembled the global distribution in CF airways, namely the majority of the cohort maintained the initially acquired clone throughout the entire period of observation. However, in Copenhagen, two clones had replaced the initially acquired individual clones in the majority of cases. Since these two clones were rare in the global *P. aeruginosa* population, they had likely spread by nosocomial superinfection.

Our phylogenetic analysis based on SNPs in the core genome also divided the population into two subpopulations derived from the evolution of the first infecting strain. The annotation of SNPs allowed us to identify mutations with moderate or high impact. The gene encoding respiratory nitrate reductase subunit gamma *nail* carried high impact variants in three closely related isolates, one early isolate, TNCF_14, and two late isolates, TNCF_130 and TNCF_151. Isolates TNCF_133 and TNCF_167_1 had high impact variants

in two genes encoding a polyprotein signal peptidase *lspA* and a hypothetical protein, and two hypothetical proteins, respectively. Other genes with high-impact variants were those encoding the ABC transporter-binding protein *aaltP* in TNCF_3, the copper resistance protein A precursor *pcoA*in TNCF_175 and a gene with unknown function in TNCF_174. With regard to moderate impact mutations, eight of them were found in genes with a putative or unknown function. The pyoverdine biosynthesis gene *pvdL* carried a total of five moderate-impact SNPs in all 40 genomes analysed, as well as the DNA gyrase subunit B *gyrB* with five variants in 36 genomes. Remarkably two aminoacid substitutions, E468-D and S749-P, were found in isolates resistant to fluoroquinolones. The topoisomerase IV subunit B *parE* gene showed three different variations within the population, including R30-C and H59-R in the late MDR isolates. The two-component regulatory system signal sensor kinase *pmrB* gene showed three different changes among the population; *glnE* and *rsme* (*yggJ*) carried three different variants, while *cbrA* and *gltB*, *nagE*, *aruF* and *pilL* had three moderate variants in five, four and three different genomes, respectively.

Molecular evolution analysis was performed to identify genes under non-neutral selective pressure. We found that at least three genes, *gyrB*, *parE* and *pmrB*, involved in the resistance to different classes of antibiotics carried mutations potentially affecting protein function. In particular, DNA gyrase *gyrB* and topoisomerase IV *parE* are both major contributors to the acquisition of resistance to fluoroquinolones [34]. Clinical isolates with the aminoacid substitution E468-D in GyrB protein is reported to be associated to a high-level of resistance to ciprofloxacin [34][212], as this variation is within the quinolone resistance-determining regions (QRDRs) of the protein, whereas the mutations found in *parE* are outside the QRDR domain. For both genes, according to the likelihood ratio test, the null hypothesis of neutrality was rejected. Therefore, non-neutral selection is acting on those genes in the population. Sensor kinase PmrB is part of the two-component regulatory system PmrA/PmrB involved in resistance to Polymyxins and other cationic antimicrobial peptides in *P. aeruginosa* CF isolates [216][217][218]. Considering that variations found in this population were not directly associated with an MDR phenotype and that this gene was not found to have non-neutral selective pressure (likelihood ratio test > 0.05), we can assume that the mutations are neutral.

Mutations in virulence genes, like pyoverdine biosynthesis gene *pvdL* and pilin biosynthesis gene *chpA* (*pilL*), are known as hallmarks of adaptation of *P. aeruginosa* strains to the CF airway environment [219]. Siderophore-mediated processes have been linked with virulence regulation of *P. aeruginosa* and its pathogenic potential [38]. However, in a study conducted on 36 CF patients, pyoverdine was undetectable in one-third of sputa positive for *P. aeruginosa* [220]. The presence of pili is necessary for the initial colonisation and the translocation of type III exotoxins [221], but adapted and late CF isolates accumulate mutations in genes associated with pili, and loss of motility is associated with a higher risk of persistent infections [213][222].

Among the 20 most variable genes (with at least three variations within the population) selected for the analysis of adaptive evolution, nine resulted to be under non-neutral pressure (namely *gyrB* and *parE*, *pilL*, *nagE*, *gltB*, *gidA* and three genes encoding hypothetical proteins). For 10 of them, the neutral (null) hypothesis could not be rejected. For one gene, *pvdL*, it was not possible to perform the test, because its sequence was incomplete, probably due to the draft nature of the genomes. All genes for which the

likelihood ratio test rejected the null hypothesis had an omega (dN/dS) > 1, suggesting they are under positive selection.

We compared the list of genes most frequently mutated in the international strain collection analysed by Greipel et al. [223] (*spuE, spuF, mexA, oprM, rpoB, fusA1, gyrA, mexS, fusA2, mexZ, mexY, parR, parS, oprD, ampD, pagL, amgS*), with the one obtained in our study: we could not find an exact correspondence between the two lists. However, the frequency of sequence variants in our population is higher in genes related or belonging to the same functional category than the ones present in the Greipel study. We found indeed the highest number of variants in the following genes: *gyrB* and *parE* directly related to *gyrA* and *parR*/*parS* respectively; furthermore, we found a frameshift mutation in *oprD* (ΔC437), present in Greipel's study too, and amino acid variations in the efflux pump *mexG* and the topoisomerase *parC*. In addition, we found a high number of variations in the pyoverdine biosynthesis gene *pvdl*, known to play a role in the adaptive process, and in the sensor kinase *pmrB*, involved in the production of cationic antimicrobial peptides and polymyxin resistance.

Six genomic islands were found in all genomes of the population, three of them were not identified, whereas the other three were tentatively assigned to LESGI-1, PAGI-2 and LESGI-3. LESGI-1 and LESGI-3 were first identified and characterised in the epidemic *P. aeruginosa* strain LESB58 [184]. LESGI-1 is described to contain phage- and transposon-related genes, together with coding sequences showing similarity with proteins of non-pseudomonad species [184]. LESGI-3 island has a mosaic compositional structure and present a significant homology to PAGI-2, PAGI-3, PAGI-5, and PAPI-1 [184][224] and, up to now, it was described to be an island unique to the LESB58 strain, since its particular structure was not found in other strains [225][226]. However, even if three protein clusters showed high identity with both LESGI-3 and PAGI-2, we saw two further protein clusters with an exclusive assignment to LESGI-3 in a different genomic region. We, therefore, consider more parsimonious to assign the first genomic region to PAGI-2 and the second genomic region, located about 1Mb downstream, to LESGI-3, rather than speculating on an event of duplication of LESGI-3. PAGI-2 was initially described in *P. aeruginosa* clone C isolates [227]. This island is divided into two main phage modules, one coding for chromosome-partitioning proteins (soj) and another containing a bacteriophage P4-related integrase [50]. PAGI-2 is present in approximately 40% of *P. aeruginosa* strains [228].

The evolution of strains in the CF airway is characterized by the loss of many virulence traits, including motility and protease secretion, along with the acquisition of multidrug resistance [23]. Functional phenotypic assays of the collection, including motility and secretion of proteases, showed a general decrease of these traits over time in the persistent isolates. In some cases, as previously reported [40][45], we observed the contemporary presence of isolates retaining traits typical of an early stage of infection (motility and secretion of proteases) and of isolates showing the typical characteristics of adaptation (loss of virulence factors, increased antibiotic resistance, overproduction of alginate and biofilm formation). Spearman's correlation analysis showed a decrease in alginate production over time. Mucoid phenotype was present mainly in earlier and intermediate isolates; previous studies have reported that *P. aeruginosa* loses mucoid phenotypes in the latest stages of CF lung disease, because its production requires high levels of energy

[18][57]; however, this is in contrast with what has been traditionally observed for the mucoid phenotype, that is associated with late stages of infection. Furthermore, in our work we observed that the same mucoid strain did not always show the exact amount of mucus when cultured on agar plates at different times; this may suggest that environment plays an important role on mucoidy, and that *in vitro* observations might significantly differ from what occurs *in vivo*, as described by Bragonzi *et al.* [229].
Swarming motility and protease production were present only in the earliest isolates. Lack of motility is usually associated with decreased virulence [230]. No isolate in our population showed twitching motility, which has been studied as an essential trait, along with mucoidy, to best predict subsequent pulmonary exacerbation [186]. The appearance of these phenotypes can be used as a potential marker of transition to chronic infection and advanced lung disease [186]. In previous studies [231][232] protease production was documented to change throughout infection, decreasing significantly in late chronic isolates, and this situation reflects our results, where we could only find protease secretion in a few early isolates. Biofilm formation assay showed that our isolates grew as sessile community mainly in the intermediate-late stage of infection. Biofilms are clinically relevant: biofilm-mediated infections that occur on medical devices like intravascular and urinary catheters, orthopaedic devices, and dialysis machines [233][234]. Chronic infections, such as recurrent ear infections and lung infections in CF patients, are caused by biofilm-dwelling bacteria [235][236][237]. Biofilms are known to be involved in 65–80% of all bacterial infections [238][234]. Also, biofilm growth offers a competitive advantage with respect to planktonic growth [239]: bacteria in biofilms are difficult to disrupt, and biofilms are often associated with antimicrobial resistance [234]. A positive correlation with the time of isolation was found for the hypermutable phenotype, which is a typical trait of *P. aeruginosa* chronic isolates [18]. Interestingly, all hypermutable strains were resistant to most of the antibiotics tested, with the only exception of TNCF_133_1 that is MDR but not hypermutable. The correlation could be explained considering that defects in the mismatch repair system cause a higher rate of mutability that can lead to the accumulation of mutations which can confer antibiotic resistance, as well as an enhanced genetic adaptation to CF airway [180][240]. Marvig et al. [45] found that different evolutionary paths of hypermutators can occur; they found a linear correlation between the number of SNPs and the time of sampling. From their collection of 55 DK2 genomes, nine sublineages had accumulated mutations at higher rates than expected, likely due to mutations in mismatch repair and error prevention genes. In total, they found 11 hypermutator strains within 55 isolates. In two patients, they found that hypermutator and normomutator clones coexisted, probably because different lineages lived in different niches within patients' lungs.
Overall MDR *P. aeruginosa* strains are developing with increasing frequency, leading to a triplication in their rates in the last two decades [241][242]. Some *P. aeruginosa* isolates have been found to be resistant to almost all or all antibiotics in clinical use [242], and estimates suggest that 25-45% of adult CF patients are chronically infected with MDR *P. aeruginosa* within their airways [243]. Antibiotic susceptibility profiles of the collection were determined for 12 molecules belonging to aminoglycosides, cephalosporines, fluoroquinolones, polymixins, β-lactams and carbapenems. While early isolates were found to be susceptible to almost all these antibiotics, resistant phenotypes dramatically

increased over time in the population. *Pseudomonas aeruginosa* is considered a paradigm of antimicrobial resistance development. It is intrinsically resistant to several antibiotics because of the low permeability of its outer membrane, the constitutive expression of various efflux pumps, and the production of antibiotic-inactivating enzymes [65]. Besides intrinsic resistance mechanisms, *P. aeruginosa* develops resistance during persistence in the airways by the accumulation of pathoadaptive mutations in genes encoding antibiotic resistance [64], e.g. β-lactamases and efflux pumps [9]. Although many mutations contributing to drug resistance have been identified, the relationship between specific mutations and the related phenotypic changes leading to resistance has yet to be fully elucidated. Genome analysis helps to predict potential molecular mechanisms of resistance and to identify gene products involved in antibiotic transport and efflux from bacterial cells. Whole-genome sequencing (WGS) has already proved to be able to predict antimicrobial susceptibility in several pathogens [244][245][52].

All the isolates in our collection were sensitive to Colistin, whereas nearly all the early isolates were susceptible to almost all the antibiotics tested, while the population became multiresistant during the persistance in the airways. Colistin (or polymyxin E) has been available on the market since 1959, but its use declined because of nephrotoxicity and neurotoxicity [246][247][248]. With the emergence of multidrug-resistant pathogens (e.g. *Acinetobacter baumannii*, *P. aeruginosa* and carbapenem-resistant Enterobacteriaceae), physicians started to use it again [249], although it remains a last-resort treatment.

Genomic analyses of the population showed a correlation between the evolution of antibiotic resistance profiles, MLST sequence types, and phylogenetic relationships. We further investigated the MDR isolates in comparison to the susceptible ones, looking specifically at the coding sequences of *P. aeruginosa* genes involved in antibiotic resistance and susceptibility. As described above, non-synonymous mutations were found in *gyrB*, *parE* and *pmrB*; additional variants present in the MDR isolates compared to the susceptible ones were: ΔC_{437} in the outer membrane porin gene *oprD* leading to a frameshift mutation in nearly all MDR isolates, P_{51}-S in MexG and N_{170}-S in the topoisomerase IV subunit A ParC.

The outer membrane protein OprD is involved in the resistance against β-lactams and carbapenems [250]. The protein contains 16 β-strands connected by short loops, eight of wich are external loops [251]. The deletion present in the MDR strains of the population disrupts the protein just before the fourth loop, and it is reported that the deletion of loops 3 and 4 results in a non-stable expression of the protein [251]. In *P. aeruginosa* repression or inactivation of OprD or a reduced protein expression contribute to moderate resistance to Imipenem [252] [253] [254], and carbapenem-resistant strains are often defective in expression of OprD [255]. Moreover, *P. aeruginosa* PA14 mutants for *oprD* showed an enhanced fitness in a murine model of mucosal colonisation and dissemination [256].

MexG, a component of the efflux pump MexGHI-OpmD, carries an amino acid substitution, P_{51}-S, in nearly all the MDR isolates; mutations in this pump are involved in the resistance to tetracycline and ticarcillin-clavulanate and implicated in the export of non-antibiotic compounds, including Vanadium [257].

Even if the N_{170}-S substitutions present in ParC in the MDR isolates is outside the QRDR domain, mutations in the topoisomerase IV subunit A *parC* gene, along with those described above in *gyrB* and *parC*, confer resistance to fluoroquinolones [258] [259] and

clinical isolates with mutations in the QRDR of *gyrA* and *parC* show high levels of fluoroquinolone resistance [260]. Aminoacid substitutions variations in *gyrB* and *parE* genes have a low frequency in clinical isolates, and they are described to have only a complementary role in fluoroquinolone resistance [258] [260]. In a recent study [261], most of the *P. aeruginosa* clinical isolates analysed had mutations in *gyrA* or *gyrB* or both *gyrA* and *parC*. The latter confers a resistant phenotype, with only a few isolates exhibiting mutations in only in *gyrB* in combination with *parE*. Marvig et al. [45] reconstructed the evolutionary history of the DK2 lineage and identified bacterial genes targeted by mutations to improve pathogen fitness, and found that several pathoadaptive genes in which they found multiple mutations were associated with antibiotic resistance such as *ampC* (β-lactams), *emrB* (quinolones), *ftsI* (penicillins, chloramphenicol, tetracyclines), *fusA* (fusidic acid), *gyrA/B* (quinolones), *mexB/Y* (β-lactams, quinolones, aminoglycosides, tetracyclines), *pmrB* (polymyxins), *pprA* (aminoglycosides), *oprD* (β-lactams), and *rpoB/C* (aminoglycosides, β-lactams, macrolides, tetracyclines).

Functional studies on specific strains. *Caenorhabditis elegans* has been used for numerous studies as an infection host for *Pseudomonas aeruginosa* and many other bacteria [204]. When *C. elegans* is fed with *P. aeruginosa* PA14, the gut is colonized and death occurs within days, alternatively known as slow killing [262][263]. In contrast, the fast killing assay results in *C. elegans* death within hours. While the fast killing assay does not necessarily require live bacteria and is caused by the production of secreted toxins including phenazines [264], the slow killing requires ingestion of live bacteria and their virulence factors [263]. *Pseudomonas aeruginosa* strains display a wide range of virulence phenotypes, where PA14 is among the most virulent strains and PAO1 among the ones with moderate slow killing activity [265]. The virulence requirements may vary within *P. aeruginosa* isolates as PAO1 was shown to induce a rapid, paralytic killing mechanism dependent on hydrogen cyanide production [266]. Our data clearly indicated that the acute-infection strain and the early CF isolates have a significantly higher killing rate compared to the late-infection isolate. Several delivered toxins have been reported as necessary for *P. aeruginosa* for killing *C. elegans* [262]. In previous investigations, we had noticed that TNCF_23 (early CF strain) and VrPa97 (acute strain) produce pyoverdine, while TNCF_175 (late CF strain) does not. This is consistent with a previous study reporting how *C. elegans* is killed by pyoverdin which uptakes iron from intracellular compartments, therefore functioning as a toxin [267].
The greater wax moth caterpillar, *Galleria mellonella,* has been used in several studies as an effective model for investigating the pathogenesis of many bacterial and fungal pathogens [205][206][207]. Advantages of this model include the ability to incubate larvae over a range of temperatures (15-37°C), ease of maintenance and handling and that the bacteria or drug inoculum can be accurately quantified prior to infection [268][269][270]. In the experiments with *Galleria mellonella*, VrPa97 appeared to be very aggressive, while TNCF_175 was significantly less virulent compared to VrPa97. TNCF_23 was instead weakly aggressive against *G. mellonella*, unlike what happened in the *C. elegans* assay. In a study of *P. aeruginosa* mutants, lipopolysaccharide-deficient isolates showed significantly reduced virulence in *G. mellonella*, whereas mutants with defects in pili, flagella, or proteases did not [271]. TNCF_23 is defective in type IV pili production, and

this may explain its reduced virulence against *G. mellonella*. The acute-infection strain VrPa97 is instead capable of killing both organisms. The late strain TNCF_175 showed low killing rates towards both *G. mellonella* and *C. elegans*, and this is consistent with a previous study that showed CF late chronic isolates to be less virulent compared to early-infection isolates [272].

In our study, we have also determined that, with the progression of the infection, immunomodulatory properties of isolates vary. Specifically, in the late stage of the infection the ability to induce cytokine secretion diminishes, while in the acute infection and early CF infection interleukin production is abundant. This is in complete agreement with previous studies in which multiple *P. aeruginosa* virulence factors (such as pilin, flagellin, proteases) have been shown to increase secretion of the chemokine IL-8 by human airway epithelial cells [201][202][203]. Loss of flagella allows bacteria to evade the immune system, thanks to the loss of engagement by phagocytic receptors that recognize flagellar components, and to the loss of immune activation through flagellin-mediated TLR signalling [273]. Loss of *P. aeruginosa* motility radically alters immune responses, but not flagellum expression itself, that results in bacterial resistance to phagocytosis by phagocytes [273]. Similarly, studies in the agar beads murine model using *P. aeruginosa* isolates from patients with CF showed that the risk of chronic infection is increased by the absence of pili and flagella [41]. In addition, TNCF_175 appeared to internalize more than VrPa97 and TNCF_23 in A549 cells. Internalization could benefit bacterial survival through evasion of host phagocytic- and antibody/complement-mediated killing mechanisms. Furthermore, in CF, a decreased internalization of *P .aeruginosa* in CFTR deficient cells may increase bacterial burdens and contribute to establish chronic infection in the lung [200][274].

To better understand the adaptation of selected strains, we observed their growth in Artificial Sputum Medium (ASM). ASM is a culture medium containing amino acids, mucin and free DNA, that mimics the composition of CF patient sputum. *Pseudomonas aeruginosa* growth in ASM should thus reflects growth during CF infection, with the formation of self-aggregating biofilm structures and population divergence [275][276][277]. ASM was originally created to study biofilm formation; in particular, it was noticed that *P. aeruginosa* grows as microcolonies in an environment that resembles CF lungs. This particular biofilm does not attach to the surface, whereas bacteria adhere to each other in the centre of the well [275]. Previous studies have used ASM models to study, for example, gene expression patterns and the effects of bacteriophages on *P. aeruginosa* [278][279][275]. Our results showed a general higher fitness of CF isolates in ASM compared with acute-infection strains or reference laboratory strains. In the competitive assay in ASM, the late isolate (TNCF_175) grew more slowly compared to the other two isolates, either when it was cultured alone or in pairs with VrPa97 or TNCF_23, suggesting the occurrence of a cell-to-cell interaction by which VrPa97 can kill FC175.

At this stage, we hypothesized that TNCF_175 was altered in one or more of its contact-dependent delivery systems. This hypothesis was corroborated by the finding of a mutation in TNCF_175 *tssK3* gene that could be associated with its lack of competitive growth ability. The mutation (C958T) leads to a premature stop-codon. The gene encodes a not yet characterized protein that is likely to be part of the baseplate in H3-T6SS. T6SS is the main contact-dependent delivery system responsible for the interactions between bacterial cells.

Several Gram-negative bacteria show at least one type of T6SS. *Pseudomonas aeruginosa* has three different T6SSs, recently found to be interdependent [137]: H1-, H2- and H3-T6SS. The extensively characterized H1-T6SS is known to be active against prokaryotic cells [116], while H2- and H3- have been shown to be active against either prokaryotic and eukaryotic cells [136][134]. T6SSs consist of effectors (proteins intended to attack neighbour cells by injecting toxins) and immunity proteins (proteins that protect the cells by attacks from T6SS of other cells) [116][128][127].
When testing T6SS functionality, we observed that TNCF_175 had an impaired T6SS, while that of TNCF_23 and VrPa97 was functional. The *tssK3*-encoded protein has currently not been characterized. Previous studies have demonstrated that its H1-T6SS homologous protein TssK is a trimer and is an essential subunit of the type VI secretion apparatus by connecting the trans-envelope membrane-complex to the phage-like contractile tail [157]. In addition, TssK has been shown to be part of the T6SS assembly platform or baseplate [280][150][152][281][157]. The same *tssK3* mutation has been found in other eight isolates from our collection: interestingly, the five latest isolates all carry the mutation, which appeared for the first time in TNCF_105, isolated in 2011. All *tssK3*-mutated strains belong to the MDR cluster of our phylogenetic analysis. In fact, the mutation seems to be conserved, suggesting that the disruption of the baseplate, and therefore of the H3-T6SS syringe, might have occurred because once the isolates have established in their niche in CF lung, no more warfare against other bacteria is required. Our results showed that bacterial cell-cell contact damages TNCF_175, and at the same time TNCF_175 cannot out-compete other strains, suggesting that TNCF_175 has both effector and immunity T6SS compartments impaired. Therefore, different mechanisms, along with the disruption of the H3-T6SS baseplate, are likely to contribute to the dramatic impairment of the whole attack/defense machinery in the late isolate TNCF_175.
To better understand the role of *tssK3* in the observed phenotypes, clean deletion mutants for this gene in the background of reference strains PA14 and PAO1 were constructed, PA14Δ*tssK3* and PAO1Δ*tssK3*. Clean mutants were subsequently complemented with a plasmid containing a constitutively expressed *tssK3* (PA14Δ*tssK3*p*tssK3* and PAO1Δ*tssK3*p*tssK3*). No significative differences were spotted in the growth rate in ASM of each strain co-cultured with VrPa97, suggesting that the *tssK3* impairment itself is not sufficient to explain TNCF_175 inability to survive in presence of VrPa97. These results suggest that *tssK3* may not be involved in T6SS-mediated immunity. Additional data were obtained by a series of *E. coli* DH5α killing assay performed with PA14, PA14Δ*tssK3*, PA14Δ*tssK3*p*tssK3*, PAO1, PAO1Δ*tssK3* and PAO1Δ*tssK3*p*tssK3*. Although data could not be statistically validated in all cases, a clear trend could be observed: both mutants, PA14Δ*tssK3* and PAO1Δ*tssK3* showed a reduced capability to kill *E. coli* compared to the relative wild-type and complemented strains. This would suggest that TssK3 is likely to play an important role in the correct functioning of H3-T6SS, allowing *P. aeruginosa* to attack neighbour cells, as previously demonstrated for TssK in H1-T6SS [159]. To investigate a possible role of *tssK3* in virulence against eukaryotic organisms as a support in toxin injection, PA14, PA14Δ*tssK3*, PA14Δ*tssK3*p*tssK3*, PAO1, PAO1Δ*tssK3* and PAO1Δ*tssK3*p*tssK3* were assessed for their capability of killing *C. elegans*. PA14, PA14Δ*tssK3* and PA14Δ*tssK3*p*tssK3* showed a remarkably high killing activity in *C. elegans*, with no significant difference among the three strains. PA14 is naturally very

aggressive against eukaryotes. Therefore it is difficult in this case to evaluate the role of *tssK3* in *C. elegans* killing, because of the presence of other virulence factors that may play a role. PA14 is well known to slowly kill *C.elegans* by accumulating and ejecting toxins in the intestinal lumen of the worm [262]. The same study showed that among 10 PA14 mutants, with different altered virulence-related genes, six of them showed a slightly decreased killing activity, while four of them showed the same aggressive behaviour against *C. elegans* as PA14 wild-type, suggesting that the combination of several factors is required for pathogenicity. PAO1 and PAO1Δ*tssK3* showed a very mild killing activity, while PAO1Δ*tssK3*p*tssK3* appeared to be noticeably more aggressive against *C. elegans*. This is probably because in the complemented strain *tssK3* is constitutively expressed, and it can thus contribute making the strain more virulent by maintaing the H3-T6SS constantly active. In PAO1 instead, *tssK3* is under the control of its native promoter that appears to be inactive in this context. It has been previously shown that PAO1 is not harmful for *C. elegans* when it is grown on Nematode Growth Medium, but it is toxic for *C. elegans* when it is grown on rich brain–heart infusion medium, by a mechanism that involves the generation of one or more neurotoxins, including hydrogen cyanide [282][266].

To sum up, our results contribute to demonstrate that chronic-infection strains in CF appear to be phenotypically "weaker" compared to the early infection strains, but at the same time they are able to persist and survive in the lungs for a long time. This is an important aspect, since persistence in the lung relies on a finely drawn up pathoadaptation, consisting in the accumulation of a set of loss-of-function mutations that allows bacteria to establish permanently in lung niches.

6. CONCLUSION AND PERSPECTIVES

A rare feature of our strain collection is the consistent number of clonal isolates obtained from a single patient over a period of 8 years, thus providing a model to look at microevolutionary trends within a highly homogenous bacterial population, and avoiding potential biases due to the host genetic background and clinical history. In spite of the close genomic relatedness of all isolates, a surprisingly high diversity was observed for most tested phenotypes, with particular reference to antibiotic susceptibility profiles. We observed an increased frequency of MDR isolates in the course of time in CF infection, which could not be explained by variations in known resistance genes. Uncharacterised variations revealed in this study should be further investigated to increase our knowledge on the emergence of MDR phenotypes.

By investigating the competitive ability of early versus late strains, we propose a role for T6SS in the adaptation process to the CF lung environment. Our data suggest that once persistence has been established, a strain no longer requires its T6SS, in which loss of function mutations may occur. Conversely, acute and early CF strains still carry a number of virulence factors, including T6SS that might provide an advantage in outcompeting other microorganisms in the initial stage of CF infection. Further studies are required to better understand the role of T6SS component TssK3. A secretion assay of Hcp3 protein to assess the effective activity of the H3-T6SS should be performed. Following the same approach as Ngyuyen et al. with the homologous TssK [159], it would be extremely useful to get a cristal of the protein to get insights into structural aspects. Transcriptomic approaches would also be helpful to better understand how the expression of genes encoding H3-T6SS units runs in the isolates belonging to our collection. It would also be useful, to verify the T3SS/T6SS switch and the underlying adaptation processes, to analyse the c-di-GMP levels in these strains. We have already obtained *tssK3* mutants in the background of reference strains PAO1 and PA14 that can be used for further analyses. However, to assess the role of the gene in clinical strains from our collection, it would be ideal to obtain mutant in the background of one of these strains. In spite of many attempts to mutate TNCF_23 during this study, no transformation was possible neither using electroporation nor conjugation, a known fact for CF strains that could be attributed to the large amount of exopolysaccharides surrounding cells, thus impeding transformation.

7. REFERENCES

[1] M. J. Welsh and A. E. Smith, “Cystic fibrosis.,” *Sci. Am.*, vol. 273, no. 6, pp. 52–9, Dec. 1995.

[2] T. F. Boat and P. W. Cheng, “Epithelial cell dysfunction in cystic fibrosis: implications for airways disease.,” *Acta Paediatr. Scand. Suppl.*, vol. 363, pp. 25-9-30, 1989.

[3] J. R. Riordan *et al.*, “Identification of the cystic fibrosis gene: cloning and characterization of complementary DNA.,” *Science*, vol. 245, no. 4922, pp. 1066–73, Sep. 1989.

[4] M. P. Rogan, D. A. Stoltz, and D. B. Hornick, “Cystic Fibrosis Transmembrane Conductance Regulator Intracellular Processing, Trafficking, and Opportunities for Mutation-Specific Treatment,” *Chest*, vol. 139, no. 6, pp. 1480–1490, Jun. 2011.

[5] B. S. Quon and S. M. Rowe, “New and emerging targeted therapies for cystic fibrosis,” *BMJ*, vol. 352, 2016.

[6] E. Quintana-Gallego, I. Delgado-Pecellín, and C. Calero Acuña, “CFTR Protein Repair Therapy in Cystic Fibrosis,” *Arch. Bronconeumol. (English Ed.*, vol. 50, no. 4, pp. 146–150, Apr. 2014.

[7] J. B. Lyczak, C. L. Cannon, and G. B. Pier, “Lung infections associated with cystic fibrosis.,” *Clin. Microbiol. Rev.*, vol. 15, no. 2, pp. 194–222, Apr. 2002.

[8] S. B. H. Ko *et al.*, “A molecular mechanism for aberrant CFTR-dependent HCO(3)(-) transport in cystic fibrosis.,” *EMBO J.*, vol. 21, no. 21, pp. 5662–72, Nov. 2002.

[9] L. Cullen and S. McClean, “Bacterial Adaptation during Chronic Respiratory Infections.,” *Pathog. (Basel, Switzerland)*, vol. 4, no. 1, pp. 66–89, Mar. 2015.

[10] C. R. Gault, L. M. Obeid, and Y. A. Hannun, “An overview of sphingolipid metabolism: From synthesis to breakdown,” *Adv. Exp. Med. Biol.*, vol. 688, pp. 1–23, 2010.

[11] M. P. Kowalski and G. B. Pier, “Localization of cystic fibrosis transmembrane conductance regulator to lipid rafts of epithelial cells is required for Pseudomonas aeruginosa-induced cellular activation.,” *J. Immunol.*, vol. 172, no. 1, pp. 418–25, Jan. 2004.

[12] I. R. Bates *et al.*, “Membrane lateral diffusion and capture of CFTR within transient confinement zones.,” *Biophys. J.*, vol. 91, no. 3, pp. 1046–58, Aug. 2006.

[13] Y. A. Hannun and L. M. Obeid, “Principles of bioactive lipid signalling: lessons from sphingolipids,” *Nat. Rev. Mol. Cell Biol.*, vol. 9, no. 2, pp. 139–150, Feb. 2008.

[14] “Ceramide in cystic fibrosis,” *Clin. Lipidol*, vol. 8, no. 6, pp. 681–692, 2013.

[15] H. Grassmé *et al.*, “CD95 Signaling via Ceramide-rich Membrane Rafts,” *J. Biol. Chem.*, vol. 276, no. 23, pp. 20589–20596, Jun. 2001.

[16] E. Gulbins and R. Kolesnick, “Raft ceramide in molecular medicine,” *Oncogene*, vol. 22, no. 45, pp. 7070–7077, Oct. 2003.

[17] Tuula A. Nurminen, Juha M. Holopainen, and Hongxia Zhao, and P. K. J. Kinnunen*, “Observation of Topical Catalysis by Sphingomyelinase Coupled To Microspheres,” 2002.

[18] A. M. Sousa and M. O. Pereira, “Pseudomonas aeruginosa Diversification during Infection Development in Cystic Fibrosis Lungs-A Review.,” *Pathog. (Basel, Switzerland)*, vol. 3, no. 3, pp. 680–703, Aug. 2014.

[19] I. J. Haq, M. A. Gray, J. P. Garnett, C. Ward, and M. Brodlie, “Airway surface liquid homeostasis in cystic fibrosis: pathophysiology and therapeutic targets,” *Thorax*, vol. 71, no. 3, pp. 284–287, Mar. 2016.

[20] D. C. Gadsby, P. Vergani, and L. Csanády, “The ABC protein turned chloride channel whose failure causes cystic fibrosis.,” *Nature*, vol. 440, no. 7083, pp. 477–83, Mar. 2006.

[21] H. G. Ahlgren *et al.*, “Clinical outcomes associated with Staphylococcus aureus and Pseudomonas aeruginosa airway infections in adult cystic fibrosis patients,” *BMC Pulm. Med.*, vol. 15, no. 1, p. 67, Dec. 2015.
[22] S. Besier *et al.*, “Prevalence and Clinical Significance of Staphylococcus aureus Small-Colony Variants in Cystic Fibrosis Lung Disease,” *J. Clin. Microbiol.*, vol. 45, no. 1, pp. 168–172, Jan. 2007.
[23] A. Folkesson *et al.*, “Adaptation of Pseudomonas aeruginosa to the cystic fibrosis airway: an evolutionary perspective.,” *Nat. Rev. Microbiol.*, vol. 10, no. 12, pp. 841–51, Dec. 2012.
[24] T. J. Kidd *et al.*, “Pseudomonas aeruginosa genotypes acquired by children with cystic fibrosis by age 5-years,” *J. Cyst. Fibros.*, vol. 14, no. 3, pp. 361–369, May 2015.
[25] E. L. Salsgiver *et al.*, “Changing Epidemiology of the Respiratory Bacteriology of Patients With Cystic Fibrosis,” *Chest*, vol. 149, no. 2, pp. 390–400, Feb. 2016.
[26] A. M. M. de Vrankrijker, T. F. W. Wolfs, and C. K. van der Ent, “Challenging and emerging pathogens in cystic fibrosis,” *Paediatr. Respir. Rev.*, vol. 11, no. 4, pp. 246–254, Dec. 2010.
[27] M. W. France, M. E. Dodd, J. R. Govan, C. J. Doherty, A. K. Webb, and A. M. Jones, “The changing epidemiology of Burkholderia species infection at an adult cystic fibrosis centre,” *J. Cyst. Fibros.*, vol. 7, no. 5, pp. 368–372, Sep. 2008.
[28] J. Bargon, N. Dauletbaev, B. Köhler, M. Wolf, H. G. Posselt, and T. O. Wagner, “Prophylactic antibiotic therapy is associated with an increased prevalence of Aspergillus colonization in adult cystic fibrosis patients.,” *Respir. Med.*, vol. 93, no. 11, pp. 835–8, Nov. 1999.
[29] M. V. Olson *et al.*, “Complete genome sequence of Pseudomonas aeruginosa PAO1, an opportunisticpathogen,” *Nature*, vol. 406, no. 6799, pp. 959–964, Aug. 2000.
[30] U. Dobrindt, B. Hochhut, U. Hentschel, and J. Hacker, “Genomic islands in pathogenic and environmental microorganisms,” *Nat. Rev. Microbiol.*, vol. 2, no. 5, pp. 414–424, May 2004.
[31] K. D. Schmidt, B. Tümmler, and U. Römling, “Comparative genome mapping of Pseudomonas aeruginosa PAO with P. aeruginosa C, which belongs to a major clone in cystic fibrosis patients and aquatic habitats.,” *J. Bacteriol.*, vol. 178, no. 1, pp. 85–93, Jan. 1996.
[32] S. E. Battle, J. Rello, and A. R. Hauser, “Genomic islands of Pseudomonas aeruginosa.,” *FEMS Microbiol. Lett.*, vol. 290, no. 1, pp. 70–8, Jan. 2009.
[33] X. Liang, X.-Q. T. Pham, M. V. Olson, and S. Lory, “Identification of a Genomic Island Present in the Majority of Pathogenic Isolates of Pseudomonas aeruginosa,” *J. Bacteriol.*, vol. 183, no. 3, pp. 843–853, Feb. 2001.
[34] K. D. Larbig *et al.*, “Gene islands integrated into tRNA(Gly) genes confer genome diversity on a Pseudomonas aeruginosa clone.,” *J. Bacteriol.*, vol. 184, no. 23, pp. 6665–80, Dec. 2002.
[35] J. He *et al.*, “The broad host range pathogen Pseudomonas aeruginosa strain PA14 carries two pathogenicity islands harboring plant and animal virulence genes.,” *Proc. Natl. Acad. Sci. U. S. A.*, vol. 101, no. 8, pp. 2530–5, Feb. 2004.
[36] J. Klockgether, O. Reva, K. Larbig, and B. Tümmler, “Sequence analysis of the mobile genome island pKLC102 of Pseudomonas aeruginosa C.,” *J. Bacteriol.*, vol. 186, no. 2, pp. 518–34, Jan. 2004.
[37] K. Mathee *et al.*, “Dynamics of Pseudomonas aeruginosa genome evolution,” *Proc. Natl. Acad. Sci.*, vol. 105, no. 8, pp. 3100–3105, Feb. 2008.
[38] C. Winstanley, S. O’Brien, and M. A. Brockhurst, “Pseudomonas aeruginosa Evolutionary Adaptation and Diversification in Cystic Fibrosis Chronic Lung Infections.,” *Trends Microbiol.*, vol. 24, no. 5, pp. 327–37, May 2016.

[39] E. E. Smith *et al.*, "Genetic adaptation by Pseudomonas aeruginosa to the airways of cystic fibrosis patients," *Proc. Natl. Acad. Sci.*, vol. 103, no. 22, pp. 8487–8492, May 2006.
[40] L. Yang *et al.*, "Evolutionary dynamics of bacteria in a human host environment," *Proc. Natl. Acad. Sci.*, vol. 108, no. 18, pp. 7481–7486, May 2011.
[41] A. Bragonzi *et al.*, "*Pseudomonas aeruginosa* Microevolution during Cystic Fibrosis Lung Infection Establishes Clones with Adapted Virulence," *Am. J. Respir. Crit. Care Med.*, vol. 180, no. 2, pp. 138–145, Jul. 2009.
[42] N. Cramer, J. Klockgether, K. Wrasman, M. Schmidt, C. F. Davenport, and B. Tümmler, "Microevolution of the major common Pseudomonas aeruginosa clones C and PA14 in cystic fibrosis lungs.," *Environ. Microbiol.*, vol. 13, no. 7, pp. 1690–704, Jul. 2011.
[43] C. Hoboth *et al.*, "Dynamics of adaptive microevolution of hypermutable Pseudomonas aeruginosa during chronic pulmonary infection in patients with cystic fibrosis.," *J. Infect. Dis.*, vol. 200, no. 1, pp. 118–30, Jul. 2009.
[44] R. L. Marvig *et al.*, "Within-host microevolution of Pseudomonas aeruginosa in Italian cystic fibrosis patients," *BMC Microbiol.*, vol. 15, no. 1, p. 218, Dec. 2015.
[45] R. L. Marvig, H. K. Johansen, S. Molin, and L. Jelsbak, "Genome Analysis of a Transmissible Lineage of Pseudomonas aeruginosa Reveals Pathoadaptive Mutations and Distinct Evolutionary Paths of Hypermutators," *PLoS Genet.*, vol. 9, no. 9, p. e1003741, Sep. 2013.
[46] R. L. Marvig, L. M. Sommer, S. Molin, and H. K. Johansen, "Convergent evolution and adaptation of Pseudomonas aeruginosa within patients with cystic fibrosis," *Nat. Genet.*, vol. 47, no. 1, pp. 57–64, Nov. 2014.
[47] R. L. Marvig, L. M. Sommer, L. Jelsbak, S. Molin, and H. K. Johansen, "Evolutionary insight from whole-genome sequencing of *Pseudomonas aeruginosa* from cystic fibrosis patients," *Future Microbiol.*, vol. 10, no. 4, pp. 599–611, Apr. 2015.
[48] D. Balasubramanian, L. Schneper, H. Kumari, and K. Mathee, "A dynamic and intricate regulatory network determines Pseudomonas aeruginosa virulence," *Nucleic Acids Res.*, vol. 41, no. 1, pp. 1–20, Jan. 2013.
[49] J. L. Fothergill, M. J. Walshaw, and C. Winstanley, "Transmissible strains of *Pseudomonas aeruginosa* in cystic fibrosis lung infections," *Eur. Respir. J.*, vol. 40, no. 1, pp. 227–238, Jul. 2012.
[50] C. Winstanley *et al.*, "Newly introduced genomic prophage islands are critical determinants of in vivo competitiveness in the Liverpool Epidemic Strain of Pseudomonas aeruginosa," *Genome Res.*, vol. 19, no. 1, pp. 12–23, Oct. 2008.
[51] D. Armstrong *et al.*, "Evidence for spread of a clonal strain of Pseudomonas aeruginosa among cystic fibrosis clinics.," *J. Clin. Microbiol.*, vol. 41, no. 5, pp. 2266–7, May 2003.
[52] C. López-Causapé *et al.*, "Evolution of the Pseudomonas aeruginosa mutational resistome in an international Cystic Fibrosis clone," *Sci. Rep.*, vol. 7, no. 1, p. 5555, Dec. 2017.
[53] D. Nguyen and P. K. Singh, "Evolving stealth: genetic adaptation of Pseudomonas aeruginosa during cystic fibrosis infections.," *Proc. Natl. Acad. Sci. U. S. A.*, vol. 103, no. 22, pp. 8305–6, May 2006.
[54] A. Mena *et al.*, "Genetic adaptation of Pseudomonas aeruginosa to the airways of cystic fibrosis patients is catalyzed by hypermutation.," *J. Bacteriol.*, vol. 190, no. 24, pp. 7910–7, Dec. 2008.
[55] H. K. Huse, T. Kwon, J. E. A. Zlosnik, D. P. Speert, E. M. Marcotte, and M. Whiteley, "Parallel Evolution in Pseudomonas aeruginosa over 39,000 Generations In Vivo," *MBio*, vol. 1, no. 4, pp. e00199-10-e00199-17, Nov. 2010.

[56] E. Mowat *et al.*, "*Pseudomonas aeruginosa* Population Diversity and Turnover in Cystic Fibrosis Chronic Infections," *Am. J. Respir. Crit. Care Med.*, vol. 183, no. 12, pp. 1674–1679, Jun. 2011.
[57] M. Hogardt and J. Heesemann, "Adaptation of Pseudomonas aeruginosa during persistence in the cystic fibrosis lung," *Int. J. Med. Microbiol.*, vol. 300, no. 8, pp. 557–562, Dec. 2010.
[58] F. Blasi and S. L. Johnston, "The role of antibiotics in asthma," *Int. J. Antimicrob. Agents*, vol. 29, no. 5, pp. 485–493, May 2007.
[59] G. Khanbabaee *et al.*, "A survey on pulmonary pathogens and their antibiotic susceptibility among cystic fibrosis patients.," *Braz. J. Infect. Dis.*, vol. 16, no. 2, pp. 122–8.
[60] F. Blasi, P. Tarsia, M. Pappalettera, M. Saporiti, and S. Aliberti, "Antibiotic therapy and prophylaxis in COPD," *Respir. Med. COPD Updat.*, vol. 2, no. 4, pp. 124–132, Feb. 2007.
[61] A. Martins, A. Hunyadi, and L. Amaral, "Mechanisms of resistance in bacteria: an evolutionary approach.," *Open Microbiol. J.*, vol. 7, pp. 53–8, 2013.
[62] M. N. Alekshun and S. B. Levy, "Molecular Mechanisms of Antibacterial Multidrug Resistance," *Cell*, vol. 128, no. 6, pp. 1037–1050, Mar. 2007.
[63] A. J. Alanis, "Resistance to Antibiotics: Are We in the Post-Antibiotic Era?," *Arch. Med. Res.*, vol. 36, no. 6, pp. 697–705, Nov. 2005.
[64] E. B. M. Breidenstein, C. de la Fuente-Núñez, and R. E. W. Hancock, "Pseudomonas aeruginosa: all roads lead to resistance," *Trends Microbiol.*, vol. 19, no. 8, pp. 419–426, Aug. 2011.
[65] R. E. Hancock, "Resistance mechanisms in Pseudomonas aeruginosa and other nonfermentative gram-negative bacteria.," *Clin. Infect. Dis.*, vol. 27 Suppl 1, pp. S93-9, Aug. 1998.
[66] X. Z. Li, H. Nikaido, and K. Poole, "Role of mexA-mexB-oprM in antibiotic efflux in Pseudomonas aeruginosa.," *Antimicrob. Agents Chemother.*, vol. 39, no. 9, pp. 1948–53, Sep. 1995.
[67] X. Z. Li, L. Zhang, and K. Poole, "Interplay between the MexA-MexB-OprM multidrug efflux system and the outer membrane barrier in the multiple antibiotic resistance of Pseudomonas aeruginosa.," *J. Antimicrob. Chemother.*, vol. 45, no. 4, pp. 433–6, Apr. 2000.
[68] S. B. Vakulenko and S. Mobashery, "Versatility of aminoglycosides and prospects for their future.," *Clin. Microbiol. Rev.*, vol. 16, no. 3, pp. 430–50, Jul. 2003.
[69] K. Tanimoto, H. Tomita, S. Fujimoto, K. Okuzumi, and Y. Ike, "Fluoroquinolone Enhances the Mutation Frequency for Meropenem-Selected Carbapenem Resistance in Pseudomonas aeruginosa, but Use of the High-Potency Drug Doripenem Inhibits Mutant Formation," *Antimicrob. Agents Chemother.*, vol. 52, no. 10, pp. 3795–3800, Oct. 2008.
[70] K. Driffield, K. Miller, J. M. Bostock, A. J. O'Neill, and I. Chopra, "Increased mutability of Pseudomonas aeruginosa in biofilms," *J. Antimicrob. Chemother.*, vol. 61, no. 5, pp. 1053–1056, Mar. 2008.
[71] I. Wiegand, A. K. Marr, E. B. M. Breidenstein, K. N. Schurek, P. Taylor, and R. E. W. Hancock, "Mutator genes giving rise to decreased antibiotic susceptibility in Pseudomonas aeruginosa.," *Antimicrob. Agents Chemother.*, vol. 52, no. 10, pp. 3810–3, Oct. 2008.
[72] A. Oliver, R. Cantón, P. Campo, F. Baquero, and J. Blázquez, "High frequency of hypermutable Pseudomonas aeruginosa in cystic fibrosis lung infection.," *Science*, vol. 288, no. 5469, pp. 1251–4, May 2000.
[73] H. G. Stickland, P. W. Davenport, K. S. Lilley, J. L. Griffin, and M. Welch, "Mutation

of *nfxB* Causes Global Changes in the Physiology and Metabolism of *Pseudomonas aeruginosa*," *J. Proteome Res.*, vol. 9, no. 6, pp. 2957–2967, Jun. 2010.
[74] F. Walsh and S. G. B. Amyes, "Carbapenem Resistance in Clinical Isolates of *Pseudomonas aeruginosa*," *J. Chemother.*, vol. 19, no. 4, pp. 376–381, Aug. 2007.
[75] M. L. Sobel, S. Neshat, and K. Poole, "Mutations in PA2491 (mexS) promote MexT-dependent mexEF-oprN expression and multidrug resistance in a clinical strain of Pseudomonas aeruginosa.," *J. Bacteriol.*, vol. 187, no. 4, pp. 1246–53, Feb. 2005.
[76] D. C. Hooper, "Emerging mechanisms of fluoroquinolone resistance.," *Emerg. Infect. Dis.*, vol. 7, no. 2, pp. 337–41.
[77] D. Hocquet *et al.*, "MexXY-OprM efflux pump is necessary for a adaptive resistance of Pseudomonas aeruginosa to aminoglycosides.," *Antimicrob. Agents Chemother.*, vol. 47, no. 4, pp. 1371–5, Apr. 2003.
[78] B. Rehm and Wiley InterScience (Online service), *Pseudomonas : model organism, pathogen, cell factory*. Wiley-VCH, 2008.
[79] G. A. O'Toole, "Microtiter dish biofilm formation assay.," *J. Vis. Exp.*, no. 47, Jan. 2011.
[80] D. Worlitzsch *et al.*, "Effects of reduced mucus oxygen concentration in airway Pseudomonas infections of cystic fibrosis patients," *J. Clin. Invest.*, vol. 109, no. 3, pp. 317–325, Feb. 2002.
[81] S. Häussler, "Multicellular signalling and growth of Pseudomonas aeruginosa," *Int. J. Med. Microbiol.*, vol. 300, no. 8, pp. 544–548, Dec. 2010.
[82] M. Kostakioti, M. Hadjifrangiskou, and S. J. Hultgren, "Bacterial Biofilms: Development, Dispersal, and Therapeutic Strategies in the Dawn of the Postantibiotic Era," *Cold Spring Harb. Perspect. Med.*, vol. 3, no. 4, pp. a010306–a010306, Apr. 2013.
[83] D. Davies, "Understanding biofilm resistance to antibacterial agents," *Nat. Rev. Drug Discov.*, vol. 2, no. 2, pp. 114–122, Feb. 2003.
[84] N. Høiby, T. Bjarnsholt, M. Givskov, S. Molin, and O. Ciofu, "Antibiotic resistance of bacterial biofilms," *Int. J. Antimicrob. Agents*, vol. 35, no. 4, pp. 322–332, Apr. 2010.
[85] T.-F. Mah, "Biofilm-specific antibiotic resistance," *Future Microbiol.*, vol. 7, no. 9, pp. 1061–1072, Sep. 2012.
[86] Y. A. Nikolaev and V. K. Plakunov, "Biofilm—'City of microbes' or an analogue of multicellular organisms?," *Microbiology*, vol. 76, no. 2, pp. 125–138, Apr. 2007.
[87] B. I. Kazmierczak, M. Schniederberend, and R. Jain, "Cross-regulation of Pseudomonas motility systems: the intimate relationship between flagella, pili and virulence," *Curr. Opin. Microbiol.*, vol. 28, pp. 78–82, Dec. 2015.
[88] M. R. Hassett *et al.*, "The Exopolysaccharide Alginate Protects The Exopolysaccharide Alginate Protects Pseudomonas aeruginosa Biofilm Bacteria from IFN-▪ -Mediated Macrophage Killing," *J Immunol Ref.*, vol. 175175117512, pp. 7512–7518, 2005.
[89] D. M. G. Cochrane, M. R. W. Brown, H. Anwar, P. H. Weller, K. Lam, and J. W. Costerton, "Antibody response to Pseudomonas aeruginosa surface protein antigens in a rat model of chronic lung infection," *J. Med. Microbiol.*, vol. 27, no. 4, pp. 255–261, Dec. 1988.
[90] J. C. Nickel, I. Ruseska, J. B. Wright, and J. W. Costerton, "Tobramycin resistance of Pseudomonas aeruginosa cells growing as a biofilm on urinary catheter material.," *Antimicrob. Agents Chemother.*, vol. 27, no. 4, pp. 619–24, Apr. 1985.
[91] Y.-S. T. Chang, J. Klockgether, and B. TÃ¼mmler, "An intragenic deletion in *pilQ* leads to nonpiliation of a *Pseudomonas aeruginosa* strain isolated from cystic fibrosis lung," *FEMS Microbiol. Lett.*, vol. 270, no. 2, pp. 201–206, May 2007.

[92] A. U. Kresse, S. D. Dinesh, K. Larbig, and U. Römling, “Impact of large chromosomal inversions on the adaptation and evolution of Pseudomonas aeruginosa chronically colonizing cystic fibrosis lungs.,” *Mol. Microbiol.*, vol. 47, no. 1, pp. 145–58, Jan. 2003.
[93] Q. Lu *et al.*, “Pseudomonas aeruginosa serotypes in nosocomial pneumonia: prevalence and clinical outcomes.,” *Crit. Care*, vol. 18, no. 1, p. R17, Jan. 2014.
[94] A. M. Hajjar, R. K. Ernst, J. H. Tsai, C. B. Wilson, and S. I. Miller, “Human Toll-like receptor 4 recognizes host-specific LPS modifications,” *Nat. Immunol.*, vol. 3, no. 4, pp. 354–359, Apr. 2002.
[95] C. Cigana *et al.*, “Pseudomonas aeruginosa exploits lipid A and muropeptides modification as a strategy to lower innate immunity during cystic fibrosis lung infection.,” *PLoS One*, vol. 4, no. 12, p. e8439, Dec. 2009.
[96] R. K. Ernst, A. M. Hajjar, J. H. Tsai, S. M. Moskowitz, C. B. Wilson, and S. I. Miller, “<I>Pseudomonas aeruginosa</I> lipid A diversity and its recognition by Toll-like receptor 4,” *J. Endotoxin Res.*, vol. 9, no. 6, pp. 395–400, Dec. 2003.
[97] R. K. Ernst *et al.*, “Specific lipopolysaccharide found in cystic fibrosis airway Pseudomonas aeruginosa.,” *Science*, vol. 286, no. 5444, pp. 1561–5, Nov. 1999.
[98] D. J. Evans, G. B. Pier, M. J. Coyne, and J. B. Goldberg, “The rfb locus from Pseudomonas aeruginosa strain PA103 promotes the expression of O antigen by both LPS-rough and LPS-smooth isolates from cystic fibrosis patients.,” *Mol. Microbiol.*, vol. 13, no. 3, pp. 427–34, Aug. 1994.
[99] D. H. Spencer *et al.*, “Whole-genome sequence variation among multiple isolates of Pseudomonas aeruginosa.,” *J. Bacteriol.*, vol. 185, no. 4, pp. 1316–25, Feb. 2003.
[100] R. K. Ernst *et al.*, “Genome mosaicism is conserved but not unique in Pseudomonas aeruginosa isolates from the airways of young children with cystic fibrosis.,” *Environ. Microbiol.*, vol. 5, no. 12, pp. 1341–9, Dec. 2003.
[101] A. Managò *et al.*, “*Pseudomonas aeruginosa* Pyocyanin Induces Neutrophil Death *via* Mitochondrial Reactive Oxygen Species and Mitochondrial Acid Sphingomyelinase,” *Antioxid. Redox Signal.*, vol. 22, no. 13, pp. 1097–1110, May 2015.
[102] V. Gasser, L. Guillon, O. Cunrath, and I. J. Schalk, “Cellular organization of siderophore biosynthesis in Pseudomonas aeruginosa: Evidence for siderosomes,” *J. Inorg. Biochem.*, vol. 148, pp. 27–34, Jul. 2015.
[103] R. Hoge, A. Pelzer, F. Rosenau, and S. Wilhelm, “" Weapons of a pathogen: Proteases and their role in virulence of Pseudomonas aeruginosa "”
[104] A. Rietsch, I. Vallet-Gely, S. L. Dove, and J. J. Mekalanos, “ExsE, a secreted regulator of type III secretion genes in Pseudomonas aeruginosa,” *Proc. Natl. Acad. Sci.*, vol. 102, no. 22, pp. 8006–8011, May 2005.
[105] K. Faure, D. Shimabukuro, T. Ajayi, L. R. Allmond, T. Sawa, and J. P. Wiener-Kronish, “O-antigen serotypes and type III secretory toxins in clinical isolates of Pseudomonas aeruginosa.,” *J. Clin. Microbiol.*, vol. 41, no. 5, pp. 2158–60, May 2003.
[106] A. Roy-Burman *et al.*, “Type III Protein Secretion Is Associated with Death in Lower Respiratory and Systemic *Pseudomonas aeruginosa* Infections,” *J. Infect. Dis.*, vol. 183, no. 12, pp. 1767–1774, Jun. 2001.
[107] A. L. Goodman, B. Kulasekara, A. Rietsch, D. Boyd, R. S. Smith, and S. Lory, “A Signaling Network Reciprocally Regulates Genes Associated with Acute Infection and Chronic Persistence in Pseudomonas aeruginosa,” *Dev. Cell*, vol. 7, no. 5, pp. 745–754, Nov. 2004.
[108] I. Ventre *et al.*, “Multiple sensors control reciprocal expression of Pseudomonas aeruginosa regulatory RNA and virulence genes,” *Proc. Natl. Acad. Sci.*, vol. 103, no.

1, pp. 171–176, Jan. 2006.
[109] J. A. Moscoso, H. Mikkelsen, S. Heeb, P. Williams, and A. Filloux, "The Pseudomonas aeruginosa sensor RetS switches Type III and Type VI secretion via c-di-GMP signalling," *Environ. Microbiol.*, vol. 13, no. 12, pp. 3128–3138, Dec. 2011.
[110] A. L. Goodman, M. Merighi, M. Hyodo, I. Ventre, A. Filloux, and S. Lory, "Direct interaction between sensor kinase proteins mediates acute and chronic disease phenotypes in a bacterial pathogen," *Genes Dev.*, vol. 23, no. 2, pp. 249–259, Jan. 2009.
[111] A. Brencic and S. Lory, "Determination of the regulon and identification of novel mRNA targets of *Pseudomonas aeruginosa* RsmA," *Mol. Microbiol.*, vol. 72, no. 3, pp. 612–632, May 2009.
[112] R. Hengge, "Principles of c-di-GMP signalling in bacteria," *Nat. Rev. Microbiol.*, vol. 7, no. 4, pp. 263–273, Apr. 2009.
[113] J. W. Hickman, D. F. Tifrea, and C. S. Harwood, "A chemosensory system that regulates biofilm formation through modulation of cyclic diguanylate levels.," *Proc. Natl. Acad. Sci. U. S. A.*, vol. 102, no. 40, pp. 14422–7, Oct. 2005.
[114] V. T. Lee, J. M. Matewish, J. L. Kessler, M. Hyodo, Y. Hayakawa, and S. Lory, "A cyclic-di-GMP receptor required for bacterial exopolysaccharide production.," *Mol. Microbiol.*, vol. 65, no. 6, pp. 1474–84, Sep. 2007.
[115] M. Starkey *et al.*, "Pseudomonas aeruginosa rugose small-colony variants have adaptations that likely promote persistence in the cystic fibrosis lung.," *J. Bacteriol.*, vol. 191, no. 11, pp. 3492–503, Jun. 2009.
[116] R. D. Hood *et al.*, "A Type VI Secretion System of Pseudomonas aeruginosa Targets a Toxin to Bacteria," *Cell Host Microbe*, vol. 7, no. 1, pp. 25–37, Jan. 2010.
[117] A. B. Russell *et al.*, "A Type VI Secretion-Related Pathway in Bacteroidetes Mediates Interbacterial Antagonism," *Cell Host Microbe*, vol. 16, no. 2, pp. 227–236, Aug. 2014.
[118] Y. Fu, M. K. Waldor, and J. J. Mekalanos, "Tn-Seq analysis of Vibrio cholerae intestinal colonization reveals a role for T6SS-mediated antibacterial activity in the host.," *Cell Host Microbe*, vol. 14, no. 6, pp. 652–63, Dec. 2013.
[119] L.-S. Ma, A. Hachani, J.-S. Lin, A. Filloux, and E.-M. Lai, "Agrobacterium tumefaciens deploys a superfamily of type VI secretion DNase effectors as weapons for interbacterial competition in planta.," *Cell Host Microbe*, vol. 16, no. 1, pp. 94–104, Jul. 2014.
[120] S. Shrivastava and S. S. Mande, "Identification and functional characterization of gene components of Type VI Secretion system in bacterial genomes.," *PLoS One*, vol. 3, no. 8, p. e2955, Aug. 2008.
[121] S. Pukatzki *et al.*, "Identification of a conserved bacterial protein secretion system in Vibrio cholerae using the Dictyostelium host model system," *Proc. Natl. Acad. Sci.*, vol. 103, no. 5, pp. 1528–1533, Jan. 2006.
[122] P. G. Leiman *et al.*, "Type VI secretion apparatus and phage tail-associated protein complexes share a common evolutionary origin."
[123] M. M. Shneider, S. A. Buth, B. T. Ho, M. Basler, J. J. Mekalanos, and P. G. Leiman, "PAAR-repeat proteins sharpen and diversify the type VI secretion system spike," *Nature*, vol. 500, no. 7462, pp. 350–353, Aug. 2013.
[124] M. Kudryashev *et al.*, "Structure of the Type VI Secretion System Contractile Sheath," *Cell*, vol. 160, no. 5, pp. 952–962, Feb. 2015.
[125] E. Durand *et al.*, "Biogenesis and structure of a type VI secretion membrane core complex," *Nature*, vol. 523, no. 7562, pp. 555–560, Jul. 2015.
[126] F. R. Cianfanelli, L. Monlezun, and S. J. Coulthurst, "Aim, Load, Fire: The Type VI Secretion System, a Bacterial Nanoweapon," *Trends Microbiol.*, vol. 24, no. 1, pp.

51–62, Jan. 2016.
[127] M. Li *et al.*, "Structural Basis for Type VI Secretion Effector Recognition by a Cognate Immunity Protein," *PLoS Pathog.*, vol. 8, no. 4, p. e1002613, Apr. 2012.
[128] A. B. Russell, R. D. Hood, N. K. Bui, M. LeRoux, W. Vollmer, and J. D. Mougous, "Type VI secretion delivers bacteriolytic effectors to target cells," *Nature*, vol. 475, no. 7356, pp. 343–347, Jul. 2011.
[129] J. Benz, C. Sendlmeier, T. R. M. Barends, and A. Meinhart, "Structural insights into the effector-immunity system Tse1/Tsi1 from Pseudomonas aeruginosa.," *PLoS One*, vol. 7, no. 7, p. e40453, Jul. 2012.
[130] J. C. Whitney *et al.*, "Genetically distinct pathways guide effector export through the type VI secretion system," *Mol. Microbiol.*, vol. 92, no. 3, pp. 529–542, May 2014.
[131] J. C. Whitney *et al.*, "An interbacterial NAD(P)(+) glycohydrolase toxin requires elongation factor Tu for delivery to target cells.," *Cell*, vol. 163, no. 3, pp. 607–19, Oct. 2015.
[132] T. G. Sana, B. Berni, and S. Bleves, "The T6SSs of Pseudomonas aeruginosa Strain PAO1 and Their Effectors: Beyond Bacterial-Cell Targeting," *Front. Cell. Infect. Microbiol.*, vol. 6, no. June, p. 61, 2016.
[133] A. B. Russell *et al.*, "Diverse type VI secretion phospholipases are functionally plastic antibacterial effectors," *Nature*, vol. 496, no. 7446, pp. 508–512, Apr. 2013.
[134] F. Jiang, N. R. Waterfield, J. Yang, G. Yang, and Q. Jin, "A Pseudomonas aeruginosa Type VI Secretion Phospholipase D Effector Targets Both Prokaryotic and Eukaryotic Cells," *Cell Host Microbe*, vol. 15, no. 5, pp. 600–610, May 2014.
[135] B. Lesic, M. Starkey, J. He, R. Hazan, and L. G. Rahme, "Quorum sensing differentially regulates Pseudomonas aeruginosa type VI secretion locus I and homologous loci II and III, which are required for pathogenesis.," *Microbiology*, vol. 155, no. Pt 9, pp. 2845–55, Sep. 2009.
[136] T. G. Sana *et al.*, "The second type VI secretion system of Pseudomonas aeruginosa strain PAO1 is regulated by quorum sensing and Fur and modulates internalization in epithelial cells.," *J. Biol. Chem.*, vol. 287, no. 32, pp. 27095–105, Aug. 2012.
[137] L. P. Allsopp *et al.*, "RsmA and AmrZ orchestrate the assembly of all three type VI secretion systems in *Pseudomonas aeruginosa*," *Proc. Natl. Acad. Sci.*, p. 201700286, Jul. 2017.
[138] E. Cascales and C. Cambillau, "Structural biology of type VI secretion systems."
[139] S. J. Coulthurst, "The Type VI secretion system – a widespread and versatile cell targeting system," *Res. Microbiol.*, vol. 164, no. 6, pp. 640–654, Jul. 2013.
[140] M.-S. Aschtgen, C. S. Bernard, S. De Bentzmann, R. Lloubès, and E. Cascales, "SciN is an outer membrane lipoprotein required for type VI secretion in enteroaggregative Escherichia coli.," *J. Bacteriol.*, vol. 190, no. 22, pp. 7523–31, Nov. 2008.
[141] M.-S. Aschtgen, M. Gavioli, A. Dessen, R. Lloubès, and E. Cascales, "The SciZ protein anchors the enteroaggregative *Escherichia coli* Type VI secretion system to the cell wall," *Mol. Microbiol.*, vol. 75, no. 4, pp. 886–899, Feb. 2010.
[142] M.-S. Aschtgen, A. Zoued, R. Lloubès, L. Journet, and E. Cascales, "The C-tail anchored TssL subunit, an essential protein of the enteroaggregative *Escherichia coli* Sci-1 Type VI secretion system, is inserted by YidC," *Microbiologyopen*, vol. 1, no. 1, pp. 71–82, Mar. 2012.
[143] E. Durand *et al.*, "Structural characterization and oligomerization of the TssL protein, a component shared by bacterial type VI and type IVb secretion systems.," *J. Biol. Chem.*, vol. 287, no. 17, pp. 14157–68, Apr. 2012.
[144] M.-S. Aschtgen, M. S. Thomas, and E. Cascales, "Anchoring the type VI secretion system to the peptidoglycan: TssL, TagL, TagP… what else?," *Virulence*, vol. 1, no. 6, pp. 535–540, Nov. 2010.

[145] B. S. Weber *et al.*, “Genetic Dissection of the Type VI Secretion System in Acinetobacter and Identification of a Novel Peptidoglycan Hydrolase, TagX, Required for Its Biogenesis.”
[146] Y. G. Santin and E. Cascales, “Domestication of a housekeeping transglycosylase for assembly of a Type VI secretion system,” *EMBO Rep.*, vol. 18, no. 1, pp. 138–149, Jan. 2017.
[147] Y. R. Brunet, J. Henin, H. Celia, and E. Cascales, “Type VI secretion and bacteriophage tail tubes share a common assembly pathway,” *EMBO Rep.*, vol. 15, no. 3, pp. 315–321, Mar. 2014.
[148] A. Mikhail Kudryashev, R. Yu-Ruei Wang, E. H. Egelman, and M. Basler Correspondence, “Structure of the Type VI Secretion System Contractile Sheath,” *Cell*, vol. 160, pp. 952–962, 2015.
[149] G. English, O. Byron, F. R. Cianfanelli, A. R. Prescott, and S. J. Coulthurst, “Biochemical analysis of TssK, a core component of the bacterial Type VI secretion system, reveals distinct oligomeric states of TssK and identifies a TssK–TssFG subcomplex,” *Biochem. J.*, vol. 461, no. 2, pp. 291–304, Jul. 2014.
[150] Y. R. Brunet, A. Zoued, F. Boyer, B. Douzi, and E. Cascales, “The Type VI Secretion TssEFGK-VgrG Phage-Like Baseplate Is Recruited to the TssJLM Membrane Complex via Multiple Contacts and Serves As Assembly Platform for Tail Tube/Sheath Polymerization,” *PLOS Genet.*, vol. 11, no. 10, p. e1005545, Oct. 2015.
[151] A. Zoued *et al.*, “Priming and polymerization of a bacterial contractile tail structure,” *Nature*, vol. 531, no. 7592, pp. 59–63, Feb. 2016.
[152] M. Basler, M. Pilhofer, G. P. Henderson, G. J. Jensen, and J. J. Mekalanos, “Type VI secretion requires a dynamic contractile phage tail-like structure.,” *Nature*, vol. 483, no. 7388, pp. 182–6, Feb. 2012.
[153] M. LeRoux *et al.*, “Quantitative single-cell characterization of bacterial interactions reveals type VI secretion is a double-edged sword.,” *Proc. Natl. Acad. Sci. U. S. A.*, vol. 109, no. 48, pp. 19804–9, Nov. 2012.
[154] M. Basler *et al.*, “Tit-for-Tat: Type VI Secretion System Counterattack during Bacterial Cell-Cell Interactions,” *Cell*, vol. 152, no. 4, pp. 884–894, Feb. 2013.
[155] Y. R. Brunet, L. Espinosa, S. Harchouni, T. Mignot, and E. Cascales, “Imaging Type VI Secretion-Mediated Bacterial Killing,” *Cell Rep.*, vol. 3, no. 1, pp. 36–41, Jan. 2013.
[156] S. Planamente, O. Salih, E. Manoli, D. Albesa-Jové, P. S. Freemont, and A. Filloux, “TssA forms a gp6-like ring attached to the type VI secretion sheath,” *EMBO J.*, vol. 35, no. 15, pp. 1613–1627, Aug. 2016.
[157] A. Zoued *et al.*, “TssK is a trimeric cytoplasmic protein interacting with components of both phage-like and membrane anchoring complexes of the type VI secretion system.,” *J. Biol. Chem.*, vol. 288, no. 38, pp. 27031–41, Sep. 2013.
[158] L. Logger, M.-S. Aschtgen, M. Guérin, E. Cascales, and E. Durand, “Molecular Dissection of the Interface between the Type VI Secretion TssM Cytoplasmic Domain and the TssG Baseplate Component,” *J. Mol. Biol.*, vol. 428, no. 22, pp. 4424–4437, Nov. 2016.
[159] V. S. Nguyen *et al.*, “Type VI secretion TssK baseplate protein exhibits structural similarity with phage receptor-binding proteins and evolved to bind the membrane complex,” *Nat. Microbiol.*, vol. 17103, no. June, pp. 1–9, 2017.
[160] A. Bankevich *et al.*, “SPAdes: a new genome assembly algorithm and its applications to single-cell sequencing.,” *J. Comput. Biol.*, vol. 19, no. 5, pp. 455–77, May 2012.
[161] T. Seemann, “Prokka: rapid prokaryotic genome annotation,” *Bioinformatics*, vol. 30, no. 14, pp. 2068–2069, Jul. 2014.
[162] A. J. Page *et al.*, “Roary: rapid large-scale prokaryote pan genome analysis,”

Bioinformatics, vol. 31, no. 22, pp. 3691–3693, Nov. 2015.
[163] P. Cingolani *et al.*, "A program for annotating and predicting the effects of single nucleotide polymorphisms, SnpEff," *Fly (Austin).*, vol. 6, no. 2, pp. 80–92, Apr. 2012.
[164] Z. Yang, "PAML 4: Phylogenetic Analysis by Maximum Likelihood," *Mol. Biol. Evol.*, vol. 24, no. 8, pp. 1586–1591, Apr. 2007.
[165] Z. Yang, *Computational Molecular Evolution*. Oxford University Press, 2006.
[166] M. Anisimova, O. Gascuel, and J. Sullivan, "Approximate Likelihood-Ratio Test for Branches: A Fast, Accurate, and Powerful Alternative," *Syst. Biol.*, vol. 55, no. 4, pp. 539–552, Aug. 2006.
[167] C. Bertelli *et al.*, "IslandViewer 4: expanded prediction of genomic islands for larger-scale datasets," *Nucleic Acids Res.*, vol. 45, no. W1, pp. W30–W35, Jul. 2017.
[168] L. Fu, B. Niu, Z. Zhu, S. Wu, and W. Li, "CD-HIT: accelerated for clustering the next-generation sequencing data," *Bioinformatics*, vol. 28, no. 23, pp. 3150–3152, Dec. 2012.
[169] S. A. Fritz and A. Purvis, "Selectivity in mammalian extinction risk and threat types: a new measure of phylogenetic signal strength in binary traits.," *Conserv. Biol.*, vol. 24, no. 4, pp. 1042–51, Aug. 2010.
[170] A. J. Drummond, M. A. Suchard, D. Xie, and A. Rambaut, "Bayesian Phylogenetics with BEAUti and the BEAST 1.7," *Mol. Biol. Evol.*, vol. 29, no. 8, pp. 1969–1973, Aug. 2012.
[171] E. J. Feil, B. C. Li, D. M. Aanensen, W. P. Hanage, and B. G. Spratt, "eBURST: inferring patterns of evolutionary descent among clusters of related bacterial genotypes from multilocus sequence typing data.," *J. Bacteriol.*, vol. 186, no. 5, pp. 1518–30, Mar. 2004.
[172] B. G. Spratt, W. P. Hanage, B. Li, D. M. Aanensen, and E. J. Feil, "Displaying the relatedness among isolates of bacterial species â€“ the eBURST approach," *FEMS Microbiol. Lett.*, vol. 241, no. 2, pp. 129–134, Dec. 2004.
[173] L. Chen, D. Zheng, B. Liu, J. Yang, and Q. Jin, "VFDB 2016: hierarchical and refined dataset for big data analysis—10 years on," *Nucleic Acids Res.*, vol. 44, no. D1, pp. D694–D697, Jan. 2016.
[174] Z. Li *et al.*, "Longitudinal Development of Mucoid <EMPH>Pseudomonas aeruginosa</EMPH> Infection and Lung Disease Progression in Children With Cystic Fibrosis," *JAMA*, vol. 293, no. 5, p. 581, Feb. 2005.
[175] I. Bianconi *et al.*, "Positive Signature-Tagged Mutagenesis in Pseudomonas aeruginosa: Tracking Patho-Adaptive Mutations Promoting Airways Chronic Infection," *PLoS Pathog Ital. Cyst. Fibros. Res. Found.*, vol. 7875725, no. 2, 2011.
[176] M. R. W. Brown 'and and J. H. S. Foster, "A simple diagnostic milk medium for Pseudomonas aeruginosa," *J. clin. Path*, vol. 23, pp. 172–177, 1970.
[177] G. A. O'Toole, "Microtiter dish biofilm formation assay.," *J. Vis. Exp.*, no. 47, Jan. 2011.
[178] H. Wickham, *Ggplot2 : elegant graphics for data analysis*. Springer, 2009.
[179] I. Bianconi *et al.*, "Draft Genome Sequences of 40 Pseudomonas aeruginosa Clinical Strains Isolated from the Sputum of a Single Cystic Fibrosis Patient Over an 8-Year Period.," *Genome Announc.*, vol. 4, no. 6, Dec. 2016.
[180] S. Feliziani *et al.*, "Coexistence and within-host evolution of diversified lineages of hypermutable Pseudomonas aeruginosa in long-term cystic fibrosis infections.," *PLoS Genet.*, vol. 10, no. 10, p. e1004651, Oct. 2014.
[181] J. Klockgether, N. Cramer, L. Wiehlmann, C. F. Davenport, and B. Tümmler, "Pseudomonas aeruginosa Genomic Structure and Diversity," *Front. Microbiol.*, vol. 2, p. 150, Jul. 2011.

[182] J. Klockgether *et al.*, “Intraclonal diversity of the Pseudomonas aeruginosa cystic fibrosis airway isolates TBCF10839 and TBCF121838: distinct signatures of transcriptome, proteome, metabolome, adherence and pathogenicity despite an almost identical genome sequence.,” *Environ. Microbiol.*, vol. 15, no. 1, pp. 191–210, Jan. 2013.
[183] V. L. Kung, E. A. Ozer, and A. R. Hauser, “The accessory genome of Pseudomonas aeruginosa.,” *Microbiol. Mol. Biol. Rev.*, vol. 74, no. 4, pp. 621–41, Dec. 2010.
[184] S. Pohl *et al.*, “The extensive set of accessory Pseudomonas aeruginosa genomic components.,” *FEMS Microbiol. Lett.*, vol. 356, no. 2, pp. 235–41, Jul. 2014.
[185] T. Seemann, “Snippy: Rapid haploid variant calling and core SNP phylogeny.” .
[186] N. Mayer-Hamblett *et al.*, “*Pseudomonas aeruginosa in vitro* Phenotypes Distinguish Cystic Fibrosis Infection Stages and Outcomes,” *Am. J. Respir. Crit. Care Med.*, vol. 190, no. 3, p. 140617081504001, Jun. 2014.
[187] L. Pirone *et al.*, “Burkholderia cenocepacia strains isolated from cystic fibrosis patients are apparently more invasive and more virulent than rhizosphere strains,” *Environ. Microbiol.*, vol. 10, no. 10, pp. 2773–2784, Oct. 2008.
[188] K. Kaniga, I. Delor, and G. R. Cornelis, “A wide-host-range suicide vector for improving reverse genetics in gram-negative bacteria: inactivation of the blaA gene of Yersinia enterocolitica.,” *Gene*, vol. 109, no. 1, pp. 137–41, Dec. 1991.
[189] D. Muhl and A. Filloux, “Site-Directed Mutagenesis and Gene Deletion Using Reverse Genetics,” in *Methods in molecular biology (Clifton, N.J.)*, vol. 1149, 2014, pp. 521–539.
[190] M. E. Kovach *et al.*, “Four new derivatives of the broad-host-range cloning vector pBBR1MCS, carrying different antibiotic-resistance cassettes,” *Gene*, vol. 166, no. 1, pp. 175–176, Dec. 1995.
[191] S. Kirchner, J. L. Fothergill, E. A. Wright, C. E. James, E. Mowat, and C. Winstanley, “Use of artificial sputum medium to test antibiotic efficacy against Pseudomonas aeruginosa in conditions more relevant to the cystic fibrosis lung.,” *J. Vis. Exp.*, no. 64, p. e3857, Jun. 2012.
[192] A. Hachani, N. S. Lossi, and A. Filloux, “A visual assay to monitor T6SS-mediated bacterial competition.,” *J. Vis. Exp.*, no. 73, p. e50103, Mar. 2013.
[193] T. Stiernagle, “Maintenance of C. elegans *,” vol. 1, 2006.
[194] M. Porta-de-la-Riva, L. Fontrodona, A. Villanueva, and J. Cerón, “Basic Caenorhabditis elegans Methods: Synchronization and Observation,” *J. Vis. Exp.*, no. 64, pp. e4019–e4019, Jun. 2012.
[195] J. W. Betts, L. M. Phee, M. Hornsey, and N. Woodford, “In vitro and in vivo Activity of Tigecycline/Colistin Combination Therapies against Carbapenem Resistant Enterobacteriaceae,” 2017.
[196] H. Motulsky and A. Christopoulos, “Analyzing Data with GraphPad Prism.”
[197] A. Hart, “Mann-Whitney test is not just a test of medians: differences in spread can be important.,” *BMJ*, vol. 323, no. 7309, pp. 391–3, Aug. 2001.
[198] A. V Alekseyenko, “Multivariate Welch t-test on distances.,” *Bioinformatics*, vol. 32, no. 23, pp. 3552–3558, Dec. 2016.
[199] J. M. Bland and D. G. Altman, “The logrank test,” *BMJ*, vol. 328, no. 7447, 2004.
[200] G. B. Pier *et al.*, “Role of Mutant CFTR in Hypersusceptibility of Cystic Fibrosis Patients to Lung Infections,” *Science (80-.).*, vol. 271, no. 5245, 1996.
[201] E. DiMango, H. J. Zar, R. Bryan, and A. Prince, “Diverse Pseudomonas aeruginosa gene products stimulate respiratory epithelial cells to produce interleukin-8.,” *J. Clin. Invest.*, vol. 96, no. 5, pp. 2204–10, Nov. 1995.
[202] M. Sonoda *et al.*, “cultured respiratory cells. aeruginosa induces inflammatory cytokines in Nitrite reductase from Pseudomonas,” *Infect. Immun*, vol. 65, no. 7,

1997.
[203] K. G. Leidal, K. L. Munson, and G. M. Denning, “Small Molecular Weight Secretory Factors from Pseudomonas aeruginosa Have Opposite Effects on IL-8 and RANTES Expression by Human Airway Epithelial Cells,” *Am. J. Respir. Cell Mol. Biol*, vol. 25, pp. 186–195, 2001.
[204] C. D. Sifri, J. Begun, and F. M. Ausubel, “The worm has turned – microbial virulence modeled in Caenorhabditis elegans,” *Trends Microbiol.*, vol. 13, no. 3, pp. 119–127, Mar. 2005.
[205] J. Glavis-Bloom, M. Muhammed, and E. Mylonakis, “Of Model Hosts and Man: Using Caenorhabditis elegans, Drosophila melanogaster and Galleria mellonella as Model Hosts for Infectious Disease Research,” Springer, New York, NY, 2012, pp. 11–17.
[206] S. A. Joyce and C. G. M. Gahan, “Molecular pathogenesis of Listeria monocytogenes in the alternative model host Galleria mellonella,” *Microbiology*, vol. 156, no. 11, pp. 3456–3468, Nov. 2010.
[207] S. Miyata, M. Casey, D. W. Frank, F. M. Ausubel, and E. Drenkard, “Use of the Galleria mellonella caterpillar as a model host to study the role of the type III secretion system in Pseudomonas aeruginosa pathogenesis.,” *Infect. Immun.*, vol. 71, no. 5, pp. 2404–13, May 2003.
[208] T. Bjarnsholt *et al.*, “*Pseudomonas aeruginosa* biofilms in the respiratory tract of cystic fibrosis patients,” *Pediatr. Pulmonol.*, vol. 44, no. 6, pp. 547–558, Jun. 2009.
[209] A. L. Barth and T. L. Pitt, “The high amino-acid content of sputum from cystic fibrosis patients promotes growth of auxotrophic Pseudomonas aeruginosa.,” *J. Med. Microbiol.*, vol. 45, no. 2, pp. 110–9, Aug. 1996.
[210] E. Mahenthiralingam, M. E. Campbell, and D. P. Speert, “Nonmotility and phagocytic resistance of Pseudomonas aeruginosa isolates from chronically colonized patients with cystic fibrosis.,” *Infect. Immun.*, vol. 62, no. 2, pp. 596–605, Feb. 1994.
[211] D. Williams *et al.*, “Divergent, coexisting Pseudomonas aeruginosa lineages in chronic cystic fibrosis lung infections.,” *Am. J. Respir. Crit. Care Med.*, vol. 191, no. 7, pp. 775–85, Apr. 2015.
[212] J. Diaz Caballero *et al.*, “Selective Sweeps and Parallel Pathoadaptation Drive Pseudomonas aeruginosa Evolution in the Cystic Fibrosis Lung.,” *MBio*, vol. 6, no. 5, pp. e00981-15, Sep. 2015.
[213] M. H. Rau *et al.*, “Early adaptive developments of Pseudomonas aeruginosa after the transition from life in the environment to persistent colonization in the airways of human cystic fibrosis hosts.,” *Environ. Microbiol.*, vol. 12, no. 6, pp. 1643–58, Jun. 2010.
[214] I. Bianconi *et al.*, “Comparative genomics and biological characterization of sequential Pseudomonas aeruginosa isolates from persistent airways infection.,” *BMC Genomics*, vol. 16, no. 1, p. 1105, Dec. 2015.
[215] N. Cramer, L. Wiehlmann, O. Ciofu, S. Tamm, N. Høiby, and B. Tümmler, “Molecular Epidemiology of Chronic Pseudomonas aeruginosa Airway Infections in Cystic Fibrosis,” *PLoS One*, vol. 7, no. 11, p. e50731, Nov. 2012.
[216] J. K. Lee, Y. S. Lee, Y. K. Park, and B. S. Kim, “Alterations in the GyrA and GyrB subunits of topoisomerase II and the ParC and ParE subunits of topoisomerase IV in ciprofloxacin-resistant clinical isolates of Pseudomonas aeruginosa,” *Int. J. Antimicrob. Agents*, vol. 25, no. 4, pp. 290–295, Apr. 2005.
[217] S. M. Moskowitz, R. K. Ernst, and S. I. Miller, “PmrAB, a two-component regulatory system of Pseudomonas aeruginosa that modulates resistance to cationic antimicrobial peptides and addition of aminoarabinose to lipid A.,” *J. Bacteriol.*, vol.

186, no. 2, pp. 575–9, Jan. 2004.
[218] K. Barrow and D. H. Kwon, “Alterations in Two-Component Regulatory Systems of phoPQ and pmrAB Are Associated with Polymyxin B Resistance in Clinical Isolates of Pseudomonas aeruginosa,” *Antimicrob. Agents Chemother.*, vol. 53, no. 12, pp. 5150–5154, Dec. 2009.
[219] S. M. Moskowitz *et al.*, “PmrB Mutations Promote Polymyxin Resistance of Pseudomonas aeruginosa Isolated from Colistin-Treated Cystic Fibrosis Patients,” *Antimicrob. Agents Chemother.*, vol. 56, no. 2, pp. 1019–1030, Feb. 2012.
[220] I. L. Lamont, P. A. Beare, U. Ochsner, A. I. Vasil, and M. L. Vasil, “Siderophore-mediated signaling regulates virulence factor production in Pseudomonas aeruginosa,” *Proc. Natl. Acad. Sci.*, vol. 99, no. 10, pp. 7072–7077, May 2002.
[221] L. W. Martin, D. W. Reid, K. J. Sharples, and I. L. Lamont, “Pseudomonas siderophores in the sputum of patients with cystic fibrosis,” *BioMetals*, vol. 24, no. 6, pp. 1059–1067, Dec. 2011.
[222] A. Bragonzi *et al.*, “*Pseudomonas aeruginosa* Microevolution during Cystic Fibrosis Lung Infection Establishes Clones with Adapted Virulence,” *Am. J. Respir. Crit. Care Med.*, vol. 180, no. 2, pp. 138–145, Jul. 2009.
[223] L. Greipel *et al.*, “Molecular epidemiology of mutations in antimicrobial resistance loci of *Pseudomonas aeruginosa* isolates from cystic fibrosis airways,” *Antimicrob. Agents Chemother.*, vol. 60, no. August, p. AAC.00724-16, 2016.
[224] J. Klockgether, D. Würdemann, O. Reva, L. Wiehlmann, and B. Tümmler, “Diversity of the abundant pKLC102/PAGI-2 family of genomic islands in Pseudomonas aeruginosa,” *J. Bacteriol.*, vol. 189, no. 6, pp. 2443–2459, 2007.
[225] M. W. Silby, C. Winstanley, S. A. C. Godfrey, S. B. Levy, and R. W. Jackson, “Pseudomonas genomes: Diverse and adaptable,” *FEMS Microbiol. Rev.*, vol. 35, no. 4, pp. 652–680, 2011.
[226] J. L. Fothergill *et al.*, “Impact of Pseudomonas aeruginosa genomic instability on the application of typing methods for chronic cystic fibrosis infections,” *J. Clin. Microbiol.*, vol. 48, no. 6, pp. 2053–2059, 2010.
[227] M. Jani, K. Mathee, and R. K. Azad, “Identification of novel genomic islands in liverpool epidemic strain of Pseudomonas aeruginosa using segmentation and clustering,” *Front. Microbiol.*, vol. 7, no. AUG, 2016.
[228] C. Winstanley *et al.*, “Newly introduced genomic prophage islands are critical determinants of in vivo competitiveness in the liverpool epidemic strain of pseudomonas aeruginosa,” *Genome Res.*, vol. 19, no. 1, pp. 12–23, 2009.
[229] A. Bragonzi *et al.*, “Sequence diversity of the mucABD locus in Pseudomonas aeruginosa isolates from patients with cystic fibrosis,” *Microbiology*, vol. 152, no. 11, pp. 3261–3269, 2006.
[230] H. B. Tang *et al.*, “Contribution of specific Pseudomonas aeruginosa virulence factors to pathogenesis of pneumonia in a neonatal mouse model of infection.,” *Infect. Immun.*, vol. 64, no. 1, pp. 37–43, Jan. 1996.
[231] P. Tingpej *et al.*, “Phenotypic characterization of clonal and nonclonal Pseudomonas aeruginosa strains isolated from lungs of adults with cystic fibrosis.,” *J. Clin. Microbiol.*, vol. 45, no. 6, pp. 1697–704, Jun. 2007.
[232] J. Manos *et al.*, “Virulence factor expression patterns in Pseudomonas aeruginosa strains from infants with cystic fibrosis,” *Eur. J. Clin. Microbiol. Infect. Dis.*, vol. 32, no. 12, pp. 1583–1592, Dec. 2013.
[233] J. W. Costerton and P. S. Stewart, “Battling biofilms.,” *Sci. Am.*, vol. 285, no. 1, pp. 74–81, Jul. 2001.
[234] J. W. Costerton, P. S. Stewart, and E. P. Greenberg, “Bacterial biofilms: a common cause of persistent infections.,” *Science*, vol. 284, no. 5418, pp. 1318–22, May 1999.

[235] J. R. Govan and V. Deretic, “Microbial pathogenesis in cystic fibrosis: mucoid Pseudomonas aeruginosa and Burkholderia cepacia.,” *Microbiol. Rev.*, vol. 60, no. 3, pp. 539–74, Sep. 1996.
[236] R. M. Donlan and J. W. Costerton, “Biofilms: survival mechanisms of clinically relevant microorganisms.,” *Clin. Microbiol. Rev.*, vol. 15, no. 2, pp. 167–93, Apr. 2002.
[237] J. W. Costerton, “Anaerobic biofilm infections in cystic fibrosis.,” *Mol. Cell*, vol. 10, no. 4, pp. 699–700, Oct. 2002.
[238] M. Hentzer, L. Eberl, and M. Givskov, “Transcriptome analysis of Pseudomonas aeruginosa biofilm development: anaerobic respiration and iron limitation,” *Biofilms*, vol. 2, no. 1, pp. 37–61, Jan. 2005.
[239] V. E. Wagner and B. H. Iglewski, “P. aeruginosa Biofilms in CF Infection,” *Clin. Rev. Allergy Immunol.*, vol. 35, no. 3, pp. 124–134, Dec. 2008.
[240] M. Hogardt, C. Hoboth, S. Schmoldt, C. Henke, L. Bader, and J. Heesemann, “Stage-Specific Adaptation of Hypermutable *Pseudomonas aeruginosa* Isolates during Chronic Pulmonary Infection in Patients with Cystic Fibrosis,” *J. Infect. Dis.*, vol. 195, no. 1, pp. 70–80, Jan. 2007.
[241] M. D. Obritsch, D. N. Fish, R. MacLaren, and R. Jung, “Nosocomial Infections Due to Multidrug-Resistant *Pseudomonas aeruginosa* : Epidemiology and Treatment Options,” *Pharmacotherapy*, vol. 25, no. 10, pp. 1353–1364, Oct. 2005.
[242] E. Lautenbach *et al.*, “Imipenem Resistance in Pseudomonas aeruginosa Emergence, Epidemiology, and Impact on Clinical and Economic Outcomes,” *Infect. Control Hosp. Epidemiol.*, vol. 31, no. 1, pp. 47–53, Jan. 2010.
[243] N. Lechtzin, M. John, R. Irizarry, C. Merlo, G. B. Diette, and M. P. Boyle, “Outcomes of adults with cystic fibrosis infected with antibiotic-resistant Pseudomonas aeruginosa.,” *Respiration.*, vol. 73, no. 1, pp. 27–33, 2006.
[244] N. Stoesser *et al.*, “Predicting antimicrobial susceptibilities for Escherichia coli and Klebsiella pneumoniae isolates using whole genomic sequence data,” *J. Antimicrob. Chemother.*, vol. 68, no. 10, pp. 2234–2244, Oct. 2013.
[245] E. Zankari *et al.*, “Genotyping using whole-genome sequencing is a realistic alternative to surveillance based on phenotypic antimicrobial susceptibility testing.,” *J. Antimicrob. Chemother.*, vol. 68, no. 4, pp. 771–7, Apr. 2013.
[246] J. Li, R. L. Nation, R. W. Milne, J. D. Turnidge, and K. Coulthard, “Evaluation of colistin as an agent against multi-resistant Gram-negative bacteria,” *Int. J. Antimicrob. Agents*, vol. 25, pp. 11–25, 2005.
[247] M. E. Falagas, I. I. Siempos, P. I. Rafailidis, I. P. Korbila, E. Ioannidou, and A. Michalopoulos, “Inhaled colistin as monotherapy for multidrug-resistant gram (–) nosocomial pneumonia: A case series,” *Respir. Med.*, vol. 103, no. 5, pp. 707–713, May 2009.
[248] S. Biswas, J.-M. Brunel, J.-C. Dubus, M. Reynaud-Gaubert, and J.-M. Rolain, “Colistin: an update on the antibiotic of the 21st century.,” *Expert Rev. Anti. Infect. Ther.*, vol. 10, no. 8, pp. 917–34, Aug. 2012.
[249] H. Giamarellou and G. Poulakou, “Multidrug-Resistant Gram-Negative Infections,” *Drugs*, vol. 69, no. 14, pp. 1879–1901, Oct. 2009.
[250] H. Li, Y. F. Luo, B. J. Williams, T. S. Blackwell, and C. M. Xie, “Structure and function of OprD protein in Pseudomonas aeruginosa: From antibiotic resistance to novel therapies,” *International Journal of Medical Microbiology*, vol. 302, no. 2. pp. 63–68, 2012.
[251] H. Huang, D. Jeanteur, F. Pattus, and R. E. Hancock, “Membrane topology and site-specific mutagenesis of Pseudomonas aeruginosa porin OprD.,” *Mol. Microbiol.*, vol. 16, no. 5, pp. 931–41, 1995.

[252] J. Quale, S. Bratu, J. Gupta, and D. Landman, “Interplay of efflux system, ampC, and oprD expression in carbapenem resistance of Pseudomonas aeruginosa clinical isolates,” *Antimicrob. Agents Chemother.*, vol. 50, no. 5, pp. 1633–1641, 2006.
[253] J.-M. Rodríguez-Martínez, L. Poirel, and P. Nordmann, “Molecular epidemiology and mechanisms of carbapenem resistance in Pseudomonas aeruginosa.,” *Antimicrob. Agents Chemother.*, vol. 53, no. 11, pp. 4783–8, 2009.
[254] K. Poole, “Pseudomonas aeruginosa: Resistance to the max,” *Front. Microbiol.*, vol. 2, no. APR, pp. 1–13, 2011.
[255] P. Naenna, P. Noisumdaeng, P. Pongpech, and C. Tribuddharat, “Detection of outer membrane porin protein, an imipenem influx channel, in Pseudomonas aeruginosa clinical isolates,” *Southeast Asian J. Trop. Med. Public Health*, vol. 41, no. 3, pp. 614–624, 2010.
[256] D. Skurnik *et al.*, “Enhanced in vivo fitness of carbapenem-resistant oprD mutants of Pseudomonas aeruginosa revealed through high-throughput sequencing,” *Proc. Natl. Acad. Sci. U. S. A.*, vol. 110, no. 51, pp. 20747–20752, 2013.
[257] S. Aendekerk, B. Ghysels, P. Cornelis, and C. Baysse, “Characterization of a new efflux pump, MexGHI-OpmD, from Pseudomonas aeruginosa that confers resistance to vanadium,” *Microbiology*, vol. 148, no. 8, pp. 2371–2381, 2002.
[258] J. K. Lee, Y. S. Lee, Y. K. Park, and B. S. Kim, “Alterations in the GyrA and GyrB subunits of topoisomerase II and the ParC and ParE subunits of topoisomerase IV in ciprofloxacin-resistant clinical isolates of Pseudomonas aeruginosa,” *Int. J. Antimicrob. Agents*, vol. 25, no. 4, pp. 290–295, 2005.
[259] H. Mouneimné, J. Robert, V. Jarlier, and E. Cambau, “Type II topoisomerase mutations in ciprofloxacin-resistant strains of Pseudomonas aeruginosa,” *Antimicrob. Agents Chemother.*, vol. 43, no. 1, pp. 62–66, 1999.
[260] P. D. Lister, D. J. Wolter, and N. D. Hanson, “Antibacterial-resistant *Pseudomonas aeruginosa*: clinical impact and complex regulation of chromosomally encoded resistance mechanisms.,” *Clin. Microbiol. Rev.*, vol. 22, no. 4, pp. 582–610, 2009.
[261] S. Bruchmann, A. Dötsch, B. Nouri, I. F. Chaberny, and S. Häussler, “Quantitative contributions of target alteration and decreased drug accumulation to pseudomonas aeruginosa fluoroquinolone resistance,” *Antimicrob. Agents Chemother.*, vol. 57, no. 3, pp. 1361–1368, 2013.
[262] M.-W. Tan, S. Mahajan-Miklos, and F. M. Ausubel, “Killing of Caenorhabditis elegans by Pseudomonas aeruginosa used to model mammalian bacterial pathogenesis,” *Microbiology*, vol. 96, pp. 715–720, 1999.
[263] R. L. Feinbaum *et al.*, “Genome-Wide Identification of Pseudomonas aeruginosa Virulence-Related Genes Using a Caenorhabditis elegans Infection Model,” 2012.
[264] B. Cezairliyan, N. Vinayavekhin, D. Grenfell-Lee, G. J. Yuen, A. Saghatelian, and F. M. Ausubel, “Identification of Pseudomonas aeruginosa Phenazines that Kill Caenorhabditis elegans,” *PLoS Pathog*, vol. 9, no. 1, 2013.
[265] D. G. Lee *et al.*, “Genomic analysis reveals that Pseudomonas aeruginosa virulence is combinatorial.,” *Genome Biol.*, vol. 7, no. 10, p. R90, 2006.
[266] L. A. Gallagher and C. Manoil, “Pseudomonas aeruginosa PAO1 kills Caenorhabditis elegans by cyanide poisoning.,” *J. Bacteriol.*, vol. 183, no. 21, pp. 6207–14, Nov. 2001.
[267] N. V Kirienko, F. M. Ausubel, and G. Ruvkun, “Mitophagy confers resistance to siderophore-mediated killing by Pseudomonas aeruginosa.,” *Proc. Natl. Acad. Sci. U. S. A.*, vol. 112, no. 6, pp. 1821–6, Feb. 2015.
[268] G. APERIS, B. BURGWYNFUCHS, C. ANDERSON, J. WARNER, S. CALDERWOOD, and E. MYLONAKIS, “Galleria mellonella as a model host to study infection by the Francisella tularensis live vaccine strain,” *Microbes Infect.*, vol. 9, no. 6, pp. 729–

734, May 2007.
[269] M. Nicoletti *et al.*, “Stenotrophomonas maltophilia strains from cystic fibrosis patients: genomic variability and molecular characterization of some virulence determinants.,” *Int. J. Med. Microbiol.*, vol. 301, no. 1, pp. 34–43, Jan. 2011.
[270] J. W. Betts, L. M. Phee, N. Woodford, and D. W. Wareham, “Activity of colistin in combination with tigecycline or rifampicin against multidrug-resistant Stenotrophomonas maltophilia,” *Eur. J. Clin. Microbiol. Infect. Dis.*, vol. 33, no. 9, pp. 1565–1572, Sep. 2014.
[271] K. F. Jarrell and A. M. Kropinski, “The virulence of protease and cell surface mutants of Pseudomonas aeruginosa for the larvae of Galleria mellonella.,” *J. Invertebr. Pathol.*, vol. 39, no. 3, pp. 395–400, May 1982.
[272] N. I. Lorè *et al.*, “Cystic Fibrosis-Niche Adaptation of Pseudomonas aeruginosa Reduces Virulence in Multiple Infection Hosts,” *PLoS One*, vol. 7, no. 4, p. e35648, Apr. 2012.
[273] E. Amiel, R. R. Lovewell, G. A. O’Toole, D. A. Hogan, and B. Berwin, “Pseudomonas aeruginosa Evasion of Phagocytosis Is Mediated by Loss of Swimming Motility and Is Independent of Flagellum Expression,” *Infect. Immun.*, vol. 78, no. 7, pp. 2937–2945, Jul. 2010.
[274] G. B. Pier, M. Grout, and T. S. Zaidi, “Cystic fibrosis transmembrane conductance regulator is an epithelial cell receptor for clearance of Pseudomonas aeruginosa from the lung,” *Med. Sci.*, vol. 94, pp. 12088–12093, 1997.
[275] D. D. Sriramulu, H. Lünsdorf, J. S. Lam, and U. Römling, “Microcolony formation: a novel biofilm model of Pseudomonas aeruginosa for the cystic fibrosis lung,” *J. Med. Microbiol.*, vol. 54, no. 7, pp. 667–676, Jul. 2005.
[276] J. Garbe *et al.*, “Characterization of JG024, a pseudomonas aeruginosa PB1-like broad host range phage under simulated infection conditions.,” *BMC Microbiol.*, vol. 10, p. 301, Nov. 2010.
[277] S. Naughton *et al.*, “Pseudomonas aeruginosa AES-1 exhibits increased virulence gene expression during chronic infection of cystic fibrosis lung.,” *PLoS One*, vol. 6, no. 9, p. e24526, 2011.
[278] C. Fung *et al.*, “Gene expression of Pseudomonas aeruginosa in a mucin-containing synthetic growth medium mimicking cystic fibrosis lung sputum,” *J. Med. Microbiol.*, vol. 59, no. 9, pp. 1089–1100, Sep. 2010.
[279] J. Garbe *et al.*, “Characterization of JG024, a pseudomonas aeruginosa PB1-like broad host range phage under simulated infection conditions,” 2010.
[280] G. English, O. Byron, F. R. Cianfanelli, A. R. Prescott, and S. J. Coulthurst, “Biochemical analysis of TssK, a core component of the bacterial Type VI secretion system, reveals distinct oligomeric states of TssK and identifies a TssK–TssFG subcomplex,” *Biochem. J.*, vol. 461, no. 2, 2014.
[281] N. M. I. Taylor *et al.*, “Structure of the T4 baseplate and its function in triggering sheath contraction,” *Nature*, vol. 533, no. 7603, pp. 346–352, 2016.
[282] C. Darby, C. L. Cosma, J. H. Thomas, and C. Manoil, “Lethal paralysis of Caenorhabditis elegans by Pseudomonas aeruginosa.,” *Proc. Natl. Acad. Sci. U. S. A.*, vol. 96, no. 26, pp. 15202–7, Dec. 1999.

ACKNOWLEDGEMENTS
First of all, I would like to warmly thank the "Associazione Trentina Fibrosi Cistica" for greatly supporting my work (donations in memory of Mauro Conotter and Sara Zini), not only economically, but also humanly. It is only because of them that I could successfully complete my PhD project and achieve many goals.
I would like to heartily offer my gratitude for all of the help and support given by my supervisor Prof. Olivier Jousson throughout my PhD.
My advisor Dr Irene Bianconi has been invaluable either for the helpful advice she has given me throughout these years, and for making my PhD project take shape.
I would like to thank Dr Alfonso Esposito for the important help he has offered me for all the bioinformatic work of my thesis.
I would like to thank Dr Kate Bailey, my initial thesis advisor, for supporting me during the first stages of my PhD.
My laboratory mates Filippo, Renato, Mattia, Elena, Viola, Federica and Toan have been incredibly supportive during the years I have spent at CIBIO, therefore I would like to heartily thank them all.
I would also like to thank all my CIBIO friends, and in particular Rosa, Isabelle, Tania, Francesca and Adrian for making my time at CIBIO a lot more valuable.
This thesis work would not have been possible without the precious collaboration of specialists from Rovereto CF support centre, therefore many thanks to Dr Ermanno Baldo, Dr Michele Schinella, Dr Paola Gualdi, Dr Marco Vizzini and Dr Grazia Dinnella for all the help and support they have offered me during my PhD.
Many thanks to Prof. Giovanni Di Bonaventura and Dr Arianna Pompilio for the fundamental and extremely appreciated contribution in the realisation of the experiments involving *Galleria mellonella*.
I would also like to thank Dr Giovanni Stefani for kindly donating me *C. elegans* from his collection, and for having taught me how to handle this fascinating organism.
I am enormously grateful to Prof. Craig Winstanley and Dr Jo Fothergill from University of Liverpool, that have hosted me in their laboratory for six months, teaching me numerous notions about *Pseudomonas aeruginosa* pathogenesis, and making me feel like I was entirely part of their group.
Prof. Alain Filloux and Dr Thomas Wood have been amazingly supportive and helpful during the four weeks I have spent at Imperial College; I am privileged to have worked with them, and I feel I have incredibly grown up as a scientist thanks to them.
A well deserved thank you goes to my new colleagues at Public Health England, who are fostering me every day, and have shown an amazing humaneness during the thesis editing period.
In addition, thanks to all my friends-of-a-life who have supported me in years.
Finally, my thanks and love to Matt and my family for putting up with me and keeping me sane throughout this time.